UAlg
UNIVERSIDADE DO ALGARVE
DEPARTAMENTO DE CIÊNCIAS BIOMÉDICAS E MEDICINA

Konjac glucomannan microcarriers: an application in the treatment of pulmonary tuberculosis

Filipa Raquel Horta Guerreiro

Tese para obtenção do grau de Doutor em Ciências Biomédicas

Trabalho realizado sob a orientação de:

Doutora Ana Margarida Grenha (Orientadora)

Doutora Maria Leonor Faleiro (Co-orientadora)

2021

This page was intentionally left in blank

UNIVERSIDADE DO ALGARVE
DEPARTAMENTO DE CIÊNCIAS BIOMÉDICAS E MEDICINA

Konjac glucomannan microcarriers: an application in the treatment of pulmonary tuberculosis

Filipa Raquel Horta Guerreiro

Tese para obtenção do grau de Doutor em Ciências Biomédicas

Trabalho realizado sob a orientação de:

Doutora Ana Margarida Grenha (Orientadora)

Doutora Maria Leonor Faleiro (Co-orientadora)

2021

This page was intentionally left in blank

Konjac glucomannan microcarriers: an application in the treatment of pulmonary tuberculosis

Declaração de autoria de trabalho:

Declaro ser a autora deste trabalho, que é original e inédito. Autores e trabalhos consultados estão devidamente citados no texto e constam da listagem de referências incluída.

Filipa Raquel Horta Guerreiro

This page was intentionally left in blank

This work was performed at:

Drug Delivery Laboratory

CBMR - Centre for Biomedical Research

CCMAR – Centro de Ciências do Mar

Faculdade de Ciências e Tecnologia – Universidade do Algarve

Campus Gambelas, 8005-139 Faro, Portugal

King's College London, Institute of Pharmaceutical Science, London, SE1 9NH, UK

This work was supported by National Portuguese funding through FCT - Fundação para a Ciência e a Tecnologia, through the PhD scholarship to Filipa Guerreiro (SFRH/BD/115628/2016) and the projects PTDC/DTP-FTO/0094/2012, UID/BIM/04773/2013, UID/Multi/04326/2019, UID/QUI/00100/2013

This page was intentionally left in blank

Acknowledgments

Ao longo destes quatro anos foram muitas as pessoas que contribuíram para a realização desta tese de doutoramento, não só a nível profissional através de todo o apoio a nível técnico e laboratorial, mas também a nível pessoal por todo o suporte emocional que proporcionaram quando foi preciso.

Em primeiro lugar agradecer à minha orientadora de tese, a Doutora Ana Grenha, por todo o apoio, disponibilidade e crescimento que me proporcionou e, tem proporcionado, desde 2014, quando entrei pela primeira vez no laboratório para realizar a minha tese de mestrado. Agradecer também à Doutora Leonor Faleiro por ter aceitado ser minha co-orientadora de tese e pelo suporte que me deu no mundo das bactérias, o qual nem sempre foi fácil. Também é importante o meu agradecimento ao Professor Doutor Ben Forbes e à Doutora Magda Swedorwska pela minha estadia no King's College London. Considero que os curtos 6 meses que estive em Londres foram aqueles que mais contribuíram, não só para o enriquecimento da tese, mas também a nível pessoal por toda a experiência de vida que me proporcionou. À Doutora Ana Costa, à Doutora María Dolores Torres da Faculdade de Ciências da Universidade de Vigo e à Doutora Manuela Gaspar da Faculdade de Farmácia da Universidade de Lisboa, o meu agradecimento pela ajuda essencial que prestaram para que certas partes do trabalho pudessem ser realizadas.

Um agradecimento a todos os colegas que passaram pelo laboratório 2.22 nos últimos 7 anos, os quais sempre mostraram disponibilidade em ajudar e que contribuíram para que pudesse chegar até aqui. Contudo, deixo aqui um agradecimento especial ao Jorge Pontes, à Susana Rodrigues e à Noelia Flórez Fernández por todos os momentos de boa disposição, onde o laboratório deixou de ser apenas mais um local de trabalho e onde encontrámos uns nos outros um apoio para as dificuldades que iam surgindo no nosso dia-a-dia.

Aos amigos de uma vida, uns mais perto outros mais longe; aos amigos mais recentes, mas que estão para ficar - a todos eles muito obrigada pelo apoio que sempre demonstraram para com as minhas decisões, pelos momentos de

convívio e descontração, os quais serviram como escape das preocupações do dia-a-dia e, pelo suporte emocional que sempre tiveram comigo nos momentos menos positivos.

Por último e, mais importante, um agradecimento à minha família e em especial aos meus pais, José António e Maria José. Foi deles que partiu o maior apoio durante todo o meu doutoramento e foi neles que muitas das frustrações foram descarregadas, sem que isso nunca interferisse no orgulho que sempre tiveram por todos os objetivos que tenho vindo a alcançar. Por isso, a acompanhar este agradecimento especial, vai um pedido de desculpas por situações e momentos que podem ter acontecido em alturas menos boas.

Muito obrigada a todos por tudo,

Filipa Guerreiro

List of contents

This page was intentionally left in blank

List of figures

List of tables

This page was intentionally left in blank

Abstract

Tuberculosis remains one of the leading causes of death worldwide.[1] The conventional therapy of this infection is based on the intake of a combination of several antitubercular drugs for a period that could reach 2 years.[2] The prolonged treatment of tuberculosis has limited the therapeutic success, as it fosters the non-compliance of the patient and, consequently, the emergence of drug resistance.[3] Thus, the development of new approaches to treat tuberculosis is demanded to address the limitations of the current treatment. Considering that 80% of tuberculosis cases are pulmonary, the direct delivery of antitubercular drugs to the lungs has been explored as therapeutic alternative in recent years. This approach is thought to potentially allow to decrease the dose and frequency of drug administration, while reducing the treatment duration and the systemic side effects associated to the conventional therapy of tuberculosis.[4] Its success requires the engineering of suitable carriers, which must reach the alveolar region, where the macrophages infected with *Mycobacterium tuberculosis* are located, and undergo phagocytosis by these cells.[5] On the other side, specific receptors existing on macrophage surface may be used as drug targets in a strategy where drug carriers may, again, play a relevant role. At this moment, there are few excipients approved for pulmonary delivery applications, which hinders the development of drug carriers.[6] The work entailing this PhD thesis proposes the development of inhalable microparticles based on konjac glucomannan (KGM), which are targeted to the alveolar macrophages. KGM is a polysaccharide composed by mannose and glucose units.[7] The rational beyond the proposed strategy relies on the fact that the presence of mannose on KGM microparticles may mediate a preferential recognition by the mannose receptors present on the macrophage surface and potentiate their phagocytosis via these receptors.[8] Inhalable microparticles were produced in the form of dry powders by a technique of spray-drying. In order to have KGM with the suitable properties for microparticle production using this technique, the polymer was initially submitted to an acid hydrolysis, which was demonstrated to not affect its physicochemical characteristics (composition and glucose/mannose ratio) and permitted a successful processing by spray-drying to produce microparticles. Isoniazid (INH) and rifabutin (RFB) are first-line antitubercular drugs and were associated to KGM

microparticles as model drugs. Various formulations of drug-loaded KGM microparticles were produced (KGM/INH/RFB = 10/1/0.5, 10/1/1, 10/2/0.5, w/w) and subsequently characterised. Drug association efficiency varied within 66% and 91%, and the release of the drugs in conditions resembling the alveolar environment showed slower release of RFB compared with INH, but complete release of both drugs within 24 h. Regarding to the aerodynamic characteristics, which are of utmost importance in lung delivery strategies, KGM microparticles exhibited aerodynamic diameters around 3 μm, regardless of the drug amounts, which evidences suitability to reach the alveolar zone. Additionally, the spherical shape and the geometric size of approximately 2 μm displayed by KGM microparticles has proven adequate for macrophage internalisation, as shown in an *in vitro* assay. In fact, approximately 100% of macrophage-like THP-1 cells in culture demonstrated to phagocytose the microparticles. Despite the uptake was demonstrated, macrophage activation upon exposure to microparticles was not observed.

As mentioned before, a relevant limitation of the pulmonary drug delivery field relies on the shortness of excipients approved for inhalation. One of the main reasons for that is the unknown fate of materials after deposition in the lungs. In this work, the swelling of (unloaded) KGM microparticles was observed to occur (40% - 50%) upon liquid contact, but size reduction (> 62% in 90 min) in presence of β-mannosidase, an enzyme present in the lung, was further demonstrated, indicating potential biodegradability upon inhalation.

The preservation of antibacterial effect of the used drugs after spray-drying was demonstrated using *Mycobacterium bovis*, evidencing an absence of effect of the process of microencapsulation. In fact, the minimum inhibitory concentration (MIC) remained similar to that determined for the free drugs. However, a preliminary study indicated that the amount of drug corresponding to MIC was not enough to kill the bacteria after infection of the macrophages (macrophage-like THP-1 cells) with *M. bovis*. The number of bacteria surviving in macrophages only decreased on the ninth day of infection. Moreover, the continued exposure of bacteria to KGM microparticles for 7 days suggested the development of a certain degree of drug resistance by *M. bovis*.

Finally, to better support the proposal of using KGM in lung delivery applications, the safety of KGM microparticles was evaluated *in vitro* and *in vivo*. With regards to the *in vitro* tests, these focused on the evaluation of toxicological profile in respiratory cells (alveolar epithelium and macrophages). Despite a wide range of concentrations was assessed to have a more comprehensive knowledge on the effect of the material and the developed drug carrier, at the concentrations expected to be realistic in approaches of lung delivery (up to 125 µg/mL) drug-loaded KGM microparticles did not show overt cell toxicity. An *in vivo* assay was also performed which focused on evaluating the toxicity of the material itself, as it is not approved for lung delivery applications. Mice receiving daily administration of unloaded KGM microparticles by inhalation for a period of two weeks have shown no signs of systemic or lung inflammatory response, which is in line with the results of macrophage activation obtained *in vitro*. Moreover, histological examination of the lung revealed no differences upon inhalation, comparing with control naïve mice, although some unexpected observations transversal to all groups require clarification. The results further demonstrated the development of eosinophilia, which is typically associated to allergic reactions. Nevertheless, no alterations were observed in serum IgE upon inhalation, which opposes to the eosinophilic effect. Overall, despite some positive indications, regulations on safety evaluation include a vast number of parameters to assess and further studies are required to deepen the assessment and support the safety of KGM for lung delivery applications.

Considering the whole set of data generated throughout the work, encouraging indications were given on the potential of KGM to be used as a pharmaceutical excipient in the formulation of inhalable antitubercular drug carriers for pulmonary tuberculosis treatment and, potentially, in other applications benefiting from macrophage targeting.

Keywords: alveolar macrophages, inhalable microparticles, isoniazid, konjac glucomannan, pulmonary drug delivery, rifabutin, spray-drying, tuberculosis.

This page was intentionally left in blan

Resumo

A tuberculose continua a ser uma das principais causas de morte em todo o mundo.[1] A terapia convencional desta infeção baseia-se na administração oral de uma combinação de vários fármacos tuberculostáticos por um período de tempo que pode alcançar os 2 anos.[2] O tratamento prolongado da tuberculose tem limitado a sua terapêutica, pois favorece a não adesão do paciente ao tratamento e, consequentemente, o aparecimento de resistência aos antibióticos.[3] Desta forma, é necessário o desenvolvimento de novas abordagens para o tratamento da tuberculose com o objetivo de ultrapassar as limitações do tratamento atual. Considerando que 80% dos casos são de tuberculose pulmonar, a administração direta de fármacos tuberculostáticos nos pulmões tem sido explorada nos últimos anos como uma alternativa terapêutica. Acredita-se que esta abordagem permitirá diminuir a dose e a frequência de administração dos antibióticos, enquanto reduz a duração do tratamento e os possíveis efeitos sistémicos associados à terapia convencional da tuberculose.[4] O sucesso desta abordagem depende da engenharia de transportadores com características adequadas, os quais devem chegar à região alveolar, onde os macrófagos infetados com *Mycobacterium tuberculosis* estão localizados, e serem internalizados por estas células.[5] Por outro lado, recetores específicos presentes na superfície dos macrófagos podem ser usados como alvos terapêuticos para a entrega dos fármacos, uma estratégia na qual os transportadores têm novamente uma função relevante. Neste momento, existem poucos excipientes aprovados para aplicações na entrega pulmonar de fármacos, o que dificulta o desenvolvimento dos transportadores.[6] O trabalho desenvolvido nesta tese de doutoramento propõe o desenvolvimento de micropartículas inaláveis à base de glucomanano de konjac (KGM) direcionadas para os macrófagos alveolares. O KGM é um polissacarídeo composto por unidades de manose e glucose.[7] Esta abordagem foca-se na presença de manose nas micropartículas de KGM, a qual poderá mediar um reconhecimento preferencial pelos recetores de manose presentes na superfície dos macrófagos alveolares e potenciar a sua fagocitose através destes.[8] As micropartículas inaláveis foram produzidas na forma de pós secos por uma técnica de secagem por pulverização, a atomização. Para que o KGM tivesse as propriedades

adequadas para a produção de micropartículas por meio desta técnica, o polímero foi inicialmente submetido a uma hidrólise ácida, a qual demonstrou não afetar as suas características físico-químicas (composição e ratio glucose/manose) e permitiu a sua atomização para a produção das micropartículas. A isoniazida (INH) e a rifabutina (RFB), dois fármacos tuberculostáticos de primeira linha usados na clínica da tuberculose, foram associadas às micropartículas de KGM como fármacos modelo. Várias formulações de micropartículas de KGM com os dois antibióticos foram produzidas (KGM/INH/RFB = 10/1/0,5, 10/1/1, 10/2/0,5, m/m) e posteriormente caracterizadas. A eficácia de associação dos fármacos variou entre 66% e 91%, e a libertação dos mesmos em condições semelhantes ao ambiente alveolar foi mais lenta para a RFB em comparação com a INH, mas ambos os antibióticos apresentaram uma libertação completa ao fim de 24 horas. Em relação às características aerodinâmicas, as quais são cruciais na entrega pulmonar de fármacos, as micropartículas de KGM apresentaram diâmetros aerodinâmicos em torno dos 3 µm, independentemente das quantidades de fármaco associadas, o que evidencia a sua capacidade para atingir a zona alveolar. Além disso, a forma esférica e o tamanho geométrico de aproximadamente 2 µm apresentados pelas micropartículas de KGM demonstraram ser adequados para a sua internalização pelos macrófagos, conforme demonstrado no ensaio *in vitro*. Aproximadamente 100% das células THP-1 diferenciadas em macrófagos fagocitaram as micropartículas de KGM. Contudo, apesar da internalização demonstrada, não foi observada a ativação dos macrófagos após a sua exposição às micropartículas.

Como mencionado anteriormente, uma limitação relevante na administração pulmonar de fármacos é a escassez de excipientes aprovados para inalação. Uma das principais razões é o destino desconhecido dos materiais após a sua deposição nos pulmões. Neste trabalho, o inchamento das micropartículas de KGM (sem antibióticos) foi observado (40% - 50%) após o contato com uma solução, mas a redução do seu tamanho (> 62% em 90 min) na presença de β-manosidase, uma enzima presente nos pulmões, foi demonstrada posteriormente, indicando uma possível biodegradabilidade após inalação.

A atividade antibacteriana dos fármacos após a sua atomização foi preservada em *Mycobacterium bovis*, o que indicou que o processo de microencapsulação não teve qualquer interferência negativa na atividade da INH e da RFB. A concentração mínima inibitória (CMI) foi semelhante àquela determinada para os fármacos não associados às micropartículas de KGM. No entanto, um estudo preliminar indicou que as quantidades de fármaco correspondente à CMI não foram suficientes para matar as bactérias após a infeção dos macrófagos (células THP-1 diferenciadas em macrófagos) com *M. bovis*. O número de bactérias sobreviventes nos macrófagos diminuiu apenas ao nono dia de infeção. Além disso, a exposição continuada das bactérias às micropartículas de KGM por 7 dias indicou o desenvolvimento de um certo grau de resistência da micobactéria.

Finalmente, o perfil toxicológico das micropartículas de KGM foi avaliado *in vitro* e *in vivo*. Em relação aos ensaios *in vitro*, estes foram focados na avaliação do perfil toxicológico em células respiratórias (epitélio alveolar e macrófagos). Apesar de terem sido avaliadas várias concentrações de forma a ter um conhecimento mais abrangente sobre o efeito do material e das micropartículas desenvolvidas, nas concentrações que se espera serem mais realistas em abordagens de entrega pulmonar (até 125 µg/mL) as micropartículas de KGM com os antibióticos não induziram um efeito de toxicidade celular evidente. O ensaio *in vivo* teve como foco avaliar a toxicidade do próprio material, uma vez que não está aprovado para aplicações de administração pulmonar. Os ratinhos que receberam uma administração diária das micropartículas de KGM sem fármacos por inalação por um período de duas semanas não mostraram sinais de resposta inflamatória sistémica ou pulmonar, o que está em concordância com os resultados obtidos no ensaio da ativação dos macrófagos *in vitro*. Além disso, a análise histológica dos pulmões não relevou diferenças após inalação comparativamente com o grupo controlo naïve, embora algumas observações inesperadas transversais a todos os grupos precisam ser clarificadas. Os resultados demonstraram ainda o desenvolvimento de eosinofilia, tipicamente associada a reações alérgicas. No entanto, não foram observadas alterações dos níveis séricos de IgE após a inalação das micropartículas de KGM, o qual se opõe ao efeito eosinofílico. No geral, apesar de algumas indicações positivas,

os regulamentos sobre a avaliação de segurança de materiais incluem um grande número de parâmetros a analisar e são necessários mais estudos para aprofundar esta avaliação de forma a garantir a segurança no uso do KGM para aplicações de administração pulmonar.

O conjunto de dados obtidos ao longo do trabalho deu indicações encorajadoras sobre o potencial do KGM para ser usado como um excipiente farmacêutico na formulação de transportadores de fármacos tuberculostáticos inaláveis para o tratamento da tuberculose pulmonar e, potencialmente, noutras aplicações que beneficiarão da veiculação para os macrófagos.

Palavras-chave: administração pulmonar de fármacos, atomização, glucomanano de konjac, isoniazida, macrófagos alveolares, micropartículas inaláveis, rifabutina, tuberculose.

List of publications and communications

Patent

Ana D Alves, Filipa S Pereira, Susana Rodrigues, **Filipa Guerreiro**, Ludmylla Cunha, Ana Grenha, Process for producing polysaccharide microparticles for alveolar macrophages targeting, microparticles obtained therein and use thereof. PCT/IB2016/052353 (under revision in the European Patents Office)

Publications

Filipa Guerreiro, Magda Swedrowska, Roshnee Patel, Noelia Flórez-Fernández, María Dolores Torres, Ana M. Rosa da Costa, Ben Forbes, Ana Grenha, 2021. Engineering of konjac glucomannan into respirable microparticles for delivery of antitubercular drugs. *International Journal of Pharmaceutics*, *604*, 120731.

Filipa Guerreiro, Jorge F. Pontes, Ana M. Rosa da Costa, Ana Grenha, 2019. Spray-drying of konjac glucomannan to produce microparticles for an application as antitubercular drug carriers. *Powder Technology*, *342*, 246-252.

Communications

Oral communications

Filipa Guerreiro, Ana M. Rosa da Costa, Ana Grenha, "Konjac glucomannan microcarriers and macrophages – a promising interaction in lung diseases treatment", Drug Delivery to the Lungs Conference, 11 December 2020 (Online).

Filipa Guerreiro, Magda Swedrowska, Ana M. Rosa da Costa, Ana Grenha, Ben Forbes, "*In vitro* behaviour of konjac glucomannan microparticles aimed at pulmonary tuberculosis therapy", Drug Delivery to the Lungs Conference, 12 December 2019, Edinburgh, Scotland.

Conference papers

Filipa Guerreiro, Magda Swedrowska, Ana M. Rosa da Costa, Ana Grenha, Ben Forbes, 2020. In vitro behaviour of konjac glucomannan microparticles aimed at pulmonary tuberculosis therapy. *Journal of Aerosol Medicine and Pulmonary Drug Delivery*, 33 (2), A12.

Filipa Guerreiro, Ana M. Rosa da Costa, Maria Leonor Faleiro, Ana Grenha, 2018. Konjac glucomannan microparticles for antitubercular drug delivery by inhalation. *Journal of Aerosol Medicine and Pulmonary Drug Delivery, 31 (2), A27-28.*

Posters in conferences

Filipa Guerreiro, Magda Swedrowska, Ana M. Rosa da Costa, Ana Grenha, Ben Forbes, "*In vitro* behaviour of konjac glucomannan microparticles aimed at pulmonary tuberculosis therapy", Drug Delivery to the Lungs Conference, 12 December 2019, Edinburgh, Scotland.

Filipa Guerreiro, Ana M. Rosa da Costa, Maria Leonor Faleiro, Ana Grenha, "Uptake of konjac glucomannan microparticles by macrophage-like cells for an application in tuberculosis therapy", 2018 Controlled Release Society Annual Meeting & Exposition, 22-24 July 2018, New York, U.S.A.

Filipa Guerreiro, Ana M. Rosa da Costa, Maria Leonor Faleiro, Ana Grenha, "Konjac glucomannan microparticles for antitubercular drug delivery by inhalation", Drug Delivery to the Lungs 2017, 6-8 December 2017, Edimburgo, Escócia.

Filipa Guerreiro, Ana M. Rosa da Costa, Maria Leonor Faleiro, Ana Grenha, "Cytotoxic evaluation and macrophage activation ability of konjac glucomannan microparticles", 21st International Symposium on Microencapsulation, 27-29 September 2017, Faro, Portugal.

Filipa Guerreiro, Ana M. Rosa da Costa, Maria Leonor Faleiro, Ana Grenha, "The effect of mannitol and leucine in konjac glucomannan spray-dried microcarriers", 2nd CBMR/ProRegeM Annual Meeting, 8 September 2017, Faro, Portugal.

Other works

Finalist of "The Pat Burnell Young Investigator Award" on Drug Delivery to the Lungs Conference 2019.

Filipa Guerreiro, Noelia Flórez-Fernández, Ana Grenha, 2020. Das árvores do Algarve para os pulmões do mundo. *Ualgoritmo - A Ciência trocada por miúdos*, *2(7)*, 35-38.

This page was intentionally left in blank

List of abbreviations and acronyms

ACK	Ammonium-chloride-potassium
AE	Association efficiency
ASL	Airway surface liquid
ATCC	American Type Cell Culture
BCG	Bacillus Calmette–Guérin
CCM	Cell culture medium
COPD	Chronic obstructive pulmonary disease
DMEM	Dulbecco's Modified Eagle's Medium
DMF	Dimethylformamide
DMSO	Dimethyl sulfoxide
DNA	Deoxyribonucleic acid
DPI(s)	Dry powder inhaler(s)
ED	Emitted dose
EDAC	1-ethyl-3-(3-dimethylaminopropyl) carbodiimide
EDTA	Ethylenediaminetetraacetic acid
FBS	Foetal Bovine Serum
FDA	Food and Drug Administration
FESEM	Field emission scanning electron microscopy
FPD	Fine particle dose
FPF	Fine particle fraction
FSC-H	Forward scatter height
FTIR	Fourier-transform infrared spectroscopy
GSD	Geometric standard deviation
HIV	Human Immunodeficiency Virus
HPLC	High performance liquid chromatography
HPSEC	High performance size exclusion chromatography
IC_{50}	Half-maximal inhibitory concentration
IgE	Immunoglobulin E

INH	Isoniazid
InhA	NADH-dependent enoyl-[Acyl-Carrier-protein] reductase
IL-1	Interleukin 1
IL-8	Interleukin 8
KGM	Konjac glucomannan
LC	Loading capacity
LDH	Lactate dehydrogenase
LPS	Lipopolysaccharide
M7H9	Middlebrook 7H9 medium
MDR-TB	Multidrug-resistant tuberculosis
MIC	Minimum inhibitory concentration
MMAD	Mass median aerodynamic diameter
MOC	Micro-orifice collector
MP(s)	Microparticle(s)
MTT	3-(4 5-dimethylthiazol-2-yl)-2 5-diphenyltetrazolium bromide
NADH	Nicotinamide adenine dinucleotide
NGI	Next Generation Impactor
NMR	Nuclear magnetic resonance spectroscopy
OADC	Oleic Albumin Dextrose Catalase
PAMPs	Pathogen-associated molecular patterns
PBS	Phosphate buffer saline
PLGA	Poly(lactic-co-glycolic acid)
PMA	Phorbol myristate acetate
PVA	Poly(vinyl alcohol)
RFB	Rifabutin
RH	Relative humidity
RIF	Rifampicin
RNA	Ribonucleic acid
SDS	Sodium dodecyl sulphate

SLF	Simulated lung fluid
SSC-H	Side scatter height
TLR	Toll-like receptors
TNF-α	Tumor necrosis factor-α
XRD-TB	Extensively drug-resistant tuberculosis
WHO	World Health Organisation

This page was intentionally left in blank

CHAPTER 1 – GENERAL INTRODUCTION

This page was intentionally left in blank

1. General introduction

1.1. Tuberculosis

1.1.1. Epidemiology

Tuberculosis has an old history in civilisation, remaining one of the main leading causes of death worldwide. According to the Global Tuberculosis Report emitted by the World Health Organisation (WHO), recent data indicate that approximately 10 million of people fall ill with tuberculosis each year and more than 1 million die from the disease. Although tuberculosis affects both sexes in all age groups, several risk factors are identified that increase the possibility of infection, including level of malnutrition, poverty, smoking, diabetes, and the existence of concomitant infection with Human Immunodeficiency Virus (HIV).[1] In cases of co-infection with HIV, tuberculosis is the leading cause of death.[9] Globally, in 2019 the regions more affected were South-East Asia (44%), Africa (25%) and Western Pacific (18%) (Figure 1.1).[1]

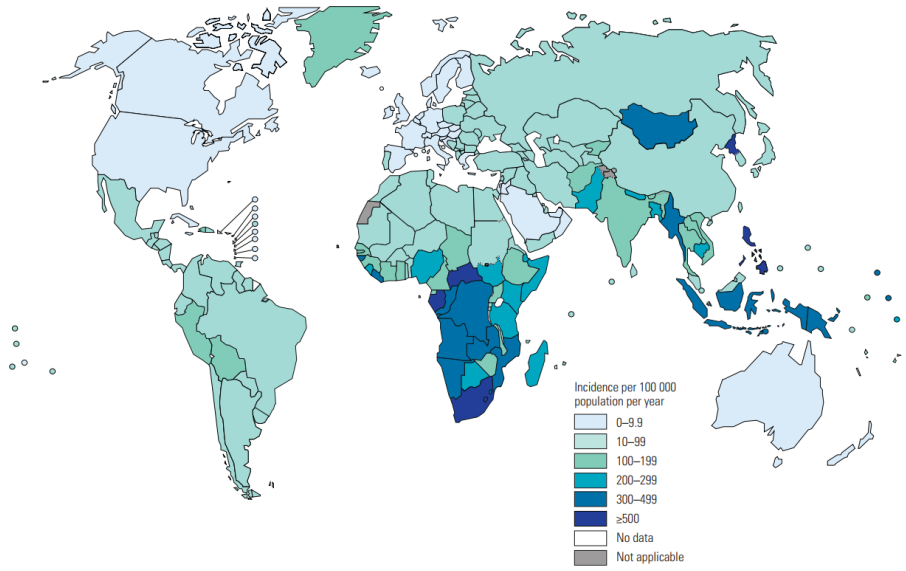

Figure 1.1. Estimated tuberculosis incidence rates in 2019.[1]

In recent years, the number of cases and deaths related with tuberculosis has been decreasing. In 2019, 1.2 million deaths from tuberculosis were estimated worldwide, half million less than the number reported in 2000. Despite the consistent decline reported in the last years, tuberculosis persists as a public

health threat, especially due to the emergence of resistance to the antibiotics conventionally used in the disease therapy. For example, around half a million people developed resistance to rifampicin (RIF), one of the first-line antitubercular drugs used in clinics. Moreover, 78% of resistance cases to RIF showed resistance to other drugs that are also used in the treatment of the disease.[1]

Aligned with global indicators, the number of cases of tuberculosis in Portugal has also registered a sustained decrease in recent years (Figure 1.2). According to data from Direção-Geral da Saúde, the incidence of tuberculosis is lower than the limit defined as low incidence (< 20/100 000 persons).[10] In 2019, a total of 1 741 cases of tuberculosis were reported, resulting in a notification rate of 16.9/100 000 persons (Figure 1.2). Eight of these cases referred to multidrug-resistant tuberculosis (MDR-TB), thus corresponding to 0.45% of the total reported cases. The largest number of cases was registered in the urban centres, Lisbon and Oporto, and the social factors found to contribute the most for this incidence were the consumption of alcohol (10.3%) and drugs (6.7%). Additionally, and as expected in the sequence of international indicators, HIV is also a risk factor for tuberculosis infection in Portugal. However, this co-infection has been decreasing over the years and, in the last decade, tuberculosis notification rate decreased from 15.7% to 10.2% among persons co-infected with HIV.[10,11]

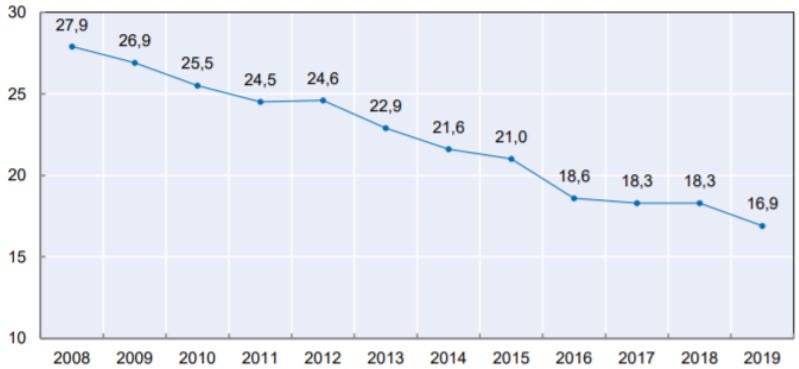

Figure 1.2. Evolution of the tuberculosis notification rate in Portugal, per 100 000 persons.[11]

The age group of children up to 5 years old is also raising concern in Portugal. The conventional Bacillus Calmette–Guérin (BCG) vaccine is no longer in the

national plan of vaccination and only children living in risk groups or in communities with a high incidence are currently vaccinated against tuberculosis. Therefore, this modification in tuberculosis prevention plan requires a monitorisation of the disease in this group of children. In 2019, 45 cases of tuberculosis were reported to occur at ages between 0 and 5 years, and only 15 of these reported cases were vaccinated with BCG when they developed the disease (33.3%).[11,12]

To end the global tuberculosis epidemic, the “End TB Strategy” was adopted by the WHO Member States during the World Health Assembly in 2014. This strategy includes achieving a 95% decline in deaths due to tuberculosis compared with 2015 and reaching an equivalent 90% reduction in tuberculosis incidence rate by 2035.[1,13]

1.1.2. Pathogenesis

Tuberculosis is an infectious disease caused by *Mycobacterium tuberculosis,* a bacillus that was discovered in 1882 by Robert Koch.[14] *M. tuberculosis* is a facultative slow-growing intracellular pathogen and it is by far the most important human pathogen amongst more than 20 species of mycobacteria known to cause disease in humans.[15–17] This pathogen is an aerobic-to-microaerophilic Gram-positive non-sporulating member of the Actinomycete family.[16] The success of *M. tuberculosis* as a pathogen and its intrinsic resistance mechanisms to many antibacterial drugs can be attributed to the complexity of the cell envelope. This is rich in lipids, such as the mycolic acids, and polysaccharides of unique chemical structure.[17,18] The lipidic nature of the cell wall makes it extremely hydrophobic and prevents the permeation of hydrophilic compounds, including many antibiotics.[19] This resistance mechanism limits both the application of available antibiotics and the development of new drugs to treat tuberculosis.[20] Moreover, beyond the innate resistance mechanisms to the antibiotics, the majority of the cases of clinical resistance to the drugs used in tuberculosis treatment is due to *M. tuberculosis* chromosomal mutations. In fact, depending on the antibiotic, there may be multiple mechanisms of resistance.[19]

M. tuberculosis infection begins with the entry of the bacillus in the respiratory tract and consequent inhalation (Figure 1.3). Upon inhalation, major lung mechanisms of defence must be faced, including the cough reflex and the mucociliary escalator. Details of the latter are described in section 1.2. If the bacteria overcome these, they will reach the alveolar region where recognition by the alveolar macrophages will take place, followed by phagocytosis.[21] These initial pathogenesis steps result in the alveolar macrophages acting as *M. tuberculosis* hosts.[22,23] Therefore, these cells play a major role throughout the course of tuberculosis infection.[24,25]

Macrophages residing in the tissues compose the first line of defence against foreign pathogens and coordinate the recruitment of leucocytes in innate immunity. These cells can control tissue homeostasis through antigen removal by phagocytosis and degradation of pathogens, apoptotic cells, and neoplastic cells.[26–28] In response to these "signals", macrophages are able to polarise, thus exhibiting distinct and defined phenotypes. These correspond to either a pro-inflammatory (classical M1) or an anti-inflammatory (alternative M2) phenotype, which are interchangeable, converting into each other depending on the microenvironment.[24,29,30] While M1 macrophages are associated to the delay of the cellular proliferation surrounding the tissue and consequent damage, M2 macrophages support cellular proliferation and promote wound healing and tissue repair through the release of anti-inflammatory cytokines.[24,29,31] The presence of a pathogen in a tissue leads to the recruitment of monocytes in circulation and, depending on the stimuli received from the pathogen, these cells will differentiate into macrophages. In the early stage of bacterial infection, macrophages express the M1 phenotype upon the recognition of pathogen-associated molecular patterns (PAMPs), leading to the bacteria phagocytosis and initiating an acute inflammatory cascade trough the high production of pro-inflammatory mediators, such as interleukin 1 (IL-1), tumour necrosis factor-α (TNF-α) and nitric oxide, which kill the pathogens and trigger an adaptive immune response.[24] The internalisation of most pathogens results in their trapping in a vacuole called phagosome, which fuses with the lysosome forming the phagolysosome in a process known as maturation. The phagolysosome exhibits

microbicidal conditions due to the presence of acid hydrolases that ensure the degradation of intracellular pathogens.[32–34]

A cascade of events similar to that described above is involved in the initial infection stages of *M. tuberculosis*.[24] Macrophages present in the alveoli keep the pulmonary surface under surveillance for inhaled pathogens. Upon arrival to the alveoli, *M. tuberculosis* PAMPs are recognised by macrophages through the receptors expressed on their surface.[26] The interaction occurring between mycobacteria and alveolar macrophages results in the activation of macrophages towards a M1 phenotype, with the consequent internalisation of the pathogen by receptor-mediated phagocytosis. The bacteria enter the cell internalised in a phagosome, as happens with other pathogens. However, *M. tuberculosis* has developed the ability to inhibit the phagosome fusion with the lysosome, thus circumventing the conventional macrophage bactericidal abilities and assuring survival (Figure 1.3).[22,23,29] The bacteria will thus replicate inside the macrophage until an adaptive immune response is developed. The M1 macrophage phenotype is characterised by the production of proteolytic enzymes and pro-inflammatory mediators by the infected cells, which mainly include IL-1, TNF-α and nitric oxide, as already referred. This increases macrophage bactericidal capacity and triggers adaptive immune response.[25,29] In this context, the released pro-inflammatory mediators attract cells to the infection site, leading to the accumulation of T and B cells along with myeloid cells (monocytes, macrophages, dendritic cells, multinucleated giant cells). This drives the formation of the granuloma, a solid host-protective structure considered the hallmark of tuberculosis. The granuloma is composed by an agglomerate of immune cells, in which differentiated macrophages (epithelioid cells, multinucleated giant cells, foamy macrophages) can be found in the centre surrounded by a lymphocytic cuff (T and B cells).[23,35–37] The centre of the granuloma is hypoxic and necrotic, a microenvironment that ensures bacterial survival in a low replicative and metabolic state.[23] Despite containing bacteria spreading and the progression of the infection, the granuloma acts as a protecting site to the bacteria, since they remain shielded from immune responses and are inaccessible to antibiotics. This in fact allows their survival for years, decades or even lifetime. During the time which the bacteria is protected and in a non-metabolic active state into the

granuloma, the infected person is asymptomatic and cannot transmit the infection to other people, being diagnosed with latent tuberculosis.[38]

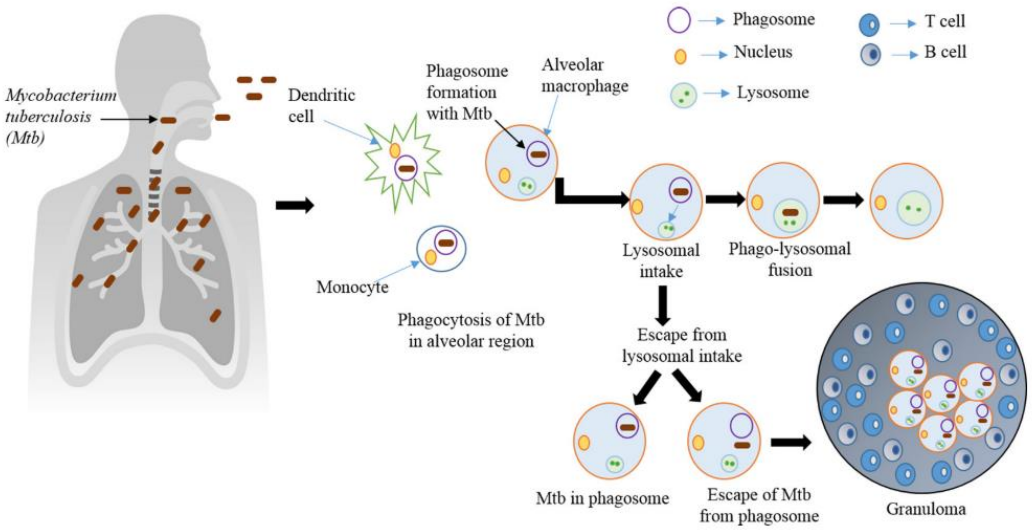

Figure 1.3. Infection mechanism of Mycobacterium tuberculosis.[38]

The resistance of the individual to the intracellular pathogens in the initial phase of tuberculosis infection is due to the action of M1 macrophages.[25,39] However, as mentioned above, macrophages have the ability to switch between M1 and M2 phenotypes. In order to avoid excessive inflammation, which could cause more damage than the infection itself due to the expression of high levels of pro-inflammatory mediators, macrophages polarise towards the M2 phenotype.[25,31] This shift of phenotype is observed during the transition from acute to chronic infection, where macrophages produce anti-inflammatory cytokines.[25]

According to the WHO, around 1.7 billion people worldwide are infected with *M. tuberculosis*, but only 5-10% of the cases will evolve to the active form of the disease during their lifetime.[40,41] Depending on the host immunity and the existence of comorbidities, the pathogen elimination/contention can occur, either in the sequence of innate immune responses (local and systemic) or because of acquired T cell immunity.[22,42] So, when the immune system is debilitated, the granuloma cannot contain the bacteria, which will replicate and disseminate from the granuloma and re-infect the lungs or spread to other organs through the bloodstream. Approximately 80% of active tuberculosis cases are pulmonary, where the lung parenchyma or the tracheobronchial area are affected.

Extrapulmonary tuberculosis can occur in many other organs as the pleura, lymph nodes, abdomen, genitourinary tract, skin, joints and bones. The infected person becomes symptomatic (fever, fatigue, lack of appetite, weight loss, persistent cough, and haemoptysis), bearing the so called active tuberculosis, with the consequent ability to transmit the infection to other people.[38]

1.1.3. Conventional treatment of tuberculosis

The first effective treatments of tuberculosis were developed in the 1940s, starting with streptomycin.[43] In the current clinical approach, the conventional treatment of tuberculosis is based on the daily intake of a combination of several first-line drugs for a period of at least 6 months.[40] In the first two months of therapy, the patients receive daily four first-line antitubercular drugs (isoniazid (INH), RIF, ethambutol and pyrazinamide). In the following four months, two or three of the drugs are maintained (INH and RIF, ethambutol is added if a third drug is to be used), being administered three times a week to eliminate the remaining bacillus and prevent a possible relapse.[6,44] If six months are not enough, the treatment of tuberculosis can be extended up to nine or twelve months, although occasionally periods up to 2 years are necessary.[45]

1.1.3.1. Multidrug-resistant tuberculosis treatment

In 2017, the WHO estimated that the treatment success rate was around 85% for cases of drug-susceptible tuberculosis. However, the emergence of MDR-TB decreased the success rate treatment to 56%, according to the last data.[40] MDR-TB appears when the patient develops resistance to at least the first-line antitubercular drugs INH and RIF,[46] the two most potent drugs, often due to issues related with adherence to the treatment, because it implies the administration of several drugs for a long period of time.[23] *M. tuberculosis* develops resistance to INH in the sequence of defective bacterial catalase enzyme responsible to convert the prodrug into the active INH, while in RIF resistance, genetic mutations in the bacterial RNA polymerase elude the action of the drug.[22]

In cases of drug resistance, the treatment regimen must be changed.[23] The recommended treatment to MDR-TB is a combination of at least four second- or third-line antitubercular drugs, which are chosen according to their efficacy, safety and cost. Examples of these are para-amino salicylic acid, cycloserine, ethionamide/prothionamide, amikacin, kanamycin, or capreomycin (second-line antitubercular drugs) and clofazimine, linezolid, amoxicillin/clavulanate, imipenem/cilastatin and clarithromycin (third-line antitubercular drugs). Moreover, the duration of MDR-TB treatment is more prolonged than that of the standard treatment, and may reach twenty or twenty-eight months, depending on the patient history.[38,47] Besides the emergence of MDR-TB worldwide, the development of extensively drug-resistant tuberculosis (XDR-TB) is exacerbating the problem of resistance to antitubercular drugs. In this category, apart from resistance to INH and RIF, there is also resistance to a fluoroquinolone and one of the three second-line injectables: amikacin, kanamycin, or capreomycin.[46] Moreover, although the definition is not yet recognised by WHO, reports on totally drug-resistant tuberculosis are starting to appear in the literature, referring to bacterial strains that are resistant to all the first- and second-line antitubercular drugs. These more severe forms of resistance require more intense and prolonged treatment than that required in MDR-TB, using more toxic, expensive and less effective drugs.[6]

In the work presented herein, the first-line antitubercular drugs INH and rifabutin (RFB) were selected as model drugs for the pharmaceutical formulations to be developed. Their selection was mainly due to different chemical properties (molecular weight, for instance) and mechanisms of action. Their specific characteristics are detailed below.

1.1.3.2. Isoniazid

Since 1950s, INH has been assuming the status of first-line drug in the treatment of latent and active tuberculosis .[38,48] INH has a high bactericidal activity, but only acts on dividing bacteria. The molecule is in fact a prodrug, as INH is then activated by catalase-peroxidase, an enzyme encoded by *M. tuberculosis* katG gene. The nicotinamide adenine dinucleotide (NADH)-INH complex resultant

from the enzyme action, induces the inhibition of cell wall mycolic acid biosynthesis by binding to the NADH-dependent enoyl acyl carrier protein reductase (InhA). The absence of mycolic acid, which is essential for the survival of the bacteria, results in its death.[2,49,50] Furthermore, INH affects the DNA, lipids, carbohydrates and NAD metabolism.[2] The resistance to INH only (INH-monoresistant tuberculosis) is the most common form of tuberculosis drug resistance,[51] which mechanism is mainly attributed to mutation of katG (60-70% of cases), InhA, ahpC and kasA genes.[49,50]

Physically, INH is a white odourless powder, easily soluble in water (140 mg/mL).[52] Its chemical structure is depicted in Figure 1.4, corresponding to a molecular weight of 137.14 g/mol.[53]

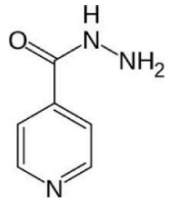

Figure 1.4. Chemical structure of isoniazid.[2]

1.1.3.3. Rifabutin

RFB is a spiro-piperidyl-rifamycin and is used in active tuberculosis treatment, being part of the group of first-line antitubercular drugs.[38,54] Discovered in 1980,[55] it received approval by the Food and Drug Administration (FDA) for the treatment of tuberculosis infection in 1992. It was widely used during the second and third decades of HIV pandemic, replacing RIF in patients co-infected with HIV, because it allows safer co-administration with protease inhibitors.[56] However, despite the efficacy of RFB is similar or higher than other antitubercular drugs, its high cost make it a second choice to treat tuberculosis.[55] As a member of the family of rifamycins, RFB mechanism of action relies on the inhibition of transcription and protein synthesis by binding to β subunit of the procaryotic DNA-dependent RNA polymerase, encoded by the *rpo*B gene. Resistance to RFB has been reported to be related with mutations of this gene found at codons 531, 526 and 513.[54]

RFB is a red-violet powder, and the molecule has very low solubility in water (0.19 mg/mL). Its molecular weight is 847.02 g/mol, corresponding to the chemical structure displayed in Figure 1.5.[57]

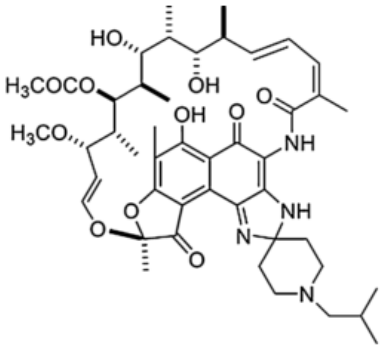

Figure 1.5. Chemical structure of rifabutin.[55]

The exposed above evidences that, despite the existence of potentially efficacious therapy of tuberculosis, there are still limitations in the treatment of the disease. Despite 80% of the cases are of pulmonary tuberculosis,[58] current therapy is mainly delivered through the oral route, requiring prolonged treatments with high doses of several antibiotics. This is the needed to have enough drug reaching the lung, where the bacteria mainly accumulate. In parallel, therapeutic incompliance, inappropriate or incorrect use of antitubercular drugs and the use of poor-quality medicines lead to rising numbers of resistance to drugs.[59] To address the issues induced by the duration of conventional tuberculosis therapy and the emergence of resistance to the antibiotics, the direct delivery of antitubercular drugs to the lungs, through inhalation, may be proposed as a viable therapeutic alternative, particularly in the cases of pulmonary tuberculosis.[60] The following sections will explore the essential aspects of such an approach.

1.2. Pulmonary delivery of drugs

The use of inhalation in therapeutic approaches is dated from 1554 BC, when the Egyptian physicists used hot vapor from the back henbane to treat patients with breathing problems.[61] Since then, the delivery of drugs to the lungs to treat respiratory diseases has been receiving the attention of clinicians and

researchers. Nowadays, pulmonary drug delivery represents a privileged choice to treat some respiratory diseases, such as asthma, chronic obstructive pulmonary disease (COPD) and cystic fibrosis. Occasionally, this delivery route has also been explored for the systemic delivery of drugs in the context diabetes, osteoporosis and pain. The good permeability, attributable to a 0.2 μm-thick epithelial cell monolayer in the alveoli, and high blood perfusion makes the organ attractive for systemic drug delivery.[62–64] Moreover, the bioavailability of drugs may benefit from the avoidance of hepatic first-pass effect.[63] When local delivery is focused, the direct delivery of drugs to the lung may provide increased local drug concentrations, while reducing the eventual systemic side effects induced by conventional administration routes. Furthermore, increasing the drug concentration in the lungs provides the possibility to reduce dosing frequency and consequent duration of the treatments, usual in some respiratory diseases.[65] Finally, in certain diseases, the proper lung cells could work as specific drug targets, when the infectious agent is an intracellular pathogen or in cases of lung cancer, for instance. The former is the case of tuberculosis, where alveolar macrophages host *M. tuberculosis* and, thus, the antitubercular drugs can directly target these cells.[66]

Drugs can be delivered to or through the lung under the form of a liquid (solution, suspension) or a dry powder. In any case, the use of an inhaler device is required. The existing devices are divided in four categories, namely nebulizers, pressurized metered-dose inhalers, dry powder inhalers (DPIs) and, more recently, soft mist inhalers.[67–69] DPIs accommodate the drugs under the form of dry powders and are currently the most used device.[64,70] They are considered the most promising device among the inhalers, because of the environmental- and patient-friendly characteristics and also because powders provide increased chemical stability.[64,68] DPIs were essentially introduced to overcome the problems with coordination of inhaler actuation and inspiration, but also to comply with safety environmental requirements.[69] However, in order to ensure powder deaggregation and maximize the emitted doses (ED) from the inhaler device, the patient must provide a considerable inhalation airflow rate, which is one of the greatest issues regarding to the mishandling of DPIs.[64,69] Besides that, the development of a dry powder formulation is more demanding in order to obtain a

suitable formulation to be delivered through a DPI and to endow the required aerodynamic properties.[68]

For several decades antibiotics have been delivered as liquid aerosols to treat lung diseases.[62] Examples of this are colistin and tobramycin, which are now already on the market as inhalable dry powders for an application in the treatment of infections associated to cystic fibrosis. In parallel, other antibiotics used in the treatment of diseases such as tuberculosis and bronchiectasis are being explored (amikacin, kanamycin, gentamycin and INH, amongst others).[66] However, there are several limitations inherent to the development of lung drug delivery formulations. The major challenge is to engineer delivery systems and drug particles that reach the desired region of the lung. Additionally, pulmonary pharmacokinetics are not linear, as happens during drug administration via other routes, mainly due to the complex architecture of the lungs,[62,64] which comprises many and subsequent bifurcations, as observed in Figure 1.6..

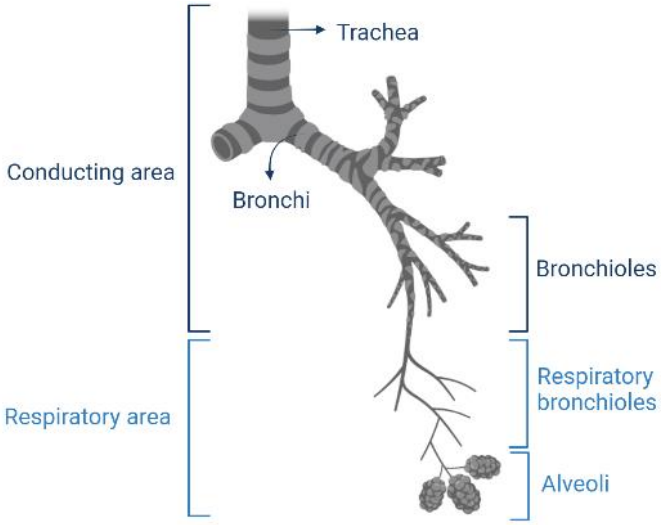

Figure 1.6. Structure of the respiratory tree detailing the conducting and respiratory areas of the respiratory system. Created in BioRender.com.

Indeed, after inhalation drug particles must travel through the respiratory tree until deposition occurs. This will happen in the mouth-throat area, conducting airways and/or the respiratory zone (Figure 1.6), which includes the alveolar space, in dependence of the particles' aerodynamic diameter. The total fraction of particles deposited in the lungs is called "lung dose". As shown in Figure 1.7, the particles with aerodynamic diameters higher than 5 µm mainly deposit in the mouth-throat

area and the central proximal airways by inertial impaction. Smaller particles, with aerodynamic diameters between 0.5 and 5 µm, deposit in the small peripheral airways by sedimentation or can reach the alveolar space and deposit by diffusion. If the particles have an aerodynamic diameter lower than 0.5 µm, deposition is hampered and exhalation will occur.[62,63]

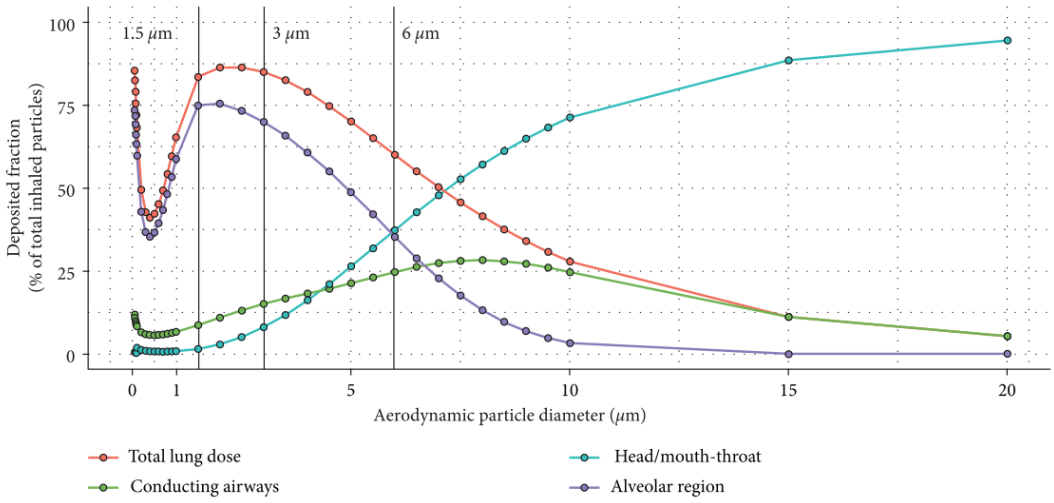

Figure 1.7. Particle size-dependent deposition stratified by respiratory tract region.[62]

Particle deposition is determinant for the success of inhalable therapies developed to treat local or systemic diseases, but other factors also influence the results. Depending on the deposition site, the particles are exposed to different clearance mechanisms that evolved to maintain the lung surface clear from potential contaminants. In this context, inhaled particles are mechanically eliminated by coughing, sneezing or swallowing when deposited in the upper region of the respiratory tract. In the tracheobronchial region, the mucociliary escalator, one of the primary innate defences of the upper respiratory tract, will remove particles produced from slowly dissolving or insoluble materials within 24 h.[61,71] This mechanism consists of goblet (mucus-producing) cells and ciliated cells covered with airway surface liquid (ASL). The mucus layer present in the ASL is responsible to entrap inhaled particles that deposit over it, which are propelled out of the trachea along with the mucus by coughing or swallowing.[72] On the other hand, particles managing to evade these mechanisms and reaching the alveolar zone will find another mechanism of defence, comprised by the

alveolar macrophages, which ensure their phagocytosis in a short time (from a few min to 1-2 h, typically). In conventional approaches where drug release to the mucosal area is expected, this reduces the amount of drug available and limits the efficacy of the treatment. However, the uptake of drugs by the alveolar macrophages, impelled by their clearance role, may be explored with great benefits in the treatment of intracellular diseases and, particularly, in the case of tuberculosis, where the intracellular pathogen *M. tuberculosis* accumulates inside these cells.[61]

With regards to drug particles expected to undergo systemic absorption, the site of deposition of inhaled particles, along with the drug nature, will also influence drug pharmacokinetics. The bronchi have an epithelium of 64 μm thickness covered by a mucus layer, conditions that do not favour drug absorption, as it would occur at a very slow rate which does not suffice to clearance mechanisms. In the bronchioles the epithelium thickness reduces to 13 μm and mucus is replaced by a lining fluid, thus providing the conditions for intermediate absorption. Finally, the alveoli display an extremely thin epithelium of 0.1-0.2 μm thickness bathed by thin layer of lining fluid, which may permit fast absorption. Along with the existence of a dense capillary net in the alveolar zone, these characteristics justify why systemic absorption substantially occurs in the alveolar region, being considered negligible in other sites. As in other epithelia, lipophilic drugs are rapidly absorbed by passive transcellular diffusion, while hydrophilic drugs are more prone to undergo paracellular diffusion across the epithelium through aqueous pores in intercellular gap junctions. Nevertheless, absorption will also be affected by the molecular weight of drug molecules.[61,62]

1.2.1. Pulmonary drug delivery systems

Since the bioavailability of the drugs in the lung is critical for the success of the therapy of pulmonary diseases, and given all the limitations and considerations exposed above, it becomes clear that successful lung delivery is inherently related with suitable engineering of drug carriers. Particulate-based drug delivery systems are considered a suitable approach to carry the drugs and increase their concentration in the lung. Particulates may be tailored to exhibit adequate

aerodynamic properties and avoid to some extent the existing clearance mechanisms, enabling a deposition in the desired place.[72] Moreover, particulates may be produced under the form of dry powders, the said microparticles, which ensures higher stability than liquid counterparts, as mentioned before. The carrier may naturally provide some protection to the encapsulated drug and enable drug targeting, depending on its composition and engineering.[72,73] Any carrier developed to deliver drugs in the lung must be biocompatible, biodegradable and non-immunogenic in the specific conditions of the administration route. It is also important that both drug and formulation exhibit high stability and that the applied production method facilitates scaling up. Moreover, there must be an adequate affinity with the selected inhaler device, so that respirability parameters can be maximised and adequate for the therapeutic end.[73] Finally, the surface properties of the carrier can influence the drug absorption, degradation, and uptake or evasion of the pulmonary clearance mechanisms, modifying the inhalable drug half-life in the lungs.[72]

Several types of carriers have been studied for pulmonary drug delivery in order to optimise the drug loading, drug release, residence time, toxicity and, at the same time, evade the lung clearance mechanisms, enzymatic degradation and rapid systemic absorption when this is not desired. Liposomes, microparticles, nanoparticles and micelles are examples of pulmonary drug delivery systems explored for the treatment of different diseases, including respiratory diseases.[72] Amongst the different carriers, microparticles defined as matrix-type particles with sizes above 1 μm, in the micrometric range, are those easily permitting tailoring of aerodynamic characteristics to allow drug deposition in the desired region, further providing protection of the drug from degradation.[74] Overall, microparticles have several advantages regarding to their use in this area. Two major aspects must be highlighted in this context: on one side, the microparticles may comprise the final drug carrier that can be delivered as dry powder, with the consequent improvement of the formulation stability comparing with liquid counterparts; on the other side, the aerodynamic properties of microparticles can be tailored to endow the carriers with the ability to deposit in the desired site of the lung.[72,73] After their deposition in the lungs, the microparticles will act locally, since their size does not permit traversing the interstitium, thus not reaching the systemic

circulation, which is an advantage of the microparticles over nanoparticles when local delivery is intended.[75] Another advantage of microparticles over nanoparticles is related with their production. While microparticles can be produced by a single step, while simultaneously allowing achieve the aerodynamic tailoring, the production of suitable nanoparticles for pulmonary drug delivery always involves extra processing.[76] Several approaches to endow nanoparticles with the suitable characteristics for lung delivery have been reported in literature, and the encapsulation of drug-loaded nanoparticles in microparticles, known as “Trojan” particles, has been explored in many works.[72] Grenha *et al*.[77] microencapsulated chitosan/tripolyphosphate nanoparticles by spray-drying, in order to produce adequate particles to deliver proteins in the lungs. Also, Tomoda *et al*.[78] produced inhalable RIF-loaded PLGA nanoparticles microencapsulated in trehalose and lactose microparticles.

The use of microparticles is also highly beneficial in drug targeting strategies in the context of infectious intracellular diseases as tuberculosis. Microparticles with an aerodynamic diameter between 0.5 and 5 µm very likely reach the alveoli upon inhalation and may be phagocytosed by the alveolar macrophages, increasing the drug concentration in the cells infected by *M. tuberculosis*.[2] Furthermore, the microencapsulation allows higher drug loading due to the size of the particles, which also increase the amount of drugs in the desired area.[74]

1.2.1.1. Polymeric microparticles

The literature reports the possibility to use many different materials to produce microparticulate carriers, from polymers to lipids and inorganic materials. However, polymeric-based microparticles are of the most described in the field of lung delivery, being explored for various applications, including the treatment of several pulmonary disorders such as asthma, COPD and infectious diseases.[2] Polymeric-based microparticles share the referred characteristics previously described for microparticles in general. However, their specific composition will necessarily affect the interaction with cellular structures. For instance, the presence of lipids on the surface of the carriers is reported to prevent their recognition and phagocytosis by macrophages.[73] On the other hand, if the

particle surface is composed of a material with high affinity for macrophages, which can be mediated by the surface receptors, the opposite will probably be observed, with a consequent potentiation of particle uptake by the macrophages.[6]

Over the years, many polymers have been explored to compose the matrix of carriers with application in lung drug delivery, regardless of their natural or synthetic origin. Some of the most reported are albumin, chitosan, gelatin and hyaluronic acid, which are of natural origin, along with poly(lactic acid), poly(vinyl alcohol) (PVA) and acrylic acid derivatives, which pertain to the category of synthetic polymers.[79] Despite some polymers are already approved by the FDA for systemic delivery, owing to the evidenced biocompatible and biodegradable character, the use of these materials in pulmonary drug delivery is, so far, limited to the experimental research. The potential lung toxicity of the polymers after inhalation and the issues related with biodegradability raise safety concerns that have been preventing their use in this area. An example is the case of poly(lactic-co-glycolic acid) PLGA, a copolymer. Its degradation could take weeks to months and the resultant accumulation of lactic and glycolic acid could lead to a significant reduction in the microenvironmental pH, which would be deleterious to the lung function.[6,79]

Amongst the polymers, polysaccharides are the most abundant and naturally available, and they have gained attention due to the general observation of properties that include biocompatibility, biodegradability and low immunogenicity.[80] These molecules are composed by repeated mono- or disaccharide units linked by enzyme-susceptible glycosidic bounds, and are usually extracted from plants (e.g. cellulose, pectin), animals (e.g. chitosan, chondroitin), microbes (e.g. xanthan gum, pullulan, dextran) and algae (e.g. alginate).[80,81] Their intrinsic characteristics, at physicochemical and biological level, have been explored for an application in the delivery of drugs. They are able to afford targeting mechanisms to specific enzymatic degradation, specific cell receptors, environmental trigging, mucosal adhesion and transportation.[81] Chitosan,[82,83] locust bean gum,[84,85] fucoidan[86,87] and chondroitin sulphate[88,89] are some examples of polysaccharides that have been studied as components of lung drug delivery systems.

1.2.2. Macrophages as therapeutic targets

Phagocytosis is a dynamic process to eliminate microbes, apoptotic cells, and other foreign particles/materials, having macrophages as its main players.[90,91] Macrophages are phagocytic targets; the interaction between a ligand and the phagocytic receptor on the macrophage surface induces a coordinated intracellular signalling cascade that leads to phagocytosis or the decision to ignore the substance.[92] The macrophage surface receptors have different degrees of ligand specificity, and can be classified according to the type of ligands they recognise.[93] These can be categorised in three main groups: non-opsonic receptors, opsonic receptors and Toll-like receptors (TLR; Figure 1.8).[29] While the non-opsonic receptors (e.g., C-type lectin and scavenger receptors) can directly recognise molecular groups on the phagocytic targets, the opsonic receptors (e.g., complement receptors and Fc receptors) recognise soluble molecules (antibodies, complement, fibronectin, etc), named as opsonins, which bind to the foreign particles and target them for ingestion.[93–95] The third category of macrophage receptors are the TLR. These receptors are located both in the cell membrane and within vacuoles, but do not mediate phagocytosis. TLR are detectors/sensors of foreign particles playing a role in the recognition of intracellular pathogens, such as bacteria, fungi and viruses.[29,94,95] Sometimes, the TLR collaborate with other non-opsonic receptors to stimulate the ingestion of foreign particles.[94]

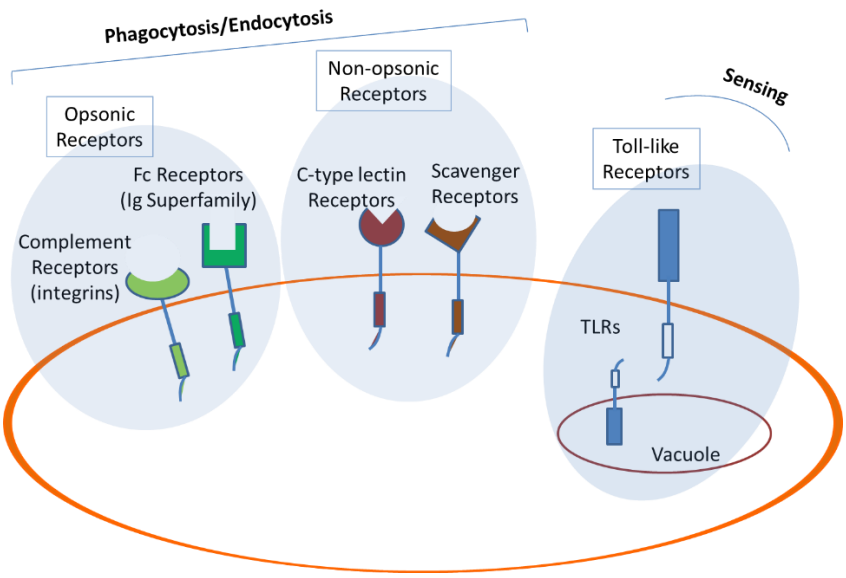

Figure 1.8. Macrophage receptors. The surface receptors can be divided in three main categories: opsonic receptors (e.g., complement receptors and Fc receptors), non-opsonic receptors (e.g., C-type lectin and scavenger receptors) and Toll-like receptors (TLRs). Adapted from Rodrigues *et al.*, 2015.[29]

The literature reports several therapeutic approaches that take benefit from the natural phagocytic ability of macrophages. Their affinity for specific ligands, mediated by the interaction with the surface receptors detailed above, permits exploring these cells as therapeutic targets and benefiting from the consequent signalling pathways.[92] The macrophage receptors are optimal structures for targeted therapies, since these reflect the physiological function of these cells (M1 or M2 phenotypes) and are used for pathogen internalisation.[29] One of the receptors most frequently used for drug targeting approaches is the mannose receptor, from the C-type lectin family, which is highly expressed on macrophage surface, including alveolar macrophages. This receptor has high affinity for mannose residues and, therefore, mannosylated carriers have been extensively proposed for the treatment of several respiratory diseases.[96,97] Indeed, the literature makes available many works concluding on the superior affinity of alveolar macrophages for mannosylated carriers comparing to non-mannosylated carriers.[98] Su *et al.*, synthetised a mannose-modified polymer-augmented liposome to enhance the delivery of streptomycin in the cytosol of the alveolar macrophages for the treatment of intracellular infections.[99] Similary,

Maretti *et al*. used mannosylated derivatives to decorate the surface of solid lipid nanoparticles loaded with RIF in the therapy of tuberculosis.[98]

In fact, tuberculosis therapy is one of the main topics where the strategy of targeting alveolar macrophages, the hosts of *M. tuberculosis,* has been strongly explored for the delivery of antitubercular drugs. This rational typically involves the possibility to decrease the dose and duration of the treatment, through the co-localization of drug and infectious agent, aiming at improving the patient compliance.[29,30] In order to explore this strategy to treat tuberculosis, the previously mentioned polymeric microparticles could be suitable carriers to deliver antitubercular drugs in the alveolar zone, facilitating subsequent uptake by the local macrophages. In fact, considering that the geometric size and shape of the carriers affect the alveolar macrophage uptake,[100] with spherical particles with sizes between 1 and 3 µm showing more favourable interaction,[72,101,102] microparticles could be tailored to meet these requisites.

1.3. Konjac glucomannan

Konjac glucomannan (KGM) is extracted from *Amorphophallus konjac*, a plant that mainly grows in subtropical regions of South East of Asia.[7,103] This plant has been explored in traditional Chinese medicine for a long time as an immunoregulator and also in healthcare food. A gel prepared from purified konjac flour has been used for detoxification, tumour-suppression, blood stasis alleviation and phlegm liquefaction for more than 2 000 years. The indigenous people of China have consumed this gel in order to treat asthma, cough, hernia, breast pain, burns, as well as haematological and skin disorders.[104]

KGM is a polysaccharide found in the roots and tubers of the *A. konjac* plant and has been receiving increased attention in the last decades. In 1997, it received from the FDA the status of generally recognised as safe (GRAS), being used as food additive. Its use has, however, been extended to other fields. Nowadays, KGM is widely used in nutraceutical and biological industry, due to its renewable, inexpensive, biodegradable and biocompatible properties.[104–107] The improvement of glucose metabolism, regulation of lipid metabolism, promotion of

intestinal activity and cholesterol reduction are some examples of the effect of KGM in healthcare.[103] Moreover, the application of KGM as part of drug delivery systems has attracted attention. One of the reasons for applications proposed in this field relies on its ability to provide the controlled release of molecules,[104] which has been shown with hormones and other macromolecules, as dextran, insulin and bovine serum albumin.[108] Similarly to other natural gums, KGM swells upon contact with water, forming a gel before dissolution. Drugs associated to KGM-based systems need to diffuse through this gel layer before being released, which explains the sustained release effect frequently associated with the material.[109] Furthermore, KGM has been explored in targeted delivery,[104] mainly as an oral colon targeted delivery system. In the gastrointestinal tract, KGM is only degraded by the enzymes present on normal colonic flora, not undergoing digestion by those produced in the upper gastrointestinal tract.[7] Therefore, the delivery of drugs targeted to the colon into hydrogels, nanoparticles or capsules based on KGM has been successfully reported in some studies over the recent years.[8,110–112]

Structurally, KGM is composed by D-mannose and D-glucose units linked by β-1,4 glycosidic bonds, in a molar ratio of mannose:glucose of 1.6:1 or 1.4:1, varying according to the plant genotypes. An acetyl group is present on KGM backbone structure attached to the C-6 position at approximately every 19 sugar residues, and some short side chains of 11-16 monosaccharides (glucose) occur at intervals of 50-60 units of the main chain linking to mannose units by joint C-3 (Figure 1.9).[7,106,113,114] The molecular weight of KGM ranges from 500 to 2 000 kDa, depending on the plant source and extraction procedure.[7,103,105,106]

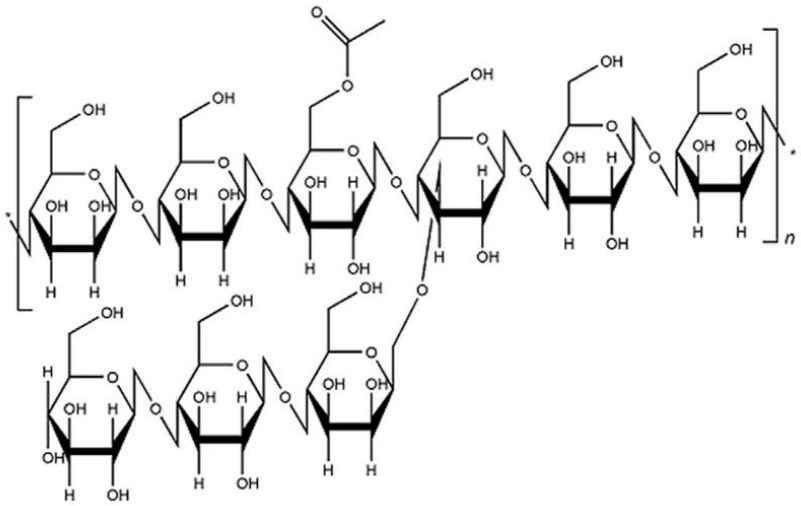

Figure 1.9. Chemical structure of KGM.[115]

Furthermore, despite yielding solutions of high viscosity, KGM is a water-soluble polysaccharide due to the presence of hydroxyl and carbonyl groups on its structure. The reported water absorption capacity of KGM is 105.4 g/g. The polymer is also known to be sensitive to high temperatures (250-350 ºC) and to the action of enzymes, such as β-D-glucanase and β-D-mannanase.[107,114] The latter group of enzymes includes the β-mannosidase, which is relevant in the present work, since its existence has been identified in the lung.[116]

1.4. Spray-drying

The production of a dry powder for inhalation with suitable characteristics for the defined therapeutic end is a challenge. As mentioned before, therapeutic success largely depends on the properties of drug particles and their ability to reach the desirable areas of the lung. Particle engineering has, thus, become a widely used process to maximise therapeutic results. Over the years, researchers have studied several techniques, such as milling, freeze-drying, spray-drying, spray-freeze-drying, and supercritical fluid-drying, to obtain particles with the ideal characteristics. Among all these techniques, spray-drying is one of the most used by the pharmaceutical industry.[117] This process was developed in 1860 and the first application reported in the pharmaceutical field was to dry medicated extracts

obtained naturally. Currently, spray-drying is frequently used to produce inhalable dry powders, allowing the engineering of carriers to encapsulate hydrophilic and hydrophobic active compounds.[117–119]

The process of spray-drying is characterised by the conversion of a solution, suspension or emulsion into a dry powder in a single step. The spray-dryer equipment produces a liquid spray in the presence of high-temperature gas stream. This results in the evaporation of the solvent in the drying chamber and the drying of the fine droplets, converting them into particles. The latter are then separated from the gas stream in a cyclonic separator, and collected in the end of the process (Figure 1.10).[117,120]

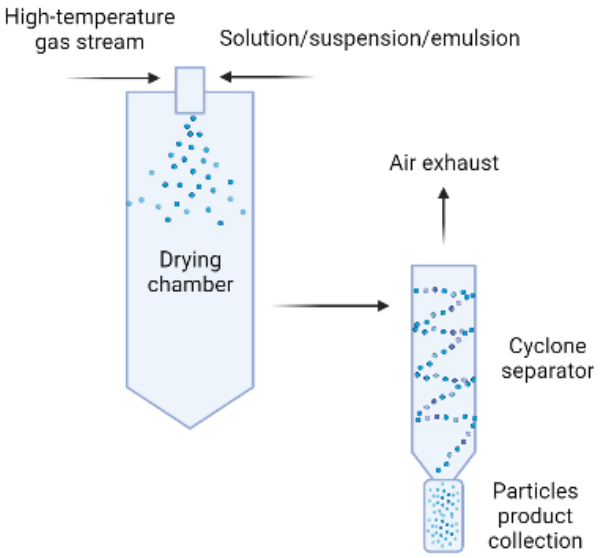

Figure 1.10. Schematic diagram of spray-drying process. Created in BioRender.com.

The wide application of spray-drying to produce inhalable dry powders, consistently implemented in industry, is due to the high flexibility of this technique. In fact, it is possible to vary several parameters of the process, which include solid content of the spraying dispersion, solvent type, and instrumental conditions (dispersion feed rate, inlet temperature, gas supply and use of different types of nozzles), with defined and predictable impact on particle properties. This permits tailoring the particles to exhibit the required characteristics for the determined application, including particle size and size distribution, morphology, moisture

content, etc. Usually, particles obtained by spray-drying exhibit homogeneous appearance regarding to the morphology.[117] Moreover, due to the short time of heat exposure (seconds or milliseconds) and the fast drying process, most of spray-dried molecules maintain their physical and chemical properties, including cases of heat-sensitive molecules, such as formulations of therapeutic peptides and proteins.[117,119,121] All the evidenced flexibility and the simplicity of the process, make it very useful in the field of dry powder production for inhalation purposes.

CHAPTER 2 – MOTIVATION AND OBJETIVES

This page was intentionally left in blank

2. Motivation and objectives

Tuberculosis is one of the main infectious diseases worldwide. According to WHO, around 10 million new cases of tuberculosis are reported every year and more than 1 million people die with this disease in that period.[1] Despite the decrease of the number of cases over the last years, the emergence of resistance to the antibiotics used in the treatment of tuberculosis has been concerning public health authorities. Conventional treatment of the disease involves the oral intake of different antibiotics for a long period of time. The prolonged treatment is considered a strong limitation, as the poor patient adherence to the treatment regimen is one of the reasons for therapeutic failure and also for the development of resistance to the antitubercular drugs.[38,122] The need for alternative therapeutic strategies to address the problems arising from conventional therapy has been being identified. Taking into account that 80% of the total cases of this disease correspond to pulmonary tuberculosis,[58] the direct delivery of the drugs to the lung, targeted to the alveolar macrophages that are the host cells of *M. tuberculosis*, could be a promising approach to treat pulmonary tuberculosis.[6,123] Such an approach could reduce the treatment duration by increasing the local dose and decreasing the frequency of drug administration.[6,23] Its success, however, is limited by the defence mechanisms of the lung,[124,125] thus requiring the development of suitable drug carriers that permit circumventing the inherent limitations.

The production of drug carriers involves the use of excipients, which is currently a hot topic in lung drug delivery. Indeed, despite many materials have been explored for an application in the field over recent years, only a few are currently approved for inhalation purposes. The discovery and approval of new materials, with improved functionality, has become imperative to widen the therapeutic opportunities.[126,127] Among the excipients that have been studied, polysaccharides comprise a popular class, mainly owing to advantages related with the higher propensity to exhibit biodegradability and biocompatibility but, in occasions, also because of their composition. In this regard, the specific composition of some polysaccharides has been explored as a means to improve the interaction of the materials and corresponding carriers with cell surface

receptors. These features provide opportunities to explore carrier composition in targeted drug delivery applications. KGM is a polysaccharide composed by mannose units,[7] which may undergo specific recognition by the mannose receptors located on the surface of macrophages.[104,128,129] Alveolar macrophages exhibit such receptors and play a very relevant role as hosts of infectious bacteria responsible for the development of diseases such as tuberculosis.[29] The favourable interaction of KGM with the surface receptors of alveolar macrophages may potentiate the internalisation of drug carriers composed by the polymer and, thus, provide the means for a more effective therapy. In parallel, adequate production techniques must be employed to obtain the carriers with high reproducibility, further endowing them with the required properties to ensure high lung deposition.[127]

Drug-loaded KGM microparticles were developed in a previous work. Guerreiro *et al*. [130] successfully incorporated INH and RFB in KGM microparticles by spray-drying. At that time, the calculation of theoretical aerodynamic parameters suggested that the produced microparticles had the suitable characteristics to reach the alveolar region. This has set the basis for the rational of the work presented in this PhD thesis, which is schematically presented in Figure 2.1.

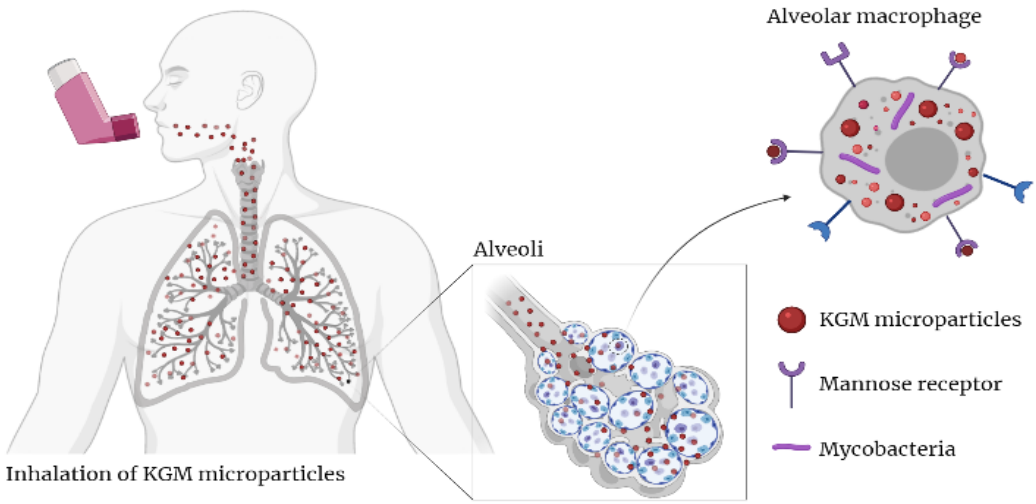

Figure 2.1. Illustration of konjac glucomannan (KGM) microparticles targeted to alveolar macrophages infected with *M. tuberculosis*. The presence of mannose units on KGM microparticles is expected to mediate recognition by mannose receptors on macrophage surface, potentiating the internalisation of microparticles and providing co-localisation with infecting bacteria. Created in BioRender.com.

Considering the motivations described above, the project underlying this PhD thesis proposed exploring further on KGM microparticles properties, in order to better analyse their potential for an application in pulmonary drug delivery aimed at the treatment of lung tuberculosis. The main objective of the project was to evaluate the use of antitubercular drug-loaded KGM microparticles as an inhalable tuberculosis therapy. The rational is mainly driven by the high mannose content of KGM, which is expected to improve the targeting ability of INH/RFB-loaded KGM microparticles towards the alveolar macrophages, thus providing the means for the co-localisation of the drugs and the pathogenic agents. For a successful approach, it was established that microparticles should meet several requirements: 1) adequate aerodynamic diameter to reach the alveoli, where alveolar macrophages are located (1-3 µm); 2) ability for macrophage targeting, including size of 1-3 µm and composition providing improved uptake; 3) absence of toxicity; 4) demonstrated antibacterial activity. In order to accomplish the main objective and meet the requirements, several partial objectives were pursued:

- To determine the aerodynamic properties of drug-loaded KGM microparticles and establish their potential to reach the alveolar region where the macrophages hosting the bacteria reside;
- To characterise the profile of drug release and evaluate the biodegradation of KGM microparticles in a medium resembling the lung environment;
- To evaluate the effect of spray-drying process on the antibacterial activity of isoniazid and rifabutin;
- To analyse the antibacterial activity of drug-loaded KGM microparticles upon bacterial infection of macrophage-like cells and study the emergence of an eventual resistance of the bacteria upon continued exposure to the formulation;
- To evaluate *in vitro* the toxicological profile of drug-loaded KGM microparticles in cell lines representative of the respiratory environment (alveolar epithelium and macrophages);
- To evaluate the interaction between KGM microparticles and macrophages through the activation of macrophage-like cells and their ability to internalise KGM microparticles;

- To evaluate *in vivo* parameters of safety upon inhalation of KGM microparticles, focusing on allergic and inflammatory biomarkers.

After all, it is expected to verify the ability of KGM microparticles as inhalable antitubercular drug carriers targeted to the alveolar zone and, specifically, to the macrophages, presenting a favourable bactericidal profile without inherent toxicity. This would comprise an effective alternative therapy with potentially decreased side effects and improved patient compliance.

CHAPTER 3 - KONJAC GLUCOMANNAN AS MATRIX MATERIAL WITH APPLICATION IN THE PRODUCTION OF INHALABLE SPRAY-DRIED MICROPARTICLES

The information in this chapter was partially published in the following publication:

Filipa Guerreiro, Magda Swedrowska, Roshnee Patel, Noelia Flórez-Fernández, María Dolores Torres, Ana M. Rosa da Costa, Bem Forbes, Ana Grenha, 2021. Engineering of konjac glucomannan into respirable microparticles for delivery of antitubercular drugs. *International Journal of Pharmaceutics*, *604*, 120731.

This page was intentionally left in blank

3. Konjac glucomannan polymer as matrix material with application in the production of inhalable spray-dried microparticles

3.1. Materials and methods

3.1.1. Hydrolysis of commercial konjac glucomannan

KGM commercial polymer (Chemos, Germany) was submitted to an acid hydrolysis in order to reduce its viscosity in water. The hydrolysis was performed following the protocol described by Cheng *et al*.[131] In a two-necked round bottom flask, 7 g of commercial KGM were added to 50 mL of 96% ethanol (AGA, Portugal) under stirring to create a suspension. Then, a nitrogen purge was performed for 5 minutes to create an inert atmosphere. After 30 min of stirring, 8 mL of 37% HCl (VWR, USA) were added to the suspension and this was sonicated for 60 min at 45 kHz (ultrasonic bath; VWR, USA). Finally, the mixture was filtered under vacuum through a No. 4 fritted funnel, and washed with 70% ethanol (AGA, Portugal), until neutral pH was achieved. To assure ethanol evaporation, the hydrolysed KGM was placed overnight in a fume hood and in the next day in a vacuum oven (VD23 Vacuum Oven; Binder, Germany) at 50 ºC. While staying in the vacuum oven, the hydrolysed sample was regularly weighed and only removed when constant weight was reached (approximately after 48 h at 50 ºC). The hydrolysis yield (%) of the hydrolysis reaction was calculated by the following equation:

$$\text{Yield} = \left(\frac{\text{Initial amount of commercial KGM}}{\text{Final amount of hydrolysed KGM}}\right) \times 100$$

The hydrolysed KGM was stored in a desiccator until further use.

3.1.2. Preparation of konjac glucomannan microparticles

A dispersion of hydrolysed KGM was prepared at the concentration of 1.5% (w/v) in ultrapure water (Milli-Q Plus; Millipore Iberica, Spain), under a temperature of approximately 70 ºC. After 3 h of stirring, the KGM dispersion was spray-dried in a Buchi B-290 laboratory mini spray-dryer (Buchi Labortechnik AG, Switzerland) equipped with a high performance cyclone in order to produce unloaded KGM microparticles. The spray flow rate was set at 473 L/h, inlet temperature was 180 ºC,

aspirator was regulated at 90% and the flow rate was 0.8 mL/min. The spray-drying yield (%) of the process was calculated from the following equation:

$$\text{Yield } = \left(\frac{\text{Weight of collected KGM microparticles}}{\text{Initial weight of solids in the dispersion}}\right) \times 100$$

3.1.3. Chemical characterisation of the konjac glucomannan polymer and microparticles

3.1.3.1. HPSEC analysis

KGM (commercial and hydrolysed) and unloaded KGM microparticles were analysed by High Performance Size Exclusion Chromatography (HPSEC) with a refractive index detector (Knauer K-2300, Berlin, Germany). Two columns OHpak SB-806M HQ of 300 × 8.0 mm were used in series with a 50 × 6.0 mm OHpak SB-G 6B guard column (Shodex, Tokyo, Japan). Milli-Q water (0.02% NaN_3) was used as mobile phase at 1 mL/min. The samples were dissolved in the eluent at 1 mg/mL (commercial KGM) or 5 mg/mL (hydrolysed KGM and microparticles) and filtered through a 0.45 µm filter disk (Frilabo, Maia, Portugal). A conventional calibration curve was set using pullulan standards. Method validation was performed following the procedure described in reference.[132] The relative errors were 6% in M_w and 5% in M_n determinations.

3.1.3.2. Nuclear magnetic resonance (NMR) spectroscopy

Nuclear magnetic resonance (NMR) spectra of commercial and hydrolysed KGM were acquired in a Bruker Avance II+ spectrometer (^{1}H: 500.13 MHz; ^{13}C: 125.77 MHz) using a BBO, TXI or CP-MAS probe, at room temperature. The ^{1}H NMR spectrum of hydrolysed KGM was also acquired at 45 ºC. Samples were previously dissolved in D_2O. ^{1}H NMR spectra were referenced to the residual internal HOD (δ 4.74 ppm). Due to partial overlap of most signals, it was not possible to perform a proper integration. Signals attributed to mannose units are referred to as M, and those of glucose units denoted as G.

KGM: ^{1}H NMR (D_2O, 500 MHz, rt): δ_H 2.09 (s, OCOC<u>H</u>$_3$), 3.26 (br s, G-H2), 3.45-3.53 (m, M-H5), 3.53-3.58 (m, G-H5), 3.58-3.62 (m, G-H3 + G-H4), 3.68 (br s, M-H6), 3.72

(br s, M-H3), 3.78-3.86 (m, M-H4), 3.87-3.95 (m, G-H6), 4.02 (br s, M-H2), 4.42 (br s, G-H1). ^{1}H NMR (D_2O, 500 MHz, 45 ºC): δ_H 2.32 (s, OCOC<u>H</u>$_3$), 3.49 (br s, G-H2), 3.67-3.73 (m, M-H5), 3.74-3.80 (m, G-H5), 3.81-3.83 (m, G-H3 + G-H4), 3.91 (br s, M-H6), 3.94 (br s, M-H3), 4.02-4.05 (m, M-H4), 4.12-4.16 (m, G-H6), 4.24 (br s, M-H2), 4.64 (shoulder, G-H1), 4.88 (br s, M-H1). ^{13}C-NMR (D_2O, 125 MHz): δ_C 24.7 (OCO<u>C</u>H$_3$), 64.7 (G-C6+M-C6), 78.2 (C2+C3+C5+M-C4), 84.0 (G-C4), 105.3 (C1), 176.5 (O<u>C</u>OCH$_3$).

3.1.3.3. Fourier transform infrared (FTIR) spectroscopy

Each polymer was blended with KBr and pressed into a tablet. For each spectrum, a 32-scan interferogram was collected in transmittance mode with a 4 cm^{-1} resolution in the 4000 - 400 cm^{-1} region.

3.1.3.4. Viscosity

The viscous behaviour of commercial and hydrolysed KGM, as well as the corresponding unloaded KGM microparticles was determined in a controlled-stress rheometer (MCR 302, Paar Physica, Austria) using a sand blasted plate-plate measuring system (0.5 mm gap, 25 mm). For this purpose, aqueous dispersions at fixed polymer content (0.5 g/L) were prepared in distilled water by stirring for 30 min at room temperature. Afterwards, samples were loaded in the rheometer measuring system, the edges were covered with paraffin oil and rested for 10 min prior to testing to enable system equilibration. The apparent viscosity flow curves (up/down) were obtained at 25 ºC following a log ramp to evaluate the hysteresis. Temperature was controlled by means of a Peltier system (± 0.01). All experiments were carried out at least in triplicate.

3.1.3.5. Oligosaccharide content

KGM (commercial and hydrolysed) and unloaded KGM microparticles were analysed by high performance liquid chromatography (HPLC) to determine the oligosaccharide

composition. A preparative hydrolysis step was needed for this procedure (4% H_2SO_4, 121 °C, 20 min). Samples were dissolved and filtered through membranes (0.45 µm). Glucose and mannose oligosaccharides were used as standards. The measurements were performed on a 1100 series Hewlett-Packard chromatographer using a 300 × 7.8 mm Aminex HPX-87H column (BioRad, Hercules, CA, USA) equipped with a refractive index detector. The analysis was performed at 60 °C and the mobile phase was 0.003M H_2SO_4 (0.6 mL/min).[133] The limit of detection (LOD) was determined as 0.8776 µg/mL for glucose and 0.7446 µg/mL for mannose, while limits of quantification (LOQ) were 0.9444 µg/mL and 0.8040 µg/mL, respectively. The oligosaccharide content was analysed in duplicate.

3.1.4. Statistical analysis

The t-test and one-way analysis of variance (ANOVA) with the pairwise multiple comparison procedure (Holm-Sidak method) were performed to compare two or multiple groups, respectively. All analyses were run using the GraphPad Prism® statistical program (Version 6.01) and differences were considered to be significant at a level of $p < 0.05$.

3.2. Results and discussion

3.2.1. Preparation of konjac glucomannan microparticles

KGM is a highly viscous polymer in solution, which makes its processing with spray-drying, as a method to obtain microparticles, a very difficult task. In order to decrease the viscosity of KGM in water and enable the spray-drying of KGM dispersions, the commercial polymer was submitted to an acid hydrolysis. The process was successful, resulting in yield of 94%. The obtained hydrolysed KGM was, thus, used to produce inhalable microparticles by spray-drying. Unloaded KGM microparticles were produced with satisfactory yield (around 73%). Nevertheless, despite several attempts were endeavoured to generate dry powders suitable for inhalation, the unloaded KGM microparticles exhibited signs of agglomeration. The absence of drugs in unloaded microparticles does not permit experimental determination of aerodynamic properties,

thus macroscopic observation assuming a significant role. In any case, the chemical characterisation of the microparticles is independent of the aerodynamic properties and was performed on the obtained unladed KGM microparticles.

3.2.2. Chemical characterisation of the konjac glucomannan polymer and microparticles

The production of microparticles using KGM as matrix material involved two steps of processing, the hydrolysis of the commercial polymer and the spray-drying of the hydrolysed product. It was, thus, considered important to evaluate the effect of both events on the polymer itself. Samples of commercial KGM, hydrolysed KGM and unloaded KGM microparticles were therefore studied regarding molar mass distribution, chemical structure, oligosaccharide content and viscosity.

3.2.2.1. Size Exclusion Chromatography

HPSEC was used to determine the effect of hydrolysis on the molecular weight of commercial KGM and of spray-drying on that of hydrolysed KGM. The results are provided in Figure 3.1 and Table 3.1. Commercial KGM was found to have a molecular weight near 2 000 kDa, in line with the literature, which reports values between 200 and 2 000 kDa.[134,135] As expected, the hydrolysed polymer presented a lower molecular weight, around 700 kDa. Following hydrolysis, an increase in the polydispersity index (PDI) occurred, consistent with a non-specific hydrolysis reaction, in which polymer chains are randomly cut. Spray-drying had no significant effect on the molecular weight of the polysaccharide, as can be seen in the chromatographic profiles. The small decrease in both Mw and PDI may be related to some loss of higher molecular weight chains due to either incomplete solubilization of the polymer in the preparation of solutions for spray-drying or their retention in the filtration process.

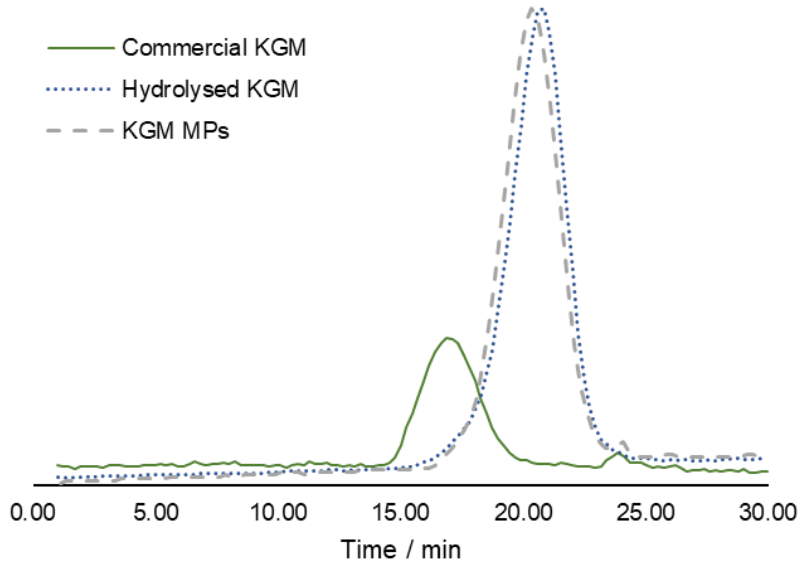

Figure 3.1. HPSEC chromatograms of commercial and hydrolysed konjac glucomannan (KGM), and unloaded KGM microparticles (MP).

Table 3.1. HPSEC analysis of commercial and hydrolysed konjac glucomannan (KGM) and unloaded KGM microparticles (MP).

Polymer	M_n (Da)*	M_w (Da)*	PDI
Commercial KGM	1 716 563	2 134 117	1.24
Hydrolysed KGM	206 787	712 413	3.45
KGM microparticles	217 241	540 644	2.49

M_n: number average molecular weight; M_w: weight average molecular weight; PDI: polydispersity index; * Relative to pullulan

3.2.2.2. Nuclear magnetic resonance (NMR) spectroscopy

The commercial and hydrolysed polymers were characterised by NMR spectroscopy. The assignment of peaks was based on reported data.[136] Due to its high viscosity in solution, the ^{1}H-NMR spectrum of commercial KGM was obtained from a very dilute solution and, therefore, presents a low resolution (Figure 3.2a). The decrease in viscosity as a consequence of hydrolysis, allowed a better resolved spectrum to be obtained for the hydrolysed polymer (Figure 3.2b). Both spectra were identical, with the signal of the acetyl protons at 2.09 ppm, the signal of the C-2 proton of glucose

units at 3.26 ppm, the C-5 protons of mannose and glucose units at 3.49 and 3.55 ppm, respectively, the glucose C-3 and C-4 protons at 3.60 ppm, the C-6 and C-3 protons of mannose units at 3.68 and 3.72 ppm, respectively, the C-4 proton of mannose at 3.81 ppm, the C-6 protons of glucose at 3.92 ppm, the C-2 proton of mannose at 4.02 ppm, and the anomeric proton of glucose units at 4.42 ppm. The signal corresponding to the anomeric proton of mannose units was masked by the peak of HOD. However, raising the temperature to 45 ºC, in order to increase the solubility of the samples, caused a downshift in all signals (Figure 3.2c), resulting in the appearance of that signal at 4.88 ppm, whilst the one of the anomeric proton of glucose appears now as a small shoulder on the solvent peak. The ^{13}C-NMR spectra (Figure 3.2d,e) were also identical, presenting a signal at 24.7 ppm attributable to the methyl carbon of acetyl groups, the signal of C-6 of glucose and mannose units at 64.7 ppm, a strong and broad signal at 78.2 ppm due to the C-2, C-3 and C-5 of glucose and mannose units and C-4 of the latter, with a shoulder 84.0 ppm due to the C-4 of glucose, a signal 105.3 ppm corresponding to the resonance of both anomeric protons, and a small signal, corresponding to the carbonyl carbon of acetyl groups, at 176.5 ppm.

These observations were as anticipated, since the breaking of some glycosidic linkages does not affect the polymer structure. Moreover, under the hydrolysis reaction conditions, the hydrolysis of the acetyl groups was not expected to occur, as this needs alkaline conditions.[136] Nevertheless, it was not possible to quantify whether this occurred to a certain extent, since none of the signals of the backbone protons was sufficiently separated to allow a proper integration.

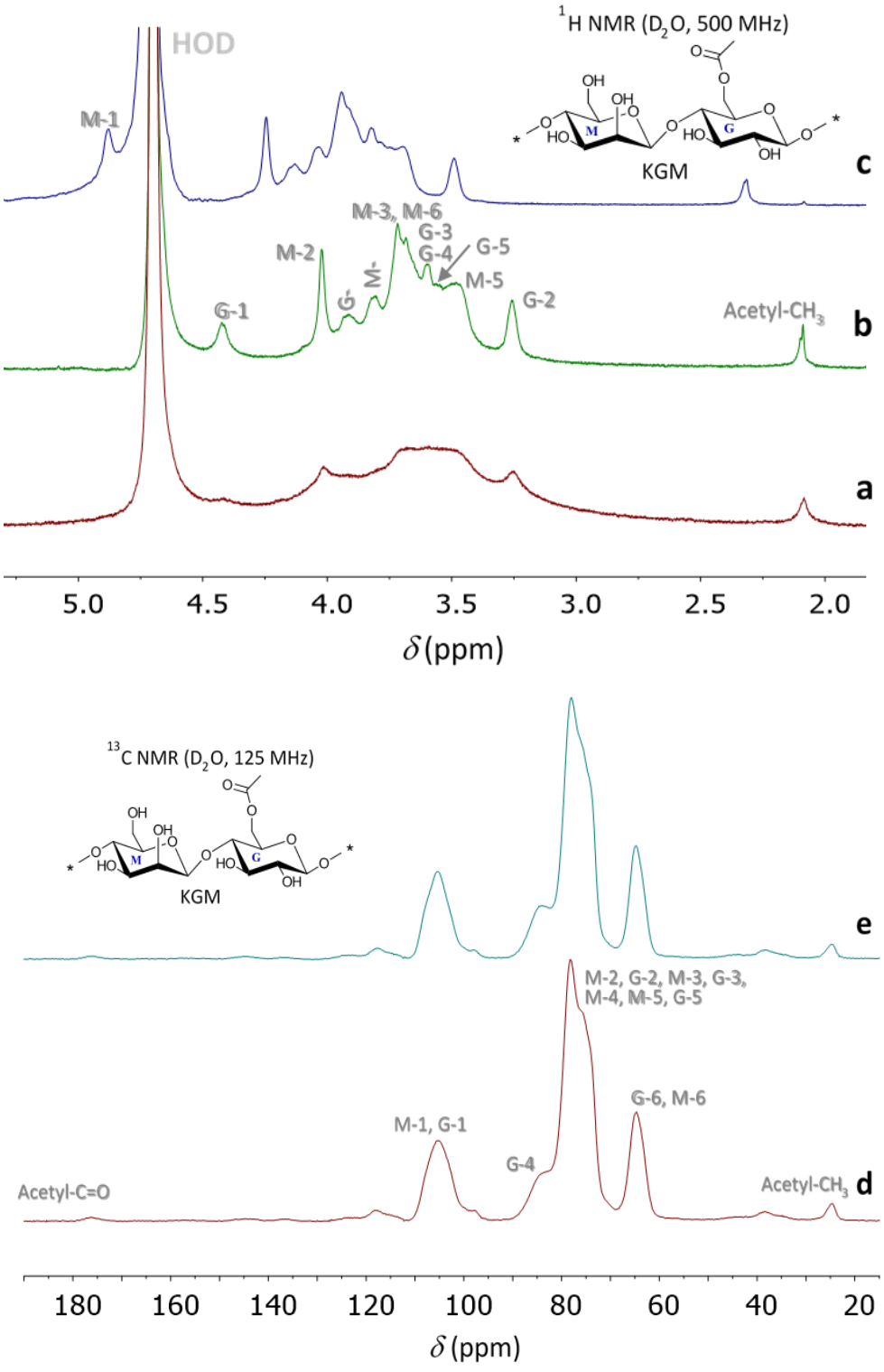

Figure 3.2. ^{1}H-NMR spectra of (a) commercial and hydrolysed konjac glucomannan (KGM) at (b) room temperature and (c) 45 ºC; ^{13}C CP-MAS spectra of (d) commercial and (e) hydrolysed KGM.

3.2.2.3. Fourier transform infrared (FTIR) spectroscopy

Commercial KGM presents a FTIR spectrum (Figure 3.3.) typical of a polysaccharide, with a strong and broad band centred around 3440 cm^{-1}, due to the stretching of O-H bonds of both the –OH groups and of adsorbed water molecules; two bands near 2900 cm^{-1}, attributed to the stretching of C-H bonds; one band at 1687 cm^{-1}, attributable to the stretching of C=O bonds from the acetyl groups that decorate the structure; a strong band at 1645 cm^{-1} corresponding to the bending of adsorbed water molecules; a strong and broad band centred near 1070 cm^{-1}, related to the skeletal vibrations (C-C, C-O and C-O-C bonds) of the polysaccharide backbone. In line with what was observed in the NMR spectroscopy, the spectrum of the hydrolysed sample is identical to that of the parent polymer. Although it is also not possible to quantify the acetyl groups from the relative intensities of the carbonyl bands in both spectra, the amount of these groups seems not to have suffered a significant reduction upon hydrolysis.

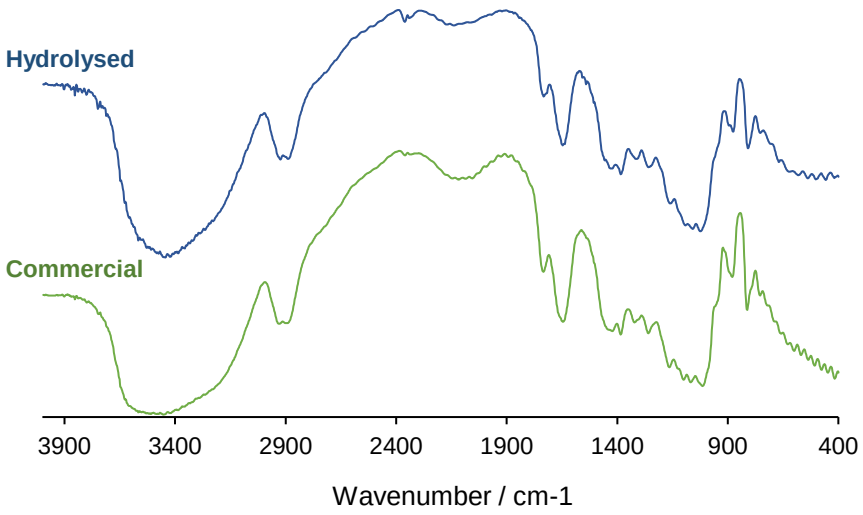

Figure 3.3. FTIR spectra of commercial and hydrolysed konjac glucomannan (KGM).

3.2.2.4. Viscosity

The apparent viscosity of commercial and hydrolysed KGM, as well as of unloaded KGM microparticles was studied. The results are displayed in Figure 3.4., where it can be clearly observed that the apparent viscosity dropped notably with increasing shear rate, all the samples exhibiting shear-thinning behaviour. This profile agrees with a typical non-entangled polymer performance in the dilute range.[137] All systems could be

adequately described by the well-known power law model (R^2 > 0.990). At the lowest tested shear rates (below 1 s^{-1}), all the samples tended to common apparent viscosity values. At intermediate shear rates (between 1 and 10 s^{-1}), no important differences were observed between the apparent viscosity of the hydrolysed KGM and the unloaded KGM microparticles, whereas higher values were identified for the commercial polymer. At the highest shear rates (above 10 s^{-1}), differences were observed between the samples, according to the following order: commercial KGM > hydrolysed KGM > unloaded KGM microparticles. Even though, the differences between the hydrolysed KGM and the unloaded KGM microparticles were very small, which is consistent with the molar mass distributions obtained by HPSEC. The higher viscosity of native KGM is a natural consequence of its higher molecular weight.

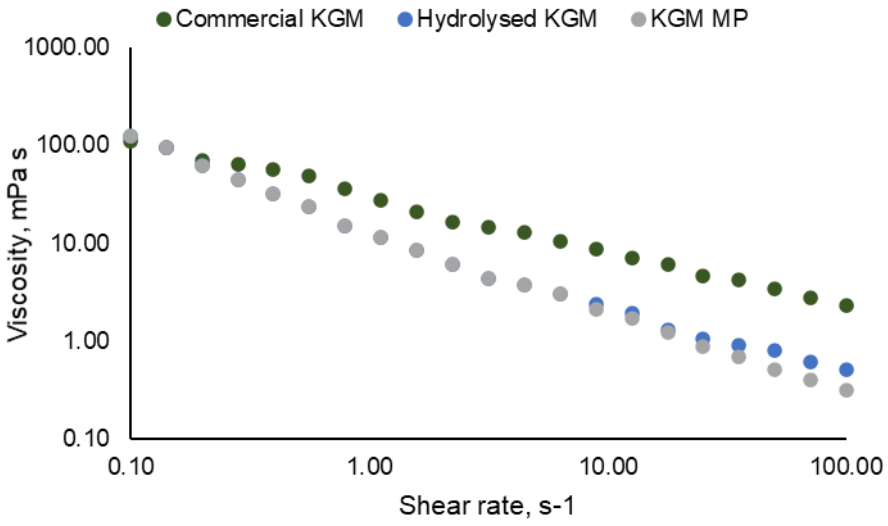

Figure 3.4. Apparent viscosity flow curves at 25 ºC for aqueous dispersions (0.5 g/L) of KGM (commercial and hydrolysed) and unloaded KGM microparticles prepared using hydrolysed KGM.

The observed shear-thinning behaviour, which is typical of dispersions of macromolecules, suggests that, at the highest shear rates, there is an alignment of the molecules with consequent release of water, favouring the fluid flow. Moreover, it is noteworthy that tested samples did not exhibit hysteresis loops, which represents a relevant advantage from the point of view of processing.

3.2.2.5. Oligosaccharide content

KGM is a slightly branched polysaccharide composed by β-1,4-linked D-mannose and D-glucose units, typically reported to be present in a molar ratio of 1.6:1 or 1.4:1, depending on the genotypes. Acetyl groups along the glucomannan back-bone are found, on average, every 9 to 19 sugar units. As the polymeric composition frequently drives the behaviours and because it can play a relevant role in certain applications of the polymer, it was considered relevant to study the impact of the hydrolysis and the spray-drying process on this parameter. To do so, the oligomer composition was determined for KGM (commercial and hydrolysed) and the unloaded KGM microparticles, the resulting data being displayed in Table 3.2.

Table 3.2. Oligomeric composition of konjac glucomannan (KGM) polymer (commercial and hydrolysed) and spray-dried unloaded KGM microparticles (n = 2).

Sample	Oligosaccharide content		Molar ratio (mannose/glucose)
	Mannose (%)	Glucose (%)	
KGM commercial polymer	59.3 ± 0.8	36.7 ± 0.2	1.6
KGM hydrolysed polymer	63.1 ± 1.7	37.8 ± 0.6	1.7
KGM microparticles	62.1 ± 0.4	37.6 ± 0.6	1.7

It can be observed that all the samples exhibited similar composition. As expected, the percentage of mannose was higher than that of glucose, and no significant differences were observed between the samples. The molar ratio determined for the commercial KGM was 1.6, the same described by several authors.[103,104] However, the hydrolysis of the polymer slightly increased the relative amount of mannose, and consequently the molar ratio from 1.6 to 1.7. Despite the decrease of molar mass and viscosity observed after the hydrolysis, the oligomeric composition was not significantly affected by the process. Regarding the KGM microparticles, which were produced from the hydrolysed polymer, the molar ratio remained unaltered comparing to that of the hydrolysed polymer, indicating that spray-drying had no noticeable effect on the oligomeric composition of KGM.

3.3. Conclusion

The use of KGM in drug delivery has been gathering attention but the high viscosity of the resulting solutions limits some applications, including processing with spray-drying. Performing an acid hydrolysis enabled decreasing the molecular weight and, consequently, the viscosity of solutions, permitting the application of the technique of spray-drying to produce KGM microparticles. NMR and FTIR spectroscopy evidenced absence of effect of the hydrolysis on the resulting KGM, which maintained its chemical structure. Furthermore, the oligomeric composition of (unloaded) KGM microparticles was similar to that of commercial and hydrolysed KGM, revealing no significant alterations after the hydrolysis and spray-drying processes, with mannose/glucose molar ratio of 1.7. KGM microparticles produced under the conditions described herein have, thus, shown to preserve the essential chemical characteristics of KGM to be used as a polymeric matrix in drug delivery applications, after hydrolysis and spray-drying processes. Nevertheless, the produced unloaded KGM microparticles exhibited a tendency towards agglomeration that must be overcome in drug-loaded carriers to permit an application in inhalation strategies.

CHAPTER 4 - ENGINEERING OF KONJAC GLUCOMANNAN INTO RESPIRABLE MICROPARTICLES FOR DELIVERY ANTITUBERCULAR DRUGS

The information in this chapter was partially published in the following publication:

Filipa Guerreiro, Magda Swedrowska, Roshnee Patel, Noelia Flórez-Fernández, María Dolores Torres, Ana M. Rosa da Costa, Bem Forbes, Ana Grenha, 2021. Engineering of konjac glucomannan into respirable microparticles for delivery of antitubercular drugs. *International Journal of Pharmaceutics*, *604*, 120731.

This page was intentionally left in blank

4. Engineering of konjac glucomannan into respirable microparticles for delivery antitubercular drugs

4.1. Materials and methods

4.1.1. Preparation and characterisation of konjac glucomannan microparticles

Drug-loaded KGM microparticles were produced using the spray-dryer (Buchi B-290 Mini Spray Dryer; Buchi Labortechnik AG, Switzerland) equipped with a high-performance cyclone. Firstly, a dispersion of hydrolysed KGM (1.5%, w/v) was prepared in warmed ultrapure water (70 ºC). INH (Sigma-Aldrich, Germany) and RFB (Chemos, Germany) were used as model antitubercular drugs and were associated to the KGM dispersion at three different INH/RFB ratios, thus leading to the preparation of three different microparticle formulations: KGM/INH/RFB = 10/1/0.5 (w/w), 10/1/1 (w/w) and 10/2/0.5 (w/w). In all cases, KGM was used at 1.5% (w/v), the same concentration that was previously used for the production of unloaded KGM microparticles. RFB was solubilised separately with 0.01M HCl (0.75%, v/v) in a test tube and added dropwise to the polymeric dispersion after its complete dissolution. The KGM/RFB dispersion was stirred overnight protected from the light to prevent degradation. INH was dissolved separately in water and subsequently added to the dispersion 2 h before spray-drying. KGM/INH/RFB microparticles were produced by spray-drying, setting the parameters as follows: spray flow rate at 473 L/h, inlet temperature of 170 ºC, aspirator at 90% and fluid flow rate of 0.8 mL/min. Three replicates of each formulation were prepared. The yield (%) of the spray-drying process was calculated as described in section 3.1.2.

4.1.2. Physical and morphological aspects of microparticles

The size and shape of unloaded KGM microparticles and the three formulations of KGM/INH/RFB microparticles were studied using Morphologi 4® (Malvern Instruments Limited, Malvern, UK). A small amount of dry powder was placed on the device and dispersed on a glass plate by compressed air. The dispersed

particles were analysed by a high-resolution microscope with a broad size range between 0.5 and 50 µm. The geometric diameter, circularity, elongation and convexity were calculated as the mean of 15 000 particles for each formulation. Morphological characterisation of drug-loaded KGM microparticles was also performed by field emission scanning electron microscopy (FESEM Ultra Plus, Zeiss, Jena, Germany). Dry powders were placed onto metal plates and 5 nm thick iridium film was sputter-coated (model Q150T S/E/ES, Quorum Technologies, Lewes, UK) on the samples before viewing.

4.1.3. Swelling behaviour of KGM microparticles

The effect of exposing the particles to different aqueous media on the particle size was studied using unloaded KGM microparticles. Microparticle dispersions at the concentration of 10 mg/mL were prepared in PBS (Sigma-Aldrich, Germany) or simulated lung fluid (SLF). The latter is composed by 1,2-dipalmitoyl-snglycero-3-phosphocholine (Avanti Polar Lipids, USA), 1,2-dipalmitoylsn-glycerol-3-phosphot-rac(1-glycerol) sodium salt (Avanti Polar Lipids, USA), cholesterol (Sigma-Aldrich, UK), albumin (Sigma-Aldrich, UK), Immunoglobulin G (Sigma-Aldrich, UK), transferrin (Sigma-Aldrich, UK), ascorbate (Sigma-Aldrich, UK), urate (Sigma-Aldrich, UK), glutathione (Sigma-Aldrich, UK), gentamicin (Sigma-Aldrich, UK) and Hanks' Balanced Salt Solution (Sigma-Aldrich, UK) and was prepared following a recently published method.[138] The microparticle dispersions were agitated at room temperature by horizontal shaking at 300 rpm. At pre-determined times up to 90 min, samples were collected, placed on a glass slide, and particle size was analysed using the Morphologi 4®. The software was programmed to measure the size of 5 000 microparticles in a scan area of 3.338 mm^2.

4.1.4. Evaluation of KGM microparticles biodegradation in the presence of β-mannosidase

The biodegradability of KGM microparticles was evaluated by incubation of unloaded carriers in medium enriched with the enzyme β-mannosidase. The assay was performed in different media: PBS; Gibco's Minimum Essential Medium (MEM; Sigma-Aldrich, UK) cell culture medium supplemented with 1% v/v Foetal Bovine Serum (FBS; Sigma-Aldrich, UK), 1% v/v L-glutamine (Sigma-Aldrich, UK), 1% v/v penicillin-streptomycin (Sigma-Aldrich, UK); and SLF. The microparticles were incubated at a concentration of 10 mg/mL and β-mannosidase (Sigma-Aldrich, UK) was added to the solutions at a concentration of 1.2 µg/L. The samples were incubated under horizontal shaking at 300 rpm and 37 ºC, over 90 min. At predetermined intervals, samples were collected and analysed using the Morphologi 4® as described above. Trypsin (Sigma-Aldrich, UK) at 0.25%, 0.025% or 0.0025% (v/v) was used to replace β-mannosidase to provide negative controls.

4.1.5. Association efficiency

To determine the association efficiency (AE) of INH and RFB and the loading capacity (LC) of microparticles, each dry powder was completely solubilised in a mixture of methanol/water (60/40, v/v) under 5 min of sonication. The 10/1/0.5 (w/w) and 10/2/0.5 (w/w) formulations were solubilised at 3 mg/mL and the 10/1/1 (w/w) formulation at 2 mg/mL. After solubilisation, the samples were filtered (0.45 µm) and analysed by HPLC (Agilent 1100 series, Concord, Germany). Chromatographic separation was performed using a LiChrospher® 100 RP-18 column (4.6 µm, 4 mm ID × 250 mm, CS Chromatographie-Service GmbH, Langerwehe, Germany) equipped with a pre-column (20 x 4 mm). The injection volume was 20 µL and both drugs were detected at a wavelength of 275 nm, at room temperature. A mobile phase of 20 mM phosphate buffer (pH = 7) (A) and acetonitrile (B) was used at a flow rate of 1.0 mL/min. The elution was conducted with a gradient starting with A/B = 95%/5% (0 – 5 min), followed by transition to 30%/70% A/B ratio (5 – 8 min) and elution at the final ratio until 19 min. The

retention times of INH and RFB were approximately 5 min and 20 min, respectively. Calibration curves (5 – 500 µg/mL) were obtained from INH and RFB standard solutions in methanol/water (60/40, v/v). AE (%) and LC (%) were calculated (n = 3) by the following equations, respectively.

$$\mathrm{AE} = \left(\frac{\text{Real drug content}}{\text{Theoretical drug content}}\right) \times 100$$

$$\mathrm{LC} = \left(\frac{\text{Real amount of drug}}{\text{Weight of microparticles}}\right) \times 100$$

4.1.6. Stability study

The stability of KGM/INH/RFB = 10/1/0.5 (w/w) microparticles was studied following the international guidelines for a new drug substance or drug product.[139,140] KGM/INH/RFB microparticles (around 30 mg) were placed in dark glass vials, hermetically closed and submitted to the conditions of accelerated and long-term storage studies in a climatic test cabinet (TK 252; Nüve Sanayi Malzemeleri ˙Imalat ve Ticaret A.S., Akyurt/Ankara, Turkey). The accelerated stability study lasted 6 months at 40 ± 2 ºC and 75 ± 5% relative humidity (RH). Regarding to the long-term stability study, KGM/INH/RFB microparticles were incubated at 25 ± 2 ºC and 60 ± 5% RH for 12 months. During the studies, the amount of drug in KGM microparticles was periodically monitored, the quantification being performed by HPLC, under the conditions described above in section 4.1.5. The free drugs, INH and RFB, were subjected to the same conditions and used as control. The study was performed using three replicates of each sample.

4.1.7. Determination of sample humidity

After being removed from the climatic test cabinet, drugs and KGM microparticles were weighed in test tubes and placed in an incubator at 105 ºC. After 24 h at this temperature, the samples were removed from the incubator and placed in a

desiccator to allow cooling down. After that, the samples were weighed and the percentage of humidity (%)calculated (n = 3) by the following equation:

$$\text{Humidity } = \left(\frac{\text{Initial powder weight} - \text{Final powder weight}}{\text{Final powder weight}}\right) \times 100$$

4.1.8. In vitro drug deposition

The aerodynamic properties of drug-loaded KGM microparticles were analysed according to the European Pharmacopoeia (Apparatus E, European Pharmacopoeia 8.0) using the Next Generation Impactor (NGI - Copley Scientific, Nottingham, UK) equipped with an induction port.[141] NGI has seven stages and a micro-orifice collector (MOC), which allow the separation of particles according to their aerodynamic diameter. The flow rate was calibrated at 60 L/min using a flow meter (TSI Series 4000, TSI Instruments Ltd, Buckinghamshire, UK) and the cut-off diameters ranged between 8.06 and 0.14 µm throughout the several stages. The collection plates were coated with ethanol and 1% (v/v) of Tween® 20 to prevent losses due to particle bounce. KGM/INH/RFB microparticles (30 mg) were loaded into a size 3 gelatine capsule (Meadow Laboratories Ltd, Romford, UK) and aerosolised using an RS01 device (IFR = 0.033 $kPa^{0.5}$/LPM, Plastiape, Lecco, Italy). After one actuation, the content of the capsule was discharged. The test duration time was 4 s and the content of three capsules was discharged for each experiment. A mixture of methanol/water (60/40, v/v) was used to rinse off the powder from the apparatus. Samples were sonicated for 5 min, filtered (0.45 µm) and analysed by HPLC following the analytical protocol described in section 4.1.5.

The quantification of drug deposited inside the impactor allows calculation of aerodynamic parameters. Mass median aerodynamic diameter (MMAD) and geometric standard deviation (GSD) were calculated by plotting the cumulative percentage of deposited drug against the NGI stage cut-off diameters (NGI stages 1 - 7 and MOC) using a log-probability scale. Fine particle dose (FPD) was defined as the mass of drug particles with size < 5 µm. The percentage of drug released from the capsules and device was considered as the emitted dose

(ED) and the fine particle fraction (FPF) was calculated as the percentage of cumulative drug mass with aerodynamic diameter lower than 5 µm.

4.1.9. In vitro drug release profile

To study the release profile of INH and RFB, a modified NGI was used to collect KGM/INH/RFB = 10/1/0.5 (w/w) microparticles in the second stage. The particles were emitted from three gelatine capsules and collected on a 0.45 µm nitrocellulose membrane. Each capsule was loaded with 30 mg of KGM microparticles and the flow rate was adjusted at 48 L/min. After the emission, the membranes with the deposited particles were cut and transferred to Transwell inserts. The inserts were transferred to a 6-well plate containing 5 mL of dissolution medium and kept under horizontal shaking (Mini Orbital Shaker SO5, Stuart Scientific, Staffordshire, UK) at 15 rpm and room temperature. The release profile of INH and RFB was determined on two different dissolution media, methanol/water (60/40, v/v) and SLF. At fixed time intervals, samples of dissolution medium were collected and replaced by the same volume of fresh medium. After 24 h of release, the membranes were sonicated, respectively, for 5 min when in methanol/water (60/40, v/v) and for 30 min when in SLF, to assure the total release of INH and RFB. The collected samples were analysed by HPLC as described in section 4.1.5. The cumulative drug release was calculated as the percentage ratio between the amount of released drug in each time interval and the total drug. The calibration curves (5–500 µg/mL) to determine the release of INH and RFB were the same obtained for the AE and LC made in methanol/water (60/40, v/v).

4.1.10. Statistical analysis

The t-test and one-way analysis of variance (ANOVA) with the pairwise multiple comparison procedure (Holm-Sidak method) were performed to compare two or multiple groups, respectively. All analyses were run using the GraphPad Prism®

statistical program (Version 6.01) and differences were considered to be significant at a level of $p < 0.05$.

4.2. Results and discussion

4.2.1. Preparation and characterisation of konjac glucomannan microparticles

Spray-dried KGM microparticles were produced associating variable amounts of INH and RFB (KGM/INH/RFB = 10/1/0.5, 10/1/1, 10/2/0.5, w/w). The selected theoretical drug loadings are in similar range of other works reporting inhalable delivery of these antitubercular drugs.[142,143] INH has similar or higher loading than RFB because the latter is more potent drug[144,145] and has been reported to be more toxic.[146] Moreover, KGM proportion was kept purposely high to foster the recognition of microparticles by macrophages in the desired application of pulmonary tuberculosis treatment, thus improving the therapeutic outcome. The microparticles, prepared with satisfactory yields around 80% (data not shown),[147] were characterised regarding size, shape and morphology.

Parameters of size and shape were analysed using the Morphologi 4® and are depicted in Table 4.1. Despite the variations in theoretical drug loading, the analysis of the three formulations revealed no significant differences regarding the referred parameters. This was somewhat expected, as the total amount of drugs loaded in the microparticles is relatively small and not likely to impact significantly on microparticle size or aspect. As observed in Table 4.1, the geometric diameters ranged between 1.87 and 2.24 µm, which may favour phagocytic uptake, a useful strategy in the treatment of intracellular diseases like tuberculosis.[148] Indeed, the literature reports preferential macrophage uptake of particles with sizes between 1 and 3 µm.[101,102] Apart from particle size, shape is another important feature in macrophage uptake process.[149] Yoo & Mitragotri[150] revealed that spherical particles were internalised by macrophages, contrary to elongated particles that mitigate phagocytosis. The produced KGM microparticles have high values of circularity (0.88 – 0.91) and low values of elongation (0.15 – 0.19), thus supporting the hypothesis that their shape could facilitate macrophage uptake. Additionally, the convexity of microparticles was found to reach a value

of 0.99 for all formulations, which is close to the maximum value of 1. This is a good indicator on the aerosolisation properties of KGM microparticles, as some studies demonstrate that appropriate surface irregularity is critical to improve microparticle dispersion and prevent agglomeration phenomena [126,151].

Table 4.1. Size and parameters of shape of konjac glucomannan (KGM) microparticles loaded with isoniazid (INH) and rifabutin (RFB) (mean ± SD, n = 3). Different letters represent significant differences in each parameter ($p < 0.05$).

KGM/INH/RFB (w/w)	Geometric diameter (μm)	Circularity	Elongation	Convexity
10/1/0.5	2.24 ± 2.18^{a}	0.91 ± 0.14^{b}	0.15 ± 0.12^{c}	0.99 ± 0.04^{d}
10/1/1	2.06 ± 2.15^{a}	0.91 ± 0.12^{b}	0.15 ± 0.12^{c}	0.99 ± 0.03^{d}
10/2/0.5	1.87 ± 2.11^{a}	0.88 ± 0.18^{b}	0.19 ± 0.16^{c}	0.99 ± 0.04^{d}

The referred data of size and shape were corroborated by the SEM analysis of KGM microparticles. Figure 4.1 shows the images of the three formulations of microparticles that were prepared in this work. KGM/INH/RFB microparticles are generally small, spherical and convex. Despite the absence of statistically significant differences in the features displayed in Table 4.1, a tendency for size decrease with the increase of the amount of associated drug is suggested by the images, as it was also observed in the mean values of geometric diameter (Table 4.1). In parallel, the presence of convexities also appeared more evident in the formulations with higher amount of drugs (KGM/INH/RFB = 10/1/1 and 10/2/0.5, w/w), which could suggest better flow properties of these formulations.

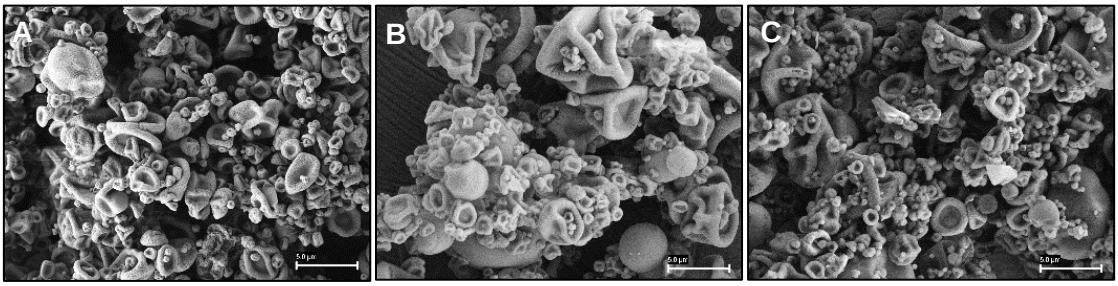

Figure 4.1. Representative microphotographs of konjac glucomannan (KGM) microparticles associating different amounts of isoniazid (INH) and rifabutin (RFB): A) KGM/INH/RFB = 10/1/0.5 (w/w); B) KGM/INH/RFB = 10/1/1 (w/w); C) KGM/INH/RFB = 10/2/0.5 (w/w). Scale bars = 5 μm.

4.2.2. Swelling of KGM microparticles and biodegradability by β-mannosidase

Considering the envisaged application of KGM microparticles as inhalable drug carriers and taking into account the shortness of exploration of the material for the objective, studying the behaviour of microparticles and the particular material upon contact with aqueous fluid was deemed adequate and informative. The literature reports KGM swelling capacity in water,[104] thus, a certain swelling degree being expected upon contact with the lung lining fluid. To perform the study, unloaded KGM microparticles were incubated in PBS and SLF and the evolution of their size and shape was compared with the dry powder in dry state. While PBS simulates the pH of the lung,[152] SLF is a faithful representative of the human respiratory tract lining fluid.[138,153] The results are depicted in Figure 4.2, showing that the contact with liquid media had no effect on particle shape, which remained spherical. The average size determined for the dry powder was 2.87 ± 2.34 μm (Figure 4.2a). The contact with either PBS or SLF resulted in microparticle swelling, as observed in Figures 4.2b and 4.2c, reaching average diameter of 4.34 ± 2.69 μm and 4.02 ± 1.60 μm, respectively. These correspond to average size increase of approximately 51% in PBS and 40% in SLF. The particle size was monitored in short intervals over 90 min and swelling was observed to occur between 20-30 min, then remained unaltered.

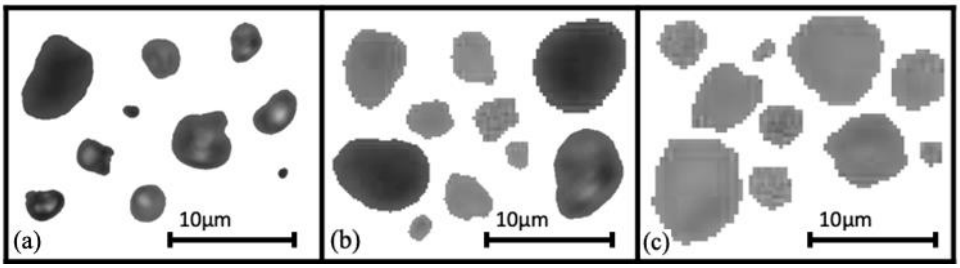

Figure 4.2. Unloaded KGM microparticles as observed with Morphologi4®, (a) as dry powder, and after 90 min incubation in (b) PBS and (c) SLF.

The literature describes the swelling of native KGM in a water-ethanol binary mixture, identifying three steps in the process: diffusion of water molecules into the polymer network leading to break of hydrogen bonds in the loose aggregation regions; diffusion of water into the tight aggregation region, increasing chain

mobility, by opening space between them, and allowing more water molecules in; hydrogen bonding between water molecules and polymeric chains.[154] Similar mechanisms are likely for PBS and SLF with the intermolecular hydrogen bonds of KGM breaking up in the liquid and water being absorbed into the structure of the polymer to form new hydrogen bonds. This causes expansion of the polymer chains and thus of the particles, leading to the swelling effect. The presence of salts in both fluids may further assist both the process of hydrogen bond breaking, due to increase in ionic strength, and the new hydrogen bonding, as some salts, like phosphate, have that ability.[155]

The swelling effect described herein is important to understand the behaviour of the carriers after reaching the deep lung and it is unclear whether this will help or hinder the interaction with macrophages. For repeat administration, it is important to evaluate conditions for the degradation of the materials used as particle matrix to avoid lung accumulation and potential toxicity. The literature reports the presence of β-mannosidase in the lungs[156] which could help on the degradation of KGM microparticles after deposition, by breaking the linkages between mannose units on the polysaccharide structure. Despite the description about lung expression, no information was found on the enzyme concentration. However, it is known that the plasma concentration of β-mannosidase is 12 µg/L.[157] To study the biodegradability of KGM microparticles in the lungs, β-mannosidase was added to KGM microparticle dispersions in PBS, cell culture medium and SLF, at the concentration of 1.2 µg/L. The obtained data are depicted in Figure 4.3.

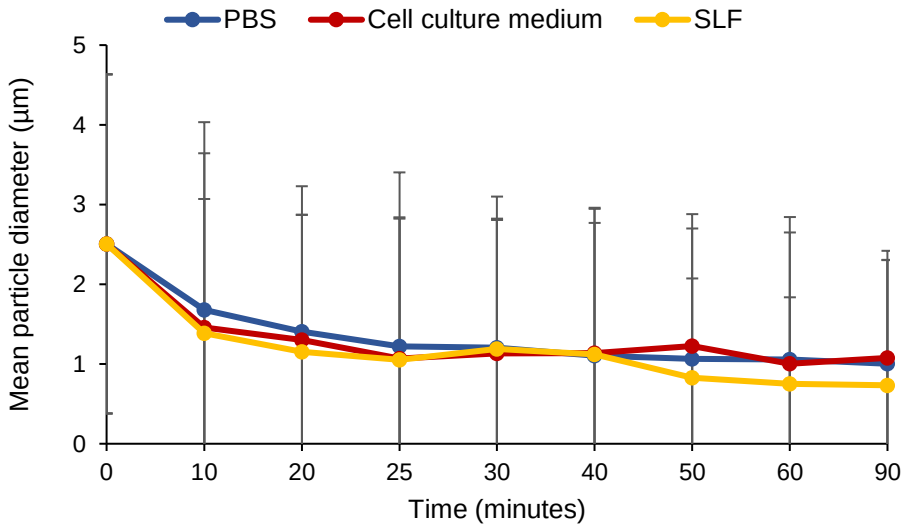

Figure 4.3. Evolution of particle size of unloaded KGM microparticles upon dispersion in PBS, cell culture medium or SLF in the presence of 1.20 µg/L β-mannosidase. Data points represent mean ± SD (n = 3; each sample 5 000 particles).

Regardless of the tested media, mean particle size was observed to decrease up to geometric diameters around 1 µm after 90 min, corresponding to size reductions of 62% - 75%. The initial swelling of the particles may enhance the access of the enzyme to the inner particle, leading to subsequent degradation of KGM microparticles. A control study was performed replacing β-mannosidase by trypsin, a serine protease expressed in several organs in the human body, including the lung.[158] In this case, no reduction was observed in microparticle size, regardless of the tested concentration (0.0025% to 0.25%, w/v, data not shown).

The particle size-time profiles show the net effect of the simultaneous dynamic processes of swelling in aqueous medium and degradation upon exposure to β-mannosidase, which have opposing effects, with the size reducing action of enzymatic activity dominating. These data provide an indication of the potential for biodegradation of KGM microparticles upon pulmonary delivery, which is favourable for the application. Further development of the KGM microparticle excipient platform should include detailed investigation of particle disintegration and polymer breakdown in more biorelevant models of the metabolic environment

in the lungs[159] and studies to attain a mechanistic understanding of how these processes affect drug release.

4.2.3. Evaluation of drug association efficiency and microparticle loading capacity

INH and RFB were associated with KGM microparticles as model antibiotics. As depicted in Table 4.2, both drugs were successfully incorporated into the microparticles, although the association of INH was significantly higher than that of RFB in the three formulations ($p < 0.05$). INH association values ranged between 78% and 91%, although an increase of theoretical drug loading in the microparticles significantly decreased the proportion of INH that was loaded ($p < 0.05$). RFB presented a different behaviour, with association efficiency ranging between 66% and 74%. An increase in the amount of RFB in the formulation, from KGM/INH/RFB = 10/1/0.5 to 10/1/1 (w/w), did not produce any alteration on drug association, which remained around 73% - 74%. However, the association of RFB was lower for the formulation 10/2/0.5 (w/w), registering 66% ($p < 0.05$). The values for the loading capacity ranged within approximately 7% - 13% and 3% - 6%, for INH and RFB, respectively. Naturally, INH showed higher loading than RFB ($p < 0.05$), mirroring the theoretical loadings. Moreover, INH and RFB loadings were found to be lower than the theoretical loadings, which were 9.1%/3.7%, 8.5%/7.3%, 15.6%/3.3% for the formulations 10/1/0.5 (w/w), 10/1/1 (w/w) and 10/2/0.5 (w/w), respectively.

Table 4.2. Association efficacy and loading capacity of isoniazid (INH) and rifabutin (RFB) in different konjac glucomannan (KGM)-based microparticles (mean ± SD, n = 6). Different letters represent significant differences in each parameter ($p < 0.05$).

KGM/INH/RFB (w/w)	Drug	Association efficiency (%)	Loading capacity (%)
10/1/0.5	INH	90.5 ± 3.4^{a}	7.5 ± 0.3^{f}
	RFB	73.6 ± 8.6^{d}	2.9 ± 0.3^{h}
10/1/1	INH	84.5 ± 4.9^{b}	7.0 ± 0.4^{f}
	RFB	73.3 ± 1.8^{d}	6.1 ± 0.2^{i}
10/2/0.5	INH	78.1 ± 3.5^{c}	13.0 ± 0.6^{g}
	RFB	65.9 ± 2.6^{e}	2.6 ± 0.1^{j}

4.2.4. Stability study

European regulations advocate the study of the stability of drug products over time under the influence of specific environmental factors, namely temperature and humidity. With regards to stability testing, the world is divided in four climatic zones and Portugal is assigned to zone II (subtropical and Mediterranean climates). The climatic zone defines the specific conditions of temperature and humidity at which drug products must be assessed.[160,161] Microparticles comprised of KGM/INH/RFB = 10/1/0.5 (w/w) were selected to perform the stability test and considered representative of the produced KGM-based microparticles. An accelerated stability study was performed at first, following ICH regulations.[139,140] As significant differences were observed in drug content, a long-term study was further performed. Free INH and RFB were used as controls in both studies.

Accelerated stability studies provide indications on phenomena that may be verified at normal storage conditions, in a narrower time. Considering the conditions established for the climatic zone II, KGM/INH/RFB = 10/1/0.5 (w/w) microparticles were stored at a temperature of 40 ± 2 ºC and RH of 75 ± 5% over 6 months. The drug amount was monitored along time and data depicted in Figure 4.4. The figure demonstrates a significant loss of INH associated to

microparticles under the conditions of the assay (Figure 4.4a). In fact, after 2 months INH amount was already below the regular 95%, reaching 57% after 6 months ($p < 0.05$). The free drug, however, maintained stability, being approximately at 95% after the 6 months. The effects of instability were even more visible in RFB (Figure 4.4b), as after 2 months only 60% of the initial amount of RFB remained in KGM microparticles ($p < 0.05$). At the end of the study (6 months), the amount of RFB in KGM microparticles was only 27%. Contrary to INH, free RFB did not show stability during the whole assay, showing a significant decrease to 84% after 6 months ($p < 0.05$).

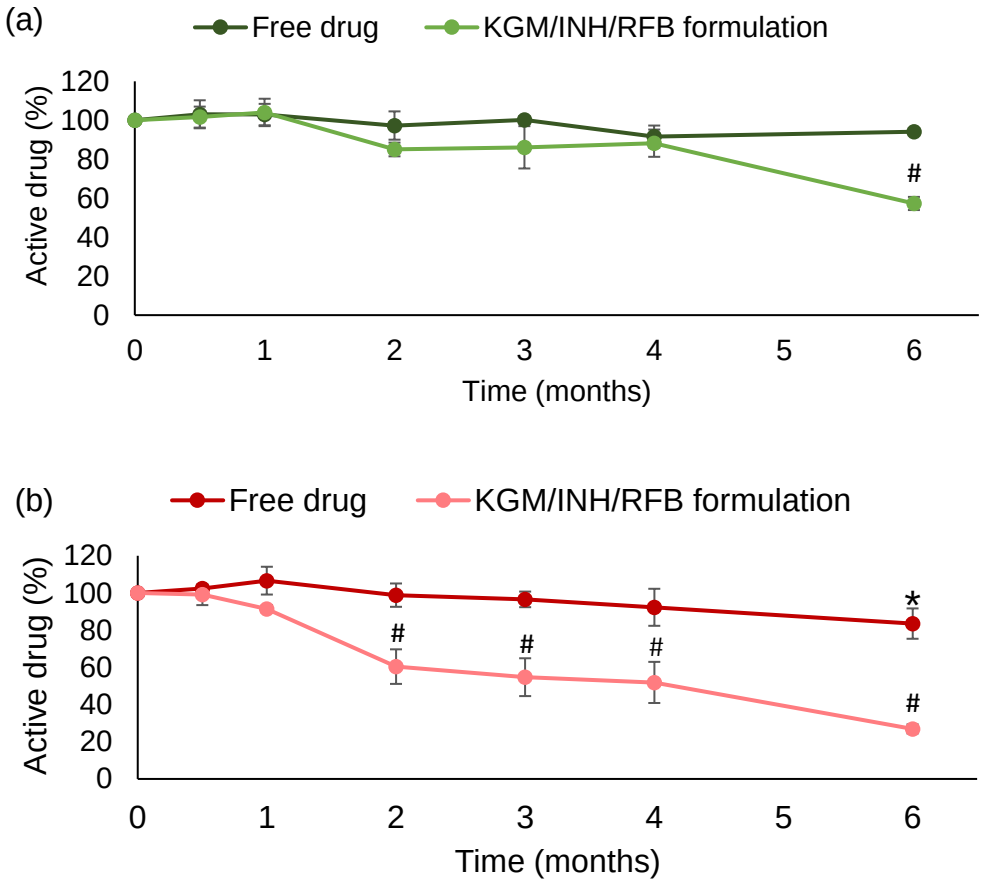

Figure 4.4. Active drug, (a) isoniazid (INH) and (b) rifabutin (RFB) quantified in the KGM microparticles (KGM/INH/RFB) and as free drug along 6 months, after incubation at 40 ± 2 ºC and 75 ± 5% relative humidity (RH). Results are expressed as mean ± SD (n = 3). Statistical significance levels are indicated as *$p < 0.05$ and $^{\#}p < 0.05$ for free drugs and KGM microparticles, respectively, compared with day 0.

Because significant change was observed in accelerated conditions, it was decided to proceed with the evaluation at the conditions considered in ICH regulation for long-term stability studies. The microparticles were then stored at 25 ± 2 ºC and 60 ± 5% RH, being monitored for 12 months. Free drugs were, again, used as controls and the results of the assay are depicted in Figure 4.5. Upon 12 months under the referred storage conditions, the active drug present in all samples was below 95%, which means that significant change was still observed even at milder storage conditions. At these conditions, both drugs reached drug contents below 95% after 3 months of microparticle storage ($p < 0.05$; Figure 4.5), being 87% for INH and 82% for RFB. The percentage of INH and RFB remaining in KGM microparticles at the end of 12 months was 69% and 55%, respectively.

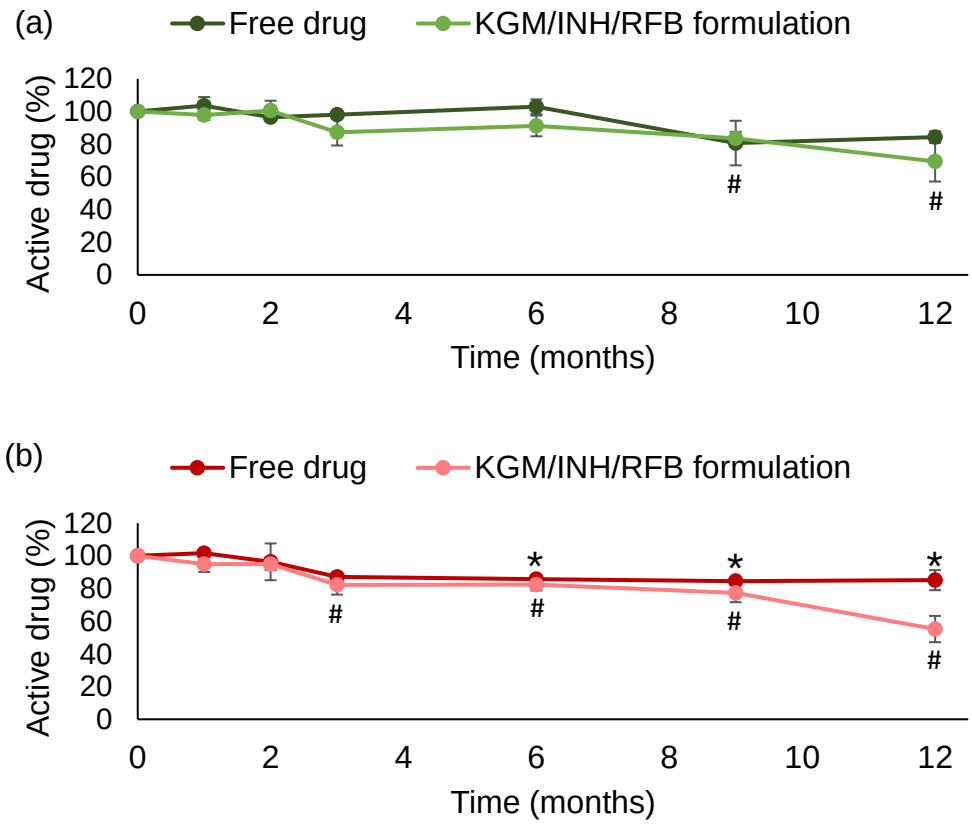

Figure 4.5. Active drug, (a) isoniazid (INH) and (b) rifabutin (RFB) quantified in the KGM microparticles (KGM/INH/RFB) and as free drug along 12 months, after incubation at 25 ± 2 ºC and 60 ± 5% relative humidity (RH). Results are expressed as mean ± SD (n = 3). Statistical significance levels are indicated as *$p < 0.05$ and $^{\#}p < 0.05$ for free drugs and KGM microparticles, respectively, compared with day 0.

Contrary to the observed in the accelerated studies, the behaviour of microencapsulated drugs was very similar to that of free drugs, a single exception being observed for RFB at the last time point (12 months).

The observed instability was somewhat unexpected. One possible explanation for the decrease of drug content could be the presence of humidity, which was not controlled any time before and could lead to drug degradation. Samples recovered from the climatic test cabinet upon 6, 9 and 12 months in the long-term assay were evaluated regarding this parameter and compared with untested samples. Surprisingly, the percentage of humidity increased in the samples stored in the climatic chamber, particularly in KGM microparticles. While untested microparticles revealed absence of humidity, the percentage of this in KGM/INH/RFB microparticles after 6, 9 and 12 months of storage was 9.3 ± 1.2%, 10.1 ± 3.2% and 18.6 ± 0.7%, respectively. In addition, the presence of humidity was also detected in the samples of free drugs, especially in RFB. After 12 months in the climatic test cabinet, the humidity percentage in INH samples was 5.3 ± 1.3% and in RFB samples was 15.9 ± 3.1%.

These findings were somewhat surprising, as theoretically, the samples were well packaged, but water absorption was found to occur somehow, which may have caused the degradation of the drugs. In the case of the KGM microparticles, considering that microparticles were produced from a polysaccharide and this has great water absorption capacity, the absorption of environmental humidity could have been potentiated, with consequent degradation of the drugs incorporated in the microparticles. This means that the packaging selected for the storage of these formulations requires particular care, principally because aerosolisation properties must also be maintained.

4.2.5. Aerodynamic characterisation of konjac glucomannan microparticles

Characterising the aerosolisation properties of KGM/INH/RFB microparticles is crucial to establish the potential of the system for inhalable applications. The microparticle formulations were evaluated using a cascade impactor (NGI) and their aerodynamic properties are shown in Table 4.3.

The emitted dose for all formulations was above 91%, indicating good dispersibility of the KGM-based microparticles regardless of some statistically significant differences ($p < 0.05$) between formulations with different proportions of INH and RFB. A MMAD around 3 µm was obtained for all three formulations, along with FPF of 55% - 60%. The latter indicates the fraction of microparticles with aerodynamic diameter below 5 µm, thus having suitable properties to reach the respiratory zone of the lungs.[162] GSD values of 2.5 – 3 µm were determined, suggesting high polydispersity of dry powders, which is coincident with SEM microphotographs.

An initial evaluation of KGM microparticles identified their potential theoretical suitability for inhalation purposes, although an experimental determination of particle aerodynamics was not performed.[115] The present work demonstrates that, as a whole, KGM microparticles possess suitable properties for deep lung delivery. The morphology of the particles contributes positively to this effect, as the convexity, previously described in section 4.2.1, improves the dispersibility of the particles, favouring the deposition in deeper zones of the lung.[126,151]

Table 4.3. Aerodynamic parameters of konjac glucomannan (KGM) microparticles loaded with isoniazid (INH) and rifabutin (RFB) (mean ± SD, n = 6). Different letters represent significant differences in each parameter ($p < 0.05$).

KGM/INH/RFB (w/w)	Drug	Emitted dose (%)	MMAD (μm)	GSD (μm)	FPD <5 μm (mg)	FPF <5 μm (%)
10/1/0.5	INH	91.8 ± 1.2^{a}	2. 89± 0.16^{d}	2.70 ± 0.12^{f}	2.71 ± 0.16^{l}	54.7 ± 2.3^{p}
	RFB	96.6 ± 1.9^{c}	3.02 ± 0.17^{e}	2.82 ± 0.09^{i}	1.40 ± 0.11^{n}	56.5 ± 2.9^{r}
10/1/1	INH	94.5 ± 1.8^{b}	3.05 ± 0.05^{d}	2.89 ± 0.10^{g}	2.64 ± 0.11^{l}	59.0 ± 1.9^{q}
	RFB	97.5 ± 1.3^{c}	3.24 ± 0.09^{e}	2.93 ± 0.10^{j}	2.62 ± 0.22^{o}	59.9 ± 1.4^{s}
10/2/0.5	INH	91.7 ± 1.3^{a}	3.05 ± 0.16^{d}	2.47 ± 0.19^{h}	5.24 ± 0.23^{m}	57.2 ± 1.8^{q}
	RFB	95.7 ± 1.6^{c}	3.17 ± 0.15^{e}	2.53 ± 0.13^{k}	1.26 ± 0.17^{n}	57.8 ± 1.6^{s}

FPD: fine particle dose; FPF: fine particle fraction; GSD: geometric standard deviation; MMAD: mass median aerodynamic diameter

The deposition profile of INH and RFB across the different stages of the NGI (Figure 4.6) can be analysed further. The first observation to highlight is that the deposition of INH and RFB was generally similar for all formulations of microparticles, which indicates a homogeneous distribution of the drugs and is consistent with the delivery of co-associated drugs. Moreover, a similar deposition profile was observed for the three formulations of KGM microparticles. Although not reaching statistical significance, the deposition of the drugs in the stages of the NGI representing the deeper zones of the lung (stages 5 to MOC) was slightly higher in the microparticles KGM/INH/RFB = 10/1/1 (w/w) (23%) comparing with the other two formulations, which obtained 20% (KGM/INH/RFB = 10/1/0.5, w/w) and 18% (KGM/INH/RFB = 10/2/0.5, w/w). This means that the former may have a greater propensity to deposit powder in the lower airways and is reflected in a higher FPF (Table 4.3) which is derived from the impactor data.

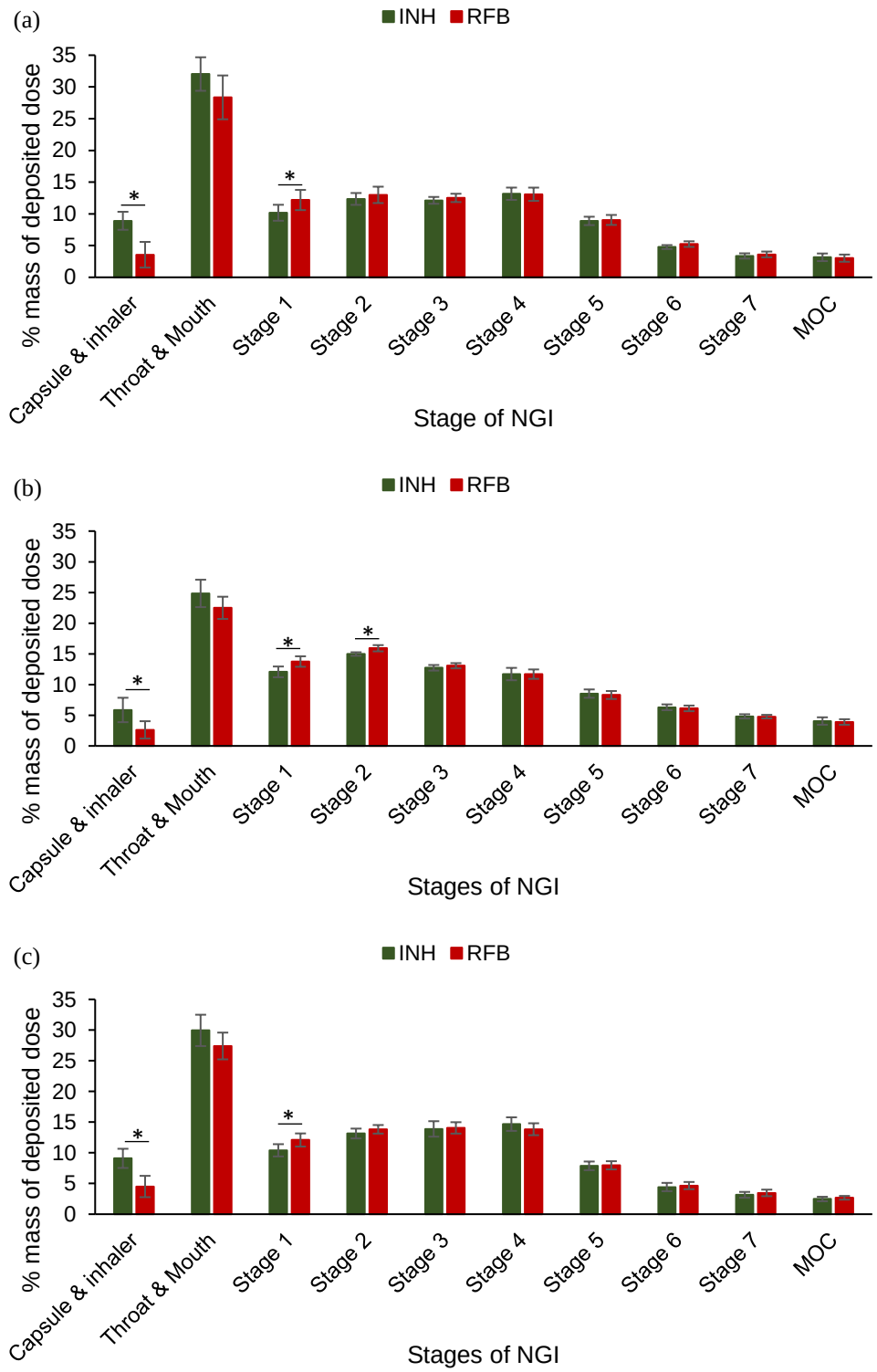

Figure 4.6. *In vitro* aerodynamic deposition of isoniazid (INH) and rifabutin (RFB) in the Next Generation Impactor (NGI) after aerosolisation of konjac glucomannan microparticles: (a) KGM/INH/RFB = 10/1/0.5 (w/w); (b) KGM/INH/RFB =10/1/1 (w/w); (c) KGM/INH/RFB =10/2/0.5 (w/w). Values are mean ± SD, n = 6. MOC: micro-orifice collector. Statistical significance is indicated with *($p < 0.05$), when comparing INH with RFB.

4.2.6. In vitro drug release

The *in vitro* release of INH and RFB was studied in two different release media, methanol/water (60/40, v/v) and SLF. Methanol/water medium was previously used to determine drug association efficiency, by releasing 100% INH and RFB. SLF is representative of the human respiratory tract lining fluid and can be used in *in vitro* studies, such as those determining the solubility of inhaled drugs, the dissolution of aerosol particles and particle-lung cell interactions.[138,153] The release profiles were determined for a representative microparticle formulation, KGM/INH/RFB 10/1/0.5 (w/w). INH exhibited a similar release profile in methanol/water and SLF (Figure 4.7a) with only small statistically significant differences observed at initial time points (up to 15 min, $p < 0.05$) and profiles that largely overlap. Approximately 50% of the drug was released in 10 min (methanol/water) and 45 min (SLF), showing a faster release in methanol/water than in SLF. After 12 h, the released antibiotic reached 84% in both dissolution media, while 96% - 97% of the drug was released in 24 h.

The release of RFB in methanol/water (Figure 4.7b) was found to be very similar to that of INH, no significant differences being observed. After 15 min, 50% of the drug was released. In turn, the release was much more sustained in SLF ($p < 0.05$); instead of a rapid initial release, only 9% of RFB was released after 15 min. Shortly after 3 h, the release rates became similar in both media. At 12 h, the released RFB was 82% and 90% in methanol/water and SLF, respectively, reaching 94% - 99% at 24 h. The release of RFB was expected to be generally slower than that of INH. This is because RFB is hydrophobic and is a larger molecule (847.02 g/mol *versus* 137.14 g/mol for INH) [53,163]. However, the release in methanol/water revealed a similar behaviour, possibly because these solvents provide a good and rapid dissolution of the carrier matrix, composed of KGM, and high solubility of RFB in the release medium due to the methanol content.[57] A preliminary evaluation performed during this study has shown that SLF is less solubilising as a dissolution medium for RFB comparing with methanol/water (26 µg/mL and 185 µg/mL, respectively).

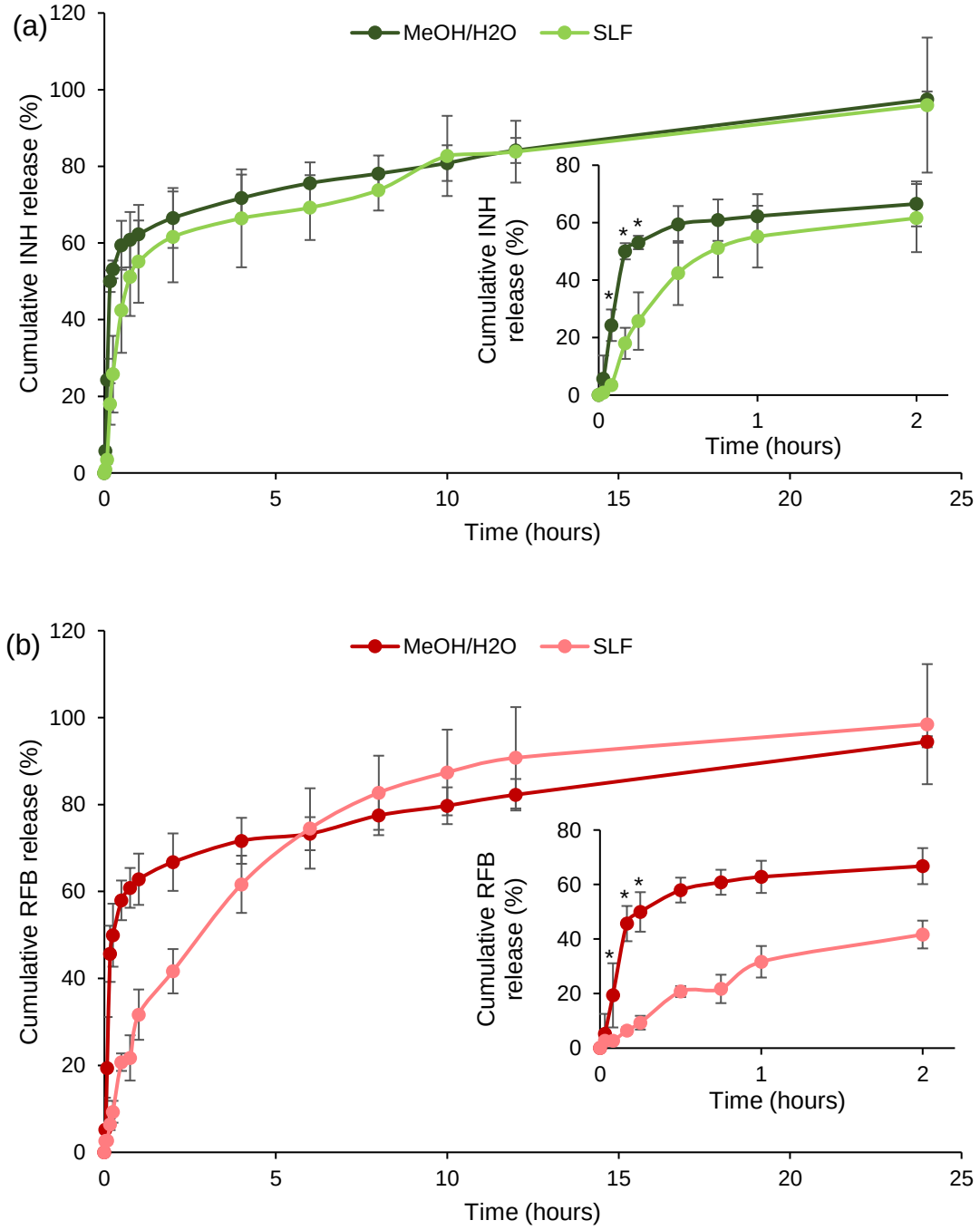

Figure 4.7. *In vitro* release profile of (a) isoniazid (INH) and (b) rifabutin (RFB) from KGM/INH/RFB = 10/1/0.5 (w/w) microparticles in methanol (MeOH)/water (H_2O) and simulated lung fluid (SLF). Graphics with expanded representation of release profiles at initial time points were inserted. Data presented as mean ± SD (n ≥ 3). Statistical significance is indicated as * ($p < 0.05$).

Drug release of the same particles in PBS pH 7.4 containing 1% (v/v) Tween 80®[115] found a faster release of both drugs, although the methodology was different, with microparticles being submerged in the release medium, which confounds a direct comparison.

4.3. Conclusion

KGM was successfully spray-dried to form microparticles loaded with a drug combination of INH and RFB and exhibited suitable characteristics for delivery to the lungs by inhalation. The aerodynamic diameter was around 3 µm, which is ideal for KGM microparticles to reach the alveolar region. The incorporation of the drugs improved the characteristics of KGM microparticles compared to the unloaded KGM microparticles which production and characterisation is described in the previous chapter. Drug release was characterised in simulated lung fluid with both drugs showing biphasic profile with faster release of 60% of drug, followed by a slower release of the drug load within 24 h. Preliminary studies have shown the potential for biodegradation of KGM microparticles in the lung environment by β-mannosidase enzyme, which is necessary for safety. Despite preliminary, data pointing to the degradation of KGM in the lungs is a promising result, as one of the major limitations of pulmonary drug delivery is the narrow list of excipients approved so far. Data of formulation stability showed significant change of drug content under the conditions of the long-term assay, which requires further clarification and sets the need for further testing.

This page was intentionally left in blank

CHAPTER 5 - *IN VITRO* ANTIBACTERIAL ACTIVITY OF KONJAC GLUCOMANNAN MICROPARTICLES AGAINST MYCOBACTERIA

This page was intentionally left in blank

5. *In vitro* antibacterial activity of konjac glucomannan microparticles against mycobacteria

5.1. Materials and methods

5.1.1. Culture of mycobacteria

The antibacterial activity of free drugs and KGM/INH/RFB microparticles was studied against *Mycobacterium bovis* BCG (DSM 43990), provided as a gift by Centro de Estudos de Doenças Crónicas da Faculdade de Ciências Médicas da Universidade Nova de Lisboa (CEDOC/FCM-UNL). The stocks of mycobacteria were stored in – 80 ºC ultralow temperature freezers (U725 Innova New Brunswick Scientific, Edison, NJ, USA). Mycobacteria were grown in Middlebrook 7H9 (M7H9) medium supplemented with 10% (v/v) OADC (oleic acid, albumin, dextrose and catalase; Lenexa, KS, USA) and 0.05% (v/v) Tween® 80. The work with the cultures of *M. bovis* was performed using a Biosafety cabinet (Bio48 Faster, Cornaredo, Italy), according to operational standards and safety requirements to prevent human and environmental contamination.

5.1.2. Cell culture

THP-1 cells (human monocytic cell line) were obtained from Leibniz-Institut DSMZ (Braunschweig, Germany). The cells were cultured in RPMI 1640 medium supplemented with FBS (10%, v/v), PenStrep (1%, v/v) and L-Glutamine (1%, v/v), and grown in suspension with a cell density between 2.0×10^5 and 1.0×10^6 cells/mL. Upon reaching the higher concentration, cells were cultivated at the concentration of 2.0×10^5 cells/mL. THP-1 cells were incubated for 48 h with phorbol 12-myristate 13-aetate (PMA, 50 nM) to obtain the macrophage phenotype before performing the experiments. The cells were used between the passages 3-20.

5.1.3. Determination of the Minimum Inhibitory Concentration (MIC)

The determination of the Minimum Inhibitory Concentration (MIC) of INH and RFB, as free drugs, and KGM/INH/RFB microparticles was performed against *M. bovis* DSM 43990 using the broth microdilution technique. To determine the MIC, solutions of INH, RFB and KGM/INH/RFB microparticles were prepared at 1 mg/mL. While INH and KGM microparticles were solubilised in M7H9 supplemented medium, RFB was dissolved in 0.01M HCl. The INH and RFB solutions were diluted to the concentration of 0.25 µg/mL in M7H9 supplemented medium. Also, the solution of KGM microparticles was diluted in M7H9 supplemented medium considering the AE of RFB in each KGM/INH/RFB formulation. Then, flat-bottom 96-well plates (Sarsted, Nümbrecht, Germany) were prepared as depicted in Figure 5.1 with the previously prepared solutions. The M7H9 supplemented medium (180 µL) was distributed over all wells, except in column 4. In this column, as well as in column 5, 180 µL of INH, RFB or KGM/INH/RFB microparticles solutions at the highest concentration were added, allowing continuous serial two-fold dilutions with M7H9 supplemented broth from columns 4 to 11. After the preparation of the serial dilutions of the drugs and KGM microparticles in the 96-well plate, the bacterial suspension, prepared as described below, was added. Firstly, mycobacteria culture was centrifuged at 5 000 rpm for 10 min (Universal 320, Hettich Lab Technology; Tuttlingen, Germany) and the supernatant eliminated. The obtained pellet was re-suspended in 5 mL of M7H9 supplemented medium and the optical density value (OD) of the resultant bacterial suspension was determined by spectrophotometry (UV-1700 Pharmaspec; Shimadazu, Japan) at 600 nm. Then, 20 µL the mycobacterial suspension, with an OD of 0.2, were added to all the wells of the plate, except in column 2, which remained only with M7H9 supplemented medium (negative control). The mycobacterial suspension, without the presence of drugs or KGM microparticles, was the positive control (column 3). The outside lane of the 96-well plate was filled with distillate water (300 µL) to avoid the evaporation of the content. The wells were sealed with parafilm and placed in the incubator (Binder, Tempe, AZ, USA) at 37 ºC for one week.

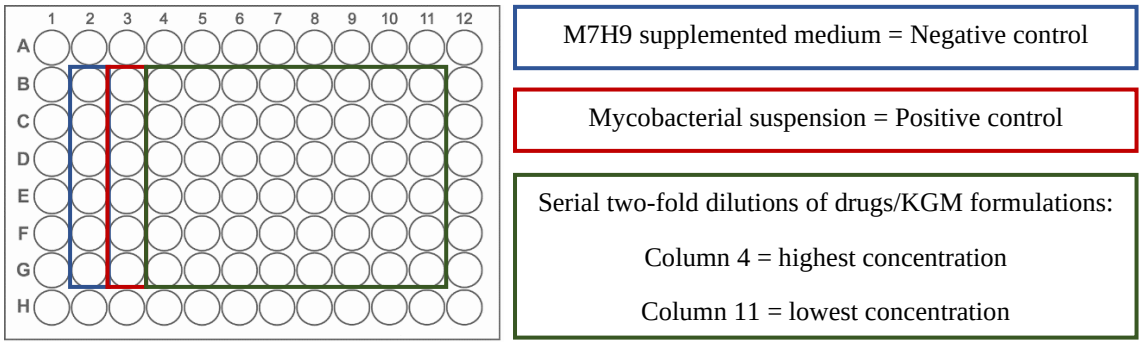

Figure 5.1. Scheme of the 96-well plate to determine the minimum inhibitory concentration (MIC) of free drugs and KGM/INH/RFB microparticles in *Mycobacterium bovis*.

After one week, 30 µL of 3-(4 5-dimethylthiazol-2-yl)-2 5-diphenyltetrazolium bromide (MTT) solution (5 mg/mL in PBS pH 7.4) were added to each well and the plate was incubated at 37 ºC for 2 h. After this period, 50 µL of DMSO were added, which induced a colour change from yellow to purple, suggesting the growth of *M. bovis*. The absorbance was quantified using a microplate reader (Infinite M200, Tecan; Männedorf, Switzerland) at 540 nm and the MIC value was considered the one that inhibited the mycobacterial growth between 95 and 100%. The MIC determination was performed in three replicates and, for each assay, two mycobacterial suspensions were prepared.

5.1.4. Evaluation of the antibacterial potential of KGM microparticles

5.1.4.1. Macrophage infection and quantification of bacteria survival

The infection of macrophages with *M. bovis* DSM 43990 was performed based on the protocol described by Nazarova & Russell, 2017.[164] Three days before the infection, THP-1 cells were seeded in 24-well plates at a cell density of 3.5 x 10^5 cells/mL using supplemented RPMI 1640 medium without antibiotics (PenStrep). Then, the plates were incubated for 48 h with PMA to allow cell differentiation into macrophages. The day before the infection, the cell culture medium (CCM) was replaced with 500 µL of fresh supplemented CCM without antibiotics and the plates were incubated for 24 h at 37 ºC. On the infection day, the mycobacterial culture was centrifuged at 5 000 rpm for 10 min (Universal 320, Hettich Lab

Technology; Tuttlingen, Germany), the supernatant discharged and the pellet re-suspended in M7H9 supplemented medium. Then, the OD value was measured by spectrophotometry (UV-1700 Pharmaspec; Shimadazu, Japan) at 600 nm. Considering that OD600=0.6 represents 1.0 x 10^8 bacteria/mL, the mycobacterial suspension was diluted in supplemented RPMI 1640 medium without antibiotics to reach a cell density of 1.0 x 10^8 bacteria/mL. Using a 1 mL tuberculin syringe with 26-gauge needle inserted, the bacterial suspension was passed in and out of the syringe for 15 times. Immediately, the volume of bacterial suspension required to obtain a multiplicity of infection (MOI) of 10:1 was added to each well pipetting up and down 5 times to mix the mycobacteria cells with the macrophage-like THP-1 cells. Then, the plates were kept under horizontal shaking (Orbital Shaker OS-10; Biosan, Latvia) at 100 rpm to increase the interaction between the cells and the bacteria. After 10 min, the plates were left inside a jar along with a sachet to create microaerophilic conditions (CampyGen™ 2.5L, Thermo Fisher Scientific, Porto Salvo, Portugal) and incubated at 37 ºC for 4 h. After the infection period, the medium was removed and replaced with 500 µL of solutions of INH and RFB or KGM/INH/RFB = 10/1/0.5 (w/w) microparticles dissolved in supplemented CCM without antibiotic. Both drugs and microparticles were dissolved at concentrations corresponding to the MIC values previously determined. Untreated infected cells were used as negative control. The infected macrophage-like THP-1 cells were incubated for 48 h, 72 h, 96 h, 7 days and 9 days at 37 ºC in microaerophilic conditions, as described above. The CCM was replaced each two days maintaining the free drugs and KGM microparticles solutions with the MIC values.

After the respective incubation periods, the infected macrophage-like THP-1 cells were washed with 1 mL of cold PBS and lysed using a solution of Triton X-100 (0.1%, v/v). The plates were incubated for 10 min at 37 ºC to allow the lysis of the infected cells.

Upon the macrophage lysis, the resultant suspension of cells and bacteria were centrifuged (16000 x g, 5 min; Heraeus Fresco 17 centrifuge; Thermo Scientific, Germany) and the supernatant discharged. The pellet was resuspended in 30 mL of MTT solution (5 mg/mL in PBS pH 7.4) and the suspension was added to a 96-well plate. The plate was incubated overnight at 37 ºC. After the incubation time,

50 µL of DMSO were added to each well to solubilise the MTT crystals, and the viable bacteria quantification was performed by spectrophotometry at 540 nm using a microplate reader (Infinite M200, Tecan; Männedorf, Switzerland).

5.1.4.2. Fluorescence microscopy

To observe the cells by fluorescence microscopy, the pellet resulting from centrifugation was resuspended in a glutaraldehyde solution (20%, v/v) to fix the cells. Then, in order to distinguish the viable and non-viable bacteria, the fixed suspension was stained using a LIVE/DEAD® BacLight™ Bacterial Viability kit (Thermo Fisher Scientific, Porto Salvo, Portugal) in a 1:1 dilution. The viable cells were stained in green by SYTO9 and the dead cells in red by propidium iodide, two components of the bacterial viability kit.

5.1.5. Impact of the continued exposure to drug-loaded microparticles

In 15 mL tubes, cultures of *M. bovis* (5 mL) were exposed to free INH, RFB and INH/RFB, and also to KGM/INH/RFB = 10/1/0.5 (w/w) microparticles at concentrations corresponding to the MIC values previously determined for 7 days. Each day, the mycobacterial cultures were centrifuged at 5 000 rpm for 10 min (Universal 320, Hettich Lab Technology; Tuttlingen, Germany), and the supernatant discharged. The pellet was resuspended in free drugs and KGM microparticles solutions after their solubilisation in M7H9 supplemented medium using the MIC values. Upon one week, the bacterial growth was quantified by MTT following the protocol described in section 5.1.3.

5.1.6. Statistical analysis

The t-test and one-way analysis of variance (ANOVA) with the pairwise multiple comparison procedure (Holm-Sidak method) were performed to compare two or multiple groups, respectively. All analyses were run using the GraphPad Prism®

statistical program (Version 6.01) and differences were considered to be significant at a level of $p < 0.05$.

5.2. Results and discussion

5.2.1. Determination of Minimum Inhibitory Concentration (MIC)

The MIC is defined as the lowest concentration of drug inhibiting 95%-100% of the growth of the wild type strains of bacteria, *M. tuberculosis* in this case, which were never exposed to a specific drug or formulation.[165] To analyse the potential of KGM microparticles against mycobacteria, the values of MIC were first determined for *M. bovis*. Mycobacterial cultures were exposed to free drugs (Table 5.1) and KGM microparticles (Table 5.2) and the mycobacteria viability exposed to the samples was determined by comparison with the untreated bacteria, which were considered as 100% of bacterial growth.

When INH and RFB were tested individually, the MIC of RFB was lower than that of INH, 0.016 and 0.250 µg/mL, respectively (Table 5.1). The obtained MIC for INH and RFB in this work are similar to the values reported in other studies,[145,166] although the MIC could be different depending on the *M. bovis* strain and on the method to determine the susceptibility.[145] In all tested combinations of INH/RFB, the MIC of RFB remained constant at 0.016 µg/mL (Table 5.1). In turn, MIC values of INH significantly decrease when comparing with values of the drug tested alone ($p < 0.05$), suggesting that INH antibacterial activity could be potentiated when the two antitubercular drugs are applied in combination.

Table 5.1. Minimum Inhibitory concentration (MIC) of isoniazid (INH) and rifabutin (RFB) as free drugs for *Mycobacterium bovis* DSM 43990. Data are presented as mean ± SEM (n = 12). Different letters represent significant differences in each parameter ($p < 0.05$).

Drugs	MIC (µg/mL)
INH	0.250^{a}
RFB	0.016^{b}
INH/RFB (1/0.5, w/w)	0.031^{c}/0.016^{b}
INH/RFB (1/1, w/w)	0.016^{d}/0.016^{b}
INH/RFB (2/0.5, w/w)	0.063^{e}/0.016^{b}

Considering that RFB had a stronger antibacterial activity than INH, probably due to the higher lipophilicity that facilitates its internalisation through the cell membrane,[167,168] the MIC determination for the KGM/INH/RFB microparticles was performed considering the loading of RFB in KGM microparticles. The MIC value of the three formulations was the same that was obtained for the combination of the free drugs. While the MIC of RFB remained in 0.016 µg/mL, the MIC of INH varied according to its concentration (Table 5.2). These results suggest that the spray-drying process did not affect the antibacterial activity of the drugs when they were incorporated into the KGM microparticles and that the KGM/INH/RFB microparticles have the capacity to inhibit the growth of the *M. bovis* DSM 43990.

Table 5.2. Minimum inhibitory concentration (MIC) of drug-loaded konjac glucomannan (KGM) microparticles for *Mycobacterium bovis* DSM 43990. Data are presented as mean ± SEM (n = 12). Different letters represent significant differences in each parameter ($p < 0.05$).

KGM/INH/RFB (w/w)	INH (µg/mL)	RFB (µg/mL)
10/1/0.5	0.031^{a}	0.016^{d}
10/1/1	0.016^{b}	0.016^{d}
10/2/0.5	0.063^{c}	0.016^{d}

5.2.2. Evaluation of the antibacterial potential of KGM microparticles

Mycobacteria are pathogens that can survive and replicate inside alveolar macrophages. Consequently, the successful of an approach targeted to these cells to treat pulmonary tuberculosis depends not only on the ability of microparticles to reach the alveolar region, but also on the capacity of the drugs to maintain the antibacterial activity against the bacteria after the microencapsulation. To evaluate the potential of KGM microparticles against internalised mycobacteria, macrophage-like THP-1 cells were infected with *M. bovis* DSM 43990 and the infected cells were exposed to the free drugs (INH/RFB; 1/0.5, w/w) and the KGM/INH/RFB = 10/1/0.5 (w/w) microparticles at the concentrations corresponding to the MIC values previously determined. Unfortunately, the assay was performed on a single occasion only and, therefore, the data must be analysed as preliminary.

Over 9 days, the percentage of *M. bovis* DSM 43990 released from the infected cells upon lysis was quantified and, contrary to the expectations, the exposure to free drugs and drug-loaded KGM microparticles did not prevent bacteria to survive in the macrophages (Figure 5.2). For 7 days there were no significant differences in the percentage of bacteria released from the cells, only on the ninth day of exposure the percentage of released bacteria was significantly lower compared with 48 h of exposure ($p < 0.05$; Figure 5.2).

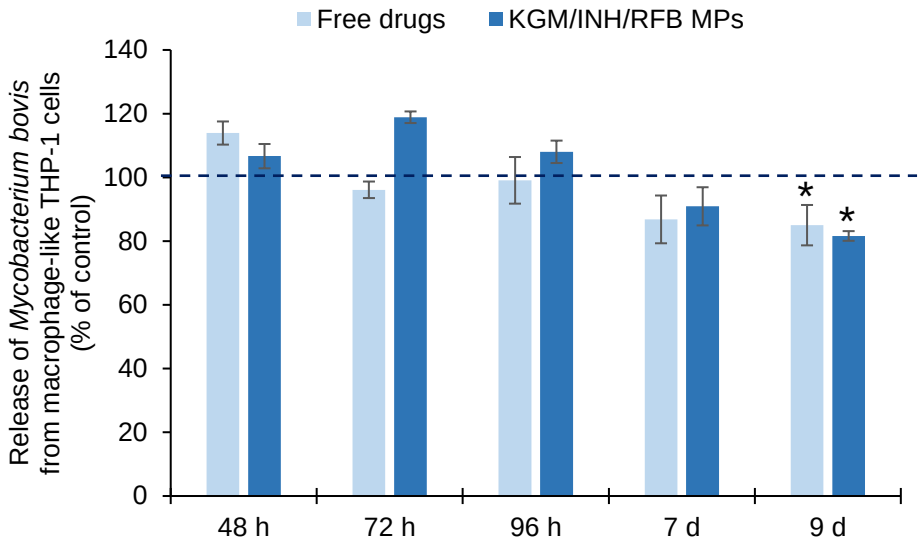

Figure 5.2. Percentage of *Mycobacterium bovis* DSM 43990 after their release from macrophage-like THP-1 cells over 9 days of exposure. Data are presented as mean ± SEM (n = 1). Statistical significance levels are indicated as *p < 0.05 compared with the time of 48 h.

In parallel with the quantification of the surviving bacteria upon macrophage-like THP-1 cells infection, the samples were also fixed and stained with LIVE/DEAD® kit and observed by epifluorescence microscopy, enabling identifying the bacterial metabolic state. While the viable cells stain green (due to the entry of SYTO9 into the bacterial cells), the dead cells exhibit red staining (due to the faster entry of propidium iodide). Regardless of the exposure time, no differences were observed in the number of viable bacteria (green) released from the cells (Figure 5.3), which are according with the obtained data of the released bacteria from macrophage-like THP-1 cells quantified by MTT, where the number of viable bacteria was similar throughout the study, except at the ninth day.

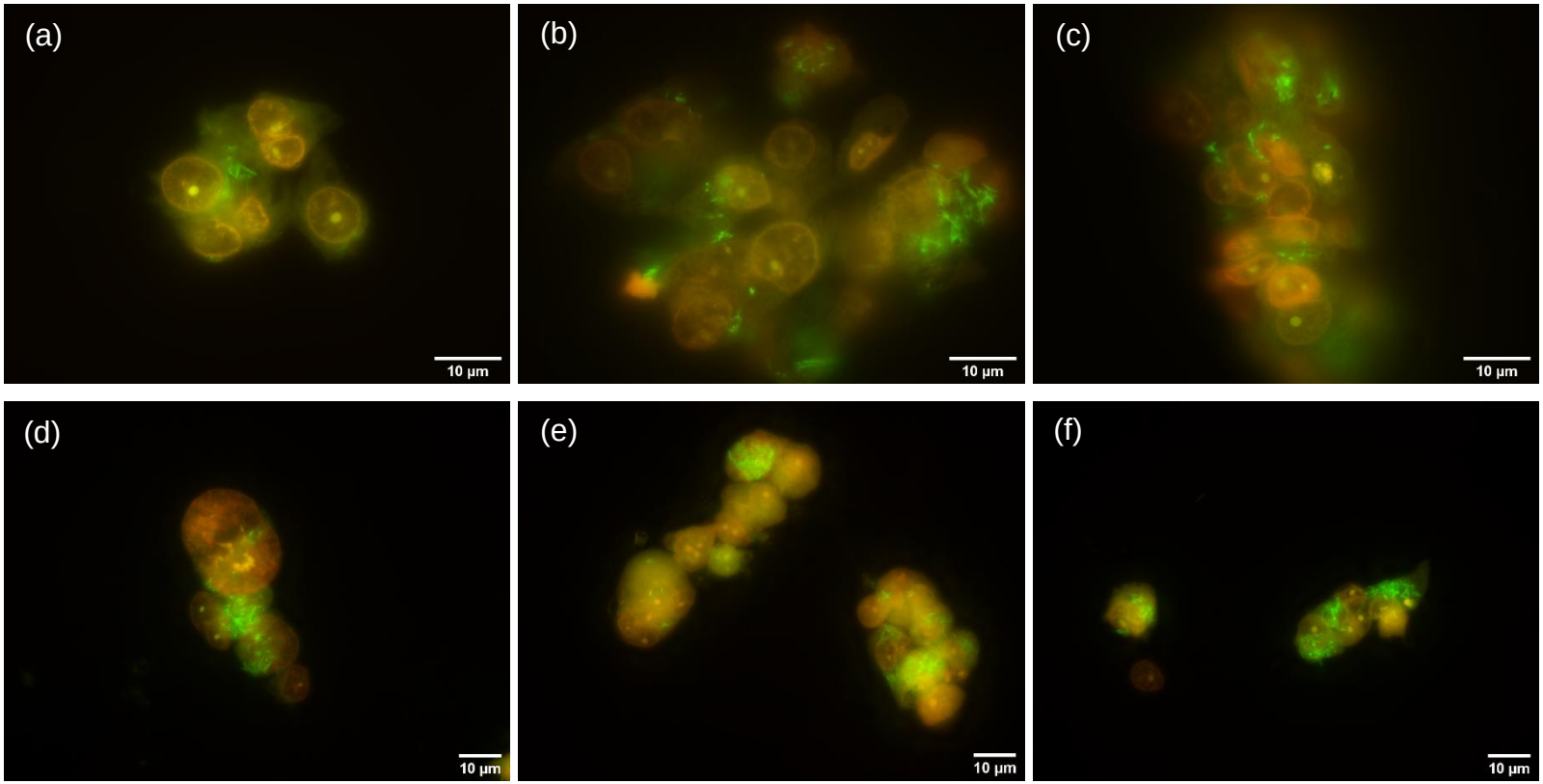

Figure 5.3. Representative images of fluorescence microscopy of released *Mycobaterium bovis* DSM 43990 from macrophage-like THP-1 cells. The cells were stained with a bacterial viability kit, which assessed the viable cells in green (SYTO9) and the dead cells in red (propidium iodide), upon (a) 48 h with cell culture medium (CCM), (b) 48 h with isoniazid (INH)/rifabutin (RFB), (c) 48 h with KGM/INH/RFB = 10/1/0.5 (w/w), (d) 7 days with CCM, (e) 7 days with INH/RFB and (f) 7 days with KGM/INH/RFB = 10/1/0.5 (w/w). Original magnifications: upper panels ×100; lower panels ×63. Scale bar = 10 μm.

The expectation was that the presence of drugs or KGM microparticles was sufficient to reduce the number of bacteria inside the macrophages, since the concentration used in the exposure after the infection was previously determined (MIC) and had the capacity to inhibit 95% of mycobacterial growth. However, it was not possible to confirm this in the present assay. A possible explanation to these data could be related with the ability of bacteria to become resistant. During the exposure, the medium was changed every two days, a period perhaps too long taking into consideration the required daily treatment in a tuberculosis infection. During the extra 24 h the mycobacteria were able to oppose the previous exposure to the drugs and even become resistant to the tested drugs. Another hypothesis to explain the observed results is the limited access of both drugs to the mycobacteria, either because the drugs or the microparticles were not internalised by the macrophages, or the drugs were not completely released from KGM microparticles. However, and as mentioned above, these results are preliminary, and the protocol needs to be optimised to establish a suitable concentration and exposure time to reach the maximum potential of KGM microparticles against mycobacteria.

5.2.3. Impact of the continued exposure to drug-loaded microparticles

Often, *M. tuberculosis* develops its own mechanisms of resistance to antitubercular drugs, which may result in the emergence of MDR-TB. The exposure of bacteria to antibiotics may result on the development of resistance[169] and, thus, it is relevant to verify the impact of microencapsulated forms of the drugs in the mycobacteria. During 7 days, *M. bovis* was exposed to the free drugs and KGM/INH/RFB = 10/1/0.5 (w/w) microparticles at concentrations corresponding to the MIC values determined previously, and the growth inhibition of bacteria quantified by MTT.

Upon 7 days of a daily exposure, it was evident the development of resistance to the samples, especially to free INH (Table 5.3). When the mycobacteria were exposed to free INH, this drug inhibited the growth of the bacteria only in 16%. On the other hand, despite the inhibition percentage induced by RFB decreased in this study compared to the MIC values previously determined (87% and > 95%,

respectively), the mycobacteria have shown to be more susceptible to this drug than INH. These data are concordant with data reported on resistance to antibiotics. The rate of reported cases of resistance is higher for INH, in comparison with other antitubercular drugs.[42,170] Furthermore, when both drugs were tested together, there was a synergic effect and the capacity of INH and RFB to inhibit the growth of *M. bovis* DSM 43990 increased with the percentage of inhibition, reaching 96% (Table 5.3). The mycobacteria were unable to resist the antibacterial activity of the drugs when they were exposed to the combination of both drugs. Regarding KGM/INH/RFB microparticles, the antibacterial efficacy of the microparticles against *M. bovis* decreased upon 7 days of continued exposure. During the MIC determination assay, the same concentration of KGM microparticles inhibited the mycobacterial growth by 95%, however, in this assay the inhibition of the mycobacterial growth decreased to 89% (Table 5.3).

Table 5.3. Inhibition of the growth of *Mycobacterium bovis* DSM 43990 determined after a daily exposure to isoniazid (INH) and rifabutin (RFB) as free drugs and KGM/INH/RFB = 10/1/0.5 (w/w) microparticles for a period of 7 days. Data are presented as mean ± SEM (n = 3).

	***Mycobacterium bovis* growth inhibition (%)**
INH	15.9 ± 1.2
RFB	87.0 ± 1.2
INH/RFB	96.1 ± 0.6
KGM/INH/RFB = 10/1/0.5 (w/w)	89.0 ± 3.2

After 7 days of a continued exposure to free drugs and KGM microparticles the inhibition percentage of growth was lower than 95%, except when the mycobacteria were exposed to the INH/RFB combination. Analysing the data as preliminary results, these suggest that *M. bovis* DSM 43990 developed resistance to the antibiotics and the KGM/INH/RFB formulation. If the exposure time was extended, with high probability the inhibition percentage of growth would continue decreasing along the time. Therefore, the study must be repeated, and the exposure time should be increased to evaluate the real impact of the continued exposure to KGM microparticles in mycobacteria.

5.3. Conclusions

For the successful therapy of an infectious disease, it is important that the drugs maintain their antibacterial activity against the pathogen when they reach the infection site. Despite the spray-drying process did not affect the antibacterial activity of INH and RFB when the drugs were incorporated into KGM microparticles, data obtained using *M. bovis* DSM 43990 suggested the development of resistance upon daily exposure to microencapsulated drugs. Upon 7 days of exposure to the free drugs and drug-loaded KGM microparticles, the inhibition percentage of mycobacteria growth decreased to values below of 95%, i.e., the concentration of drugs, microencapsulated or free, needed to inhibit the growth of *M. bovis* was higher than in the assay of MIC determination. Also, data obtained upon the infection of macrophage-like THP-1 cells may suggest a possible resistance of *M. bovis* to the drugs and KGM microparticles, since the number of viable bacteria surviving inside the cells was very similar over the study. However, on the other hand, the fact that the number of viable bacteria remains almost the same after the lysis of the infected cells could be due to other reasons instead of an acquired drug resistance, such as the limited access of *M. bovis* to the drugs. A deficient internalisation of KGM/INH/RFB microparticles by macrophages is a possible cause that could explain why the *M. bovis* DSM 43990 survived to the drugs in free and microencapsulated form. Nevertheless, these are preliminary results and further studies must be performed to clarify the real potential of KGM microparticles against mycobacteria.

This page was intentionally left in blank

CHAPTER 6 - *IN VITRO* AND *IN VIVO* SAFETY PROFILE OF KONJAC GLUCOMANNAN MICROPARTICLES AND INTERACTION WITH MACROPHAGES

This page was intentionally left in blank

6. *In vitro* and *in vivo* safety profile of konjac glucomannan microparticles and interaction with macrophages

6.1. Materials and methods

6.1.1. Cell culture

A549 cells (human alveolar epithelial adenocarcinoma) and THP-1 cells derived from a human monocytic cell line, were provided by the American Type Culture Collection (ATCC, Middlesex, UK) and used to analyse in vitro the cytocompatibility of drugs, raw material (KGM) and microparticle formulations. Cells were cultured in 75 cm^2 flasks in a 5% CO2/95% humidified atmospheric air incubator at 37 ºC. A549 cells were maintained in culture in Dulbecco's Modified Eagle's Medium (DMEM) supplemented with FBS (10%, v/v), PenStrep (1%, v/v), L-Glutamine (1%, v/v) and non-essential amino acids (1%, v/v). CCM was exchanged every 2-3 days and the cells were sub-cultivated weekly. A549 cells were used between the passages 25-36. Regarding THP-1 cells, these were cultured as described in section 5.1.2.

6.1.2. Evaluation of cytocompatibility

6.1.2.1. Metabolic activity

The metabolic activity of the cells upon a specific exposure time to free drugs, KGM and KGM microparticles was analysed using the MTT assay. Thus, samples of KGM and KGM microparticles were solubilised in CCM without FBS at 2 000 µg/mL, representing the highest concentration assessed in the assay. From this concentration, a serial dilution of 1:2 was performed, and different concentrations tested (31.25 - 2 000 µg/mL). The toxicological profile of free drugs was also evaluated at concentrations similar to those corresponding to the three drug-loaded KGM microparticles. While INH was directly solubilised in CCM, RFB was previously solubilised in 0.01M HCl (7.5 mg/mL) and diluted in CCM to reach the desired concentrations. The cell viability was assessed in A549 and macrophage-like THP-1 cells after a period of exposure of 3 h and 24 h. To perform the assay, A549 and THP-1 cells were seeded in 96-well plates at a cell density of 1 x 10^4

cells/well and 3.5 x 10^5 cells/mL, respectively, and the plates were incubated at 37 ºC and 5% CO_2/95% humidified atmospheric air. While A549 cells were incubated only for 24 h to assure cell adherence to the plates, THP-1 cells were incubated for 48 h with PMA (50 nM) to allow the differentiation required to acquire the macrophage-like phenotype. After the referred periods, CCM was removed and replaced by 100 µL of each sample, and incubation allowed for 3 h and 24 h. CCM was used as a positive control of cell viability and sodium dodecyl sulphate (SDS; 2%, v/v) as negative control. After the exposure time, the samples were removed and 30 µL of MTT solution (5 mg/mL in PBS pH 7.4) added to each well. Upon 4 h of incubation, the MTT was replaced by 100 µL of SDS 10% (v/v) in a 1:1 mixture of DMF:water, and the plates were incubated at 37 ºC overnight in order to solubilised formazan crystals. The absorbance was measured by spectrophotometry (Infinite M200, Tecan; Männedorf, Switzerland) at a wavelength of 570 nm, with the application of background correction at 650 nm. Cell viability (%) was calculated using the following equation:

$$\text{Cell viability} = \left(\frac{\text{A} - \text{S}}{\text{CM} - \text{S}}\right) \times 100$$

Where A is the absorbance obtained for each of the concentrations of the test substance, CM is the absorbance obtained for untreated cells (incubated with CCM only) and S is the absorbance obtained for 2% SDS. The CM reading was assumed to correspond to 100% cell viability. The assay was performed on three occasions with six replicates at each concentration of test substance in each instance.

6.1.2.2. Cell membrane integrity

The integrity of cell membrane was evaluated by measuring the amount of lactate dehydrogenase (LDH) in the supernatant of the A549 and macrophage-like THP-1 cells exposed for 24 h to the free drugs, KGM and KGM microparticles. The LDH assay was performed simultaneously with the MTT assay. However, only the released LDH induced by the exposure to the concentrations of 500 and 1 000 µg/mL of KGM samples tested in MTT assay was analysed. The release of LDH induced by exposure to INH and RFB as free drugs was also evaluated at

concentrations similar to those corresponding to microparticle drug loading. After 24 h of exposure, 75 µL of the cell supernatant were collected from each well, centrifuged (16000 x g, 5 min; Heraeus Fresco 17 centrifuge; Thermo Scientific, Germany) and placed on a 96-well plate. CCM was used as a negative control of LDH release, while Triton X-100 (dilution 1:10, v/v) was used as positive control and assumed as the 100% of release of LDH. Then, to each well were added 75 µL of the LDH reagent from the kit (TaKaRa; Tokyo, Japan) following the indications of the supplier. The LDH reaction was stopped by the addition of 37.5 µL/well of 1M HCl. The samples were analysed spectrophotometrically at 490 nm using background correction at 690 nm (Infinite M200, Tecan; Männedorf, Switzerland). The release of LDH (%) was measured using the following equation:

$$\text{LDH release} = \left(\frac{\text{A}}{\text{CM}}\right) \times 100$$

Where A represents the absorbance obtained for the LDH released by the cells exposed to the test substance and CM is the absorbance obtained for untreated with cells (incubated with CCM). The assay was performed on three occasions with three replicates at each condition.

6.1.3. Macrophage activation

The activation of macrophages was evaluated by measuring the amount of TNF-α and interleukin 8 (IL-8) produced by macrophage-like THP-1 cells after exposure to either KGM or KGM microparticles (KGM/INH/RFB = 10/1/0.5, w/w). THP-1 cells were seeded in 96-well plates at a density of 3.5 x 10^5 cells/mL and incubated for 48 h in the presence of 50 nM PMA to assure the differentiation of the cells into macrophages. KGM and KGM microparticles were solubilised in CCM at the concentration of 1 mg/mL and incubated with the cells (100 µL/well) after media removal. CCM was used as a negative control and lipopolysaccharide (LPS, 100 µg/mL) as a positive control. After 24 h of incubation with the samples, the cell supernatants were collected and TNF-α and IL-8 quantified with ELISA kits (Quantikine® HS, R&D Systems, Minneapolis, MN, USA) following the supplier indications. The amount of each cytokine was quantified by measuring

the absorbance at 450 nm with a background correction at 540 nm (Infinite M200, Tecan; Männedorf, Switzerland). The produced levels of TNF-α and IL-8 were expressed in pg/mL based on reference standard curves.

6.1.4. Uptake of konjac glucomannan microparticles by macrophages

6.1.4.1. Labelling of poly(vinyl alcohol) and konjac glucomannan

Poly(vinyl alcohol) (PVA; Sigma-Aldrich, Germany) and hydrolysed KGM were labelled with fluorescein prior to the production of the fluorescent microparticles to be used in the evaluation of the uptake by macrophages. To prepare the fluorescent polymers, PVA and KGM (500 mg) were inserted in two round bottom flasks and solubilised in 50 mL of 10^{-4} M HCl (pH = 4) to a final concentration of 1% (w/v). To help the solubilisation of PVA, the dispersion was placed in a water bath at 80 ºC for 2 h. The amount of fluorescein needed to label each polymer was calculated according to the number of hexoses in the respective structures. To label PVA, 21.5 mg of fluorescein (Sigma-Aldrich, Germany) were dissolved in 8 mL of 70% ethanol and added to the PVA dispersion, along with 16.5 mg of 1-ethyl-3-(3-dimethylaminopropyl) carbodiimide (EDAC; Sigma-Aldrich, Germany) dissolved in 8 mL of ultrapure water. Regarding to the KGM, 24 mg of fluorescein and 15 mg of EDAC were dissolved in 8 mL of 70% ethanol and ultrapure water, respectively, and added to the KGM dispersion. After 72 h under stirring and protected from the light, the PVA and KGM dispersions were transferred to a dialysis membrane (Sigma Aldrich, Germany; Mw cut off of 2000 Da) to eliminate unreacted fluorescein and other reaction sub products and maintained in water for approximately one week. During that time, the water resulting from the dialysis was changed twice daily. Finally, both suspensions were placed in 50 mL tubes and placed at -20 ºC. After initial freezing, samples were placed at -80 ºC overnight and finally lyophilized for 48 h (FreeZone Benchtop Freeze Dry System, LABCONCO, USA). The obtained fluorescent polymers were stored in a desiccator until the production of the respective microparticles by spray-drying.

6.1.4.2. Preparation of fluorescently-labelled poly(vinyl alcohol) and konjac glucomannan microparticles

Fluorescently-labelled PVA was milled in a glass mortar and solubilised in ultrapure water at a final concentration of 2% (w/v). The PVA dispersion was transferred to a water bath at 80 ºC and was maintained under stirring until complete dissolution was observed. After that, the dispersion was spray-dried (Buchi B-290 Mini Spray Dryer; Buchi Labortechnik AG, Switzerland) at an inlet temperature of 155 ºC, setting the aspirator at 80%, the fluid flow rate at approximately 1 mL/min and the spray flow rate at 473 L/h. Regarding to the production of fluorescently-labelled KGM microparticles, these were obtained following the same conditions and spray-drying parameters described in section 3.1.2. to produce the unloaded KGM microparticles.

6.1.4.3. Uptake of konjac glucomannan microparticles by macrophages

To determine the uptake of KGM microparticles by macrophage-like cells, differentiated THP-1 cells were exposed to the fluorescently-labelled microparticles. To do so, THP-1 cells were seeded in Petri dishes (35 mm diameter) containing 3 mL of the respective medium (medium detailed in section 5.1.2.) at the concentration of 3.5 x 10^6 cells/mL. The cells were incubated with PMA for 48 h to assure their differentiation into the macrophage phenotype. After differentiation, the CCM in the dishes was removed and the KGM microparticles aerosolised onto the cell layer using a Dry powder Insufflator™ (Model DP-4, Penn-Century™, Wyndmoor, PA, USA). The cells were exposed to two different doses of microparticles, 100 and 300 µg/cm^2, for a period of 2 h, being incubated at 37 ºC. Similar conditions were used to assess fluorescently-labelled PVA microparticles, which were used as negative control in the assay. After the exposure time of 2 h, cells exposed to PVA or KGM microparticles were washed with 5 mL of cold PBS supplemented with 3% FBS (PBS.3% FBS, v/v) for three times. Then, the cells were scraped and centrifuged (1500 rpm, 4 min, room temperature) in 2 mL of PBS.3% FBS. The cells supernatant was discharged, and the cell pellet re-suspended in 5 mL of PBS.3% FBS. This process was repeated for three times. After the last centrifugation, the cell supernatant was

removed and the pellet re-suspended and incubated with the APC-CD11b antibody (1:100 dilution in PBS.3% FBS) for 1 h on ice. After the period of incubation, 5 mL of PBS.3% FBS were added to the cells and a final cycle of centrifugation applied. The supernatant was removed and the cells re-suspended in 1 mL of PBS.3% FBS. The cell suspension was transferred to cytometry tubes (BD Biosciences) and maintained on ice until the cytometric analysis was performed (BD Biosciences FACSCalibur, Belgium).

Flow cytometry was used to quantify the percentage of cells phagocytosing the fluorescently-labelled microparticles. Forward scatter height (FSC-H) and side scatter height (SSC-H) channels were used to measure size and granularity of cells, respectively. In parallel, scatter light was used to identify the population of viable cells. A total of 10 000 events were counted for each sample and cells exhibiting a double fluorescent signal (APC from antibody and FITC from labelled microparticles) were considered as those phagocytosing the microparticles. The analysis was replicated three times for each dose.

6.1.5. In vivo evauation of safety

6.1.5.1. Animals

Male BALB/c mice (21-27 days) were purchased to Charles River (France). The animals were maintained in standard hygienic conditions with access to commercial chow and acidified drinking water *ad libitum*. All the experiments performed with the animals were approved by the ethical committee of the Faculty of Pharmacy of the University of Lisbon in accordance with the European Union Directive (2010/63/EU) and Portuguese laws (DL 113/2013, 2880/2015, 260/2016 and 1/2019) for the use and care of animals in research.

6.1.5.2. Pulmonary administration

Animals (6-8 weeks; 22-28 g), were divided in three groups, each composed of six animals, corresponding to naïve (control), KGM 1x and KGM 10x. Animals pertaining to the group KGM 1x were exposed to a single dose of KGM

microparticles (acute exposure), while those of group KGM 10x received ten doses of microparticles over 2 weeks (subacute exposure). Unloaded KGM microparticles were used for this effect. The naïve group received no treatment. The administration of the dry powders corresponding to KGM microparticles was performed using a simple home-made apparatus. Briefly, mice were restrained in a 50 mL tube and their nose positioned in a small hole in the bottom of the tube to promote powder inhalation. The lower part of the 50 mL tube was connected to a 15 mL tube using a baby bottle teat. KGM dry powder was weighed in the 15 mL tube and delivered using a small pump connected to the upper part of the tube creating an air stream that allows the aerosolisation of the powder (Figure 6.1). Each delivered dose comprised 60 mg of unloaded KGM microparticles to which mice were exposed during 2 min. Previous experiments demonstrated that only about 10% of the powder is in fact inhaled by the animals, thus resulting in an approximate dose of 240 mg/kg.[171] The weight of the animals was registered before each administration.

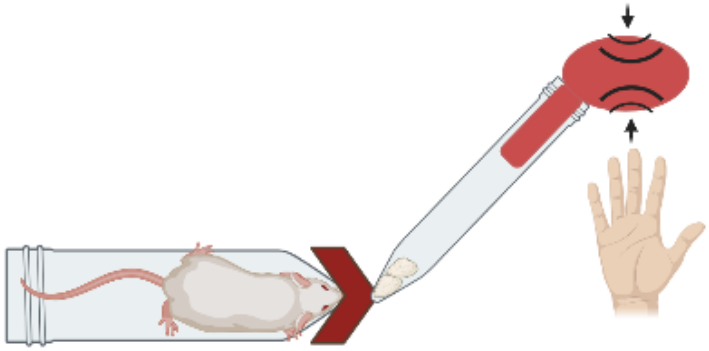

Figure 6.1. Illustration of the pulmonary administration of unloaded konjac glucomannan (KGM) microparticles to mice. KGM microparticles were weighed in a 15 mL tube and dispersed. The dispersion of the powder allowed its inhalation by mice placed in a 50 mL tube. Created in BioRender.com.

One day after the last administration, animals from all groups were anesthetised with isoflurane (IsoVet® 1000 mg/g, Piramal Healthcare, UK) and blood subsequently extracted from the retinal blood vessels (retro-orbital bleeding technique). The blood was collected to vials containing ethylene diamine tetra acetic acid (EDTA). The animals were sacrificed by cervical displacement under anaesthesia and organs of relevance collected and stored for further analysis,

including liver, spleen, lung, and kidneys. The bronchoalveolar lavage fluid (BALF) was also collected, according to the procedure detailed below.

6.1.5.3. Bronchoalveolar lavage

In order to collect the BALF, the lavage was performed based on the protocol proposed by Van Hoecke *et al*.[172] After animal sacrifice, 700 µL of sterile balanced salt solution with 100 µM of EDTA were injected through the trachea and then collected to a 15 mL tube, which was then placed on ice. The lavage was repeated three times. The collected BALF was then centrifuged for 7 minutes at 400 x g and 4 ºC, and the supernatant collected and stored at - 80 ºC for further analysis.

6.1.5.4. *In vivo* safety evaluation

The safety of the unloaded KGM microparticles was evaluated based on several parameters quantified in blood and BALF samples (leucocyte counts, IgE, LDH, total protein) and also on the histological analysis of the collected organs.

6.1.5.4.1. Leucocyte count and diferentiation

Blood samples from the mice of the various groups were collected and analysed to determine the leucocyte count and differentiation (DNAtech, Lisbon, Portugal).

6.1.5.4.2. IgE evaluation

The analysis of IgE levels in plasma and BALF samples collected from mice was performed using a mouse immunoglobulin E (IgE) kit (RayBiotech; Norcross, GA, USA), following the indications of the supplier. Plasma samples were obtained after blood centrifugation (2 000 g, 10 min) in a refrigerated centrifuge, Sigma-

202 MK and diluted 1:100, while the BALF samples were applied without any dilution.

6.1.5.4.3. LDH quantification

LDH release assay was performed in BALF samples collected from mice. BALF (75 µL) was placed on a 96-well plate and 75 µL of the LDH reagent (LDH determination kit, TaKaRa, Japan) was added to each well following the indications of the supplier. The LDH reaction was stopped by the addition of 37.5 µL of 1 M HCl after 20 min of incubation protected from light at room temperature. The samples were analysed spectrophotometrically at 490 nm and background corrected at 690 nm (Infinite M200, Tecan; Männedorf, Switzerland). The released LDH (%) was determined by application of the following equation:

$$\text{LDH release} = \left(\frac{\text{A}}{\text{CM}}\right) \times 100$$

Where A represents the absorbance obtained in the wells corresponding to the groups exposed to KGM (1x or 10x) and CM is the absorbance obtained for naïve group (control group). The assay was performed in duplicate.

6.1.5.4.4. Total protein quantification

The levels of total protein were analysed in BALF samples collected from mice, using the Bradford assay (Bio-Rad; Algés, Portugal) and following the indications of the supplier. Eighty µL of BALF samples were placed on a 96-well plate and 20 µL of reagent added to each well. After 5 min of incubation protected from light, the samples were analysed spectrophotometrically at 595 nm (Infinite M200, Tecan; Männedorf, Switzerland) and the total amount of protein quantified using a calibration curve (0-160 µg/mL) with bovine serum albumin as standard.

6.1.5.4.5. Tissue Index

The organs of interest such as liver, spleen, lung, and kidneys were collected after sacrifice and weighed. The respective tissue index (%) was determined according to the following equation and comparisons established with the naïve group (control group)[171]:

$$\text{Tissue index} = \sqrt{\frac{\text{Organ weight}}{\text{Animal weight}}} \times 100$$

6.1.5.4.6. Histology

Lungs were collected and stored in formalin solution (10%, v/v; Sigma-Aldrich, Germany) for subsequent histological analysis. These were performed at the Instituto Nacional de Investigação Agrária e Veterinária (INIAV), I.P. (Lisbon, Portugal).

6.1.6. Statistical analysis

The t-test and one-way analysis of variance (ANOVA) with the pairwise multiple comparison procedure (Holm-Sidak method) were performed to compare two or multiple groups, respectively. All analyses were run using the GraphPad Prism® statistical program (Version 6.01) and differences were considered to be significant at a level of $p < 0.05$.

6.2. Results and discussion

6.2.1. Evaluation of cytocompatiblity

6.2.1.1. Metabolic activity

Considering that this work proposes an inhalable therapy of lung tuberculosis in which drug carriers are targeted to the alveolar macrophages, the host cells of *M. tuberculosis*, it was deemed relevant to evaluate the cytocompatibility of the

carriers in cells relevant to that specific context. A549 cells, representative of the alveolar epithelium, and macrophage-like THP-1 cells were selected for the purpose. The cell viability was evaluated through the quantification of the cell metabolic activity (MTT assay) upon exposure to drug-loaded microparticles. Free drugs (INH and RFB) and the microparticle matrix material (KGM) were also evaluated as controls. The MTT assay is based on a colorimetric method that relies on the enzymatic reduction of the yellow tetrazolium salt, MTT, by enzymes present only in metabolically active cells, to form purple formazan crystals. After the solubilisation of these crystals, a coloured solution is produced that might be analysed by spectrophotometry. The intensity of the colour depends on the formazan concentration and is assumed as directly proportional to the number of viable cells.[173]

Exposure periods of 3 h and 24 h were chosen to perform the assay. The period of 3 h is considered of short-term contact but is a period ensuring the phagocytosis of the great majority of particles by the macrophages in the lungs after inhalation.[174] In turn, 24 h comprise a more prolonged time of exposure, necessary to evaluate cytotoxic events. INH and RFB were tested as free drugs in concentrations that were calculated to represent those present in the drug-loaded microparticles (~3 – 400 µg/mL), considering the concentrations of these tested in the MTT assay. The assessment of KGM and KGM microparticles was performed at seven different concentrations, the highest being 2 000 µg/mL and serial dilutions of 1:2 being then applied. The obtained data are described below.

INH was tested at a maximum concentration of 400 µg/mL, while this was of 200 µg/mL for RFB, respecting the amounts loaded in the microparticles. Figure 6.2a depicts the results obtained after an exposure of 3 h to the free drugs, generally revealing an absence of effect of the drugs on cell viability in both cell lines. In fact, cell viability remained approximately at 70% or higher in all tested conditions, this value representing the threshold below which a cytotoxic response is considered, according to ISO 10993.[175] Nevertheless, a slight tendency for cell viability decrease was observed upon exposure of A549 cells to the higher concentrations of RFB.

The prolongation of the exposure to 24 h (Figure 6.2b) revealed a time-dependent effect, with the viability of both cell lines decreasing significantly with the increase of the exposure time ($p < 0.05$). Furthermore, a concentration-dependent effect was clearly visible, particularly at concentrations above 50 µg/mL, where increased drug concentration resulted in significantly lower cell viability ($p < 0.05$; Figure 6.2b). The effects were predominantly evident for RFB. Indeed, while the higher concentrations of INH (200 and 400 µg/mL) resulted in minimum cell viability around 60%, which was only visible in A549 cells, RFB elicited cell viability levels of 5 – 20% when tested at the higher concentration (200 µg/mL).

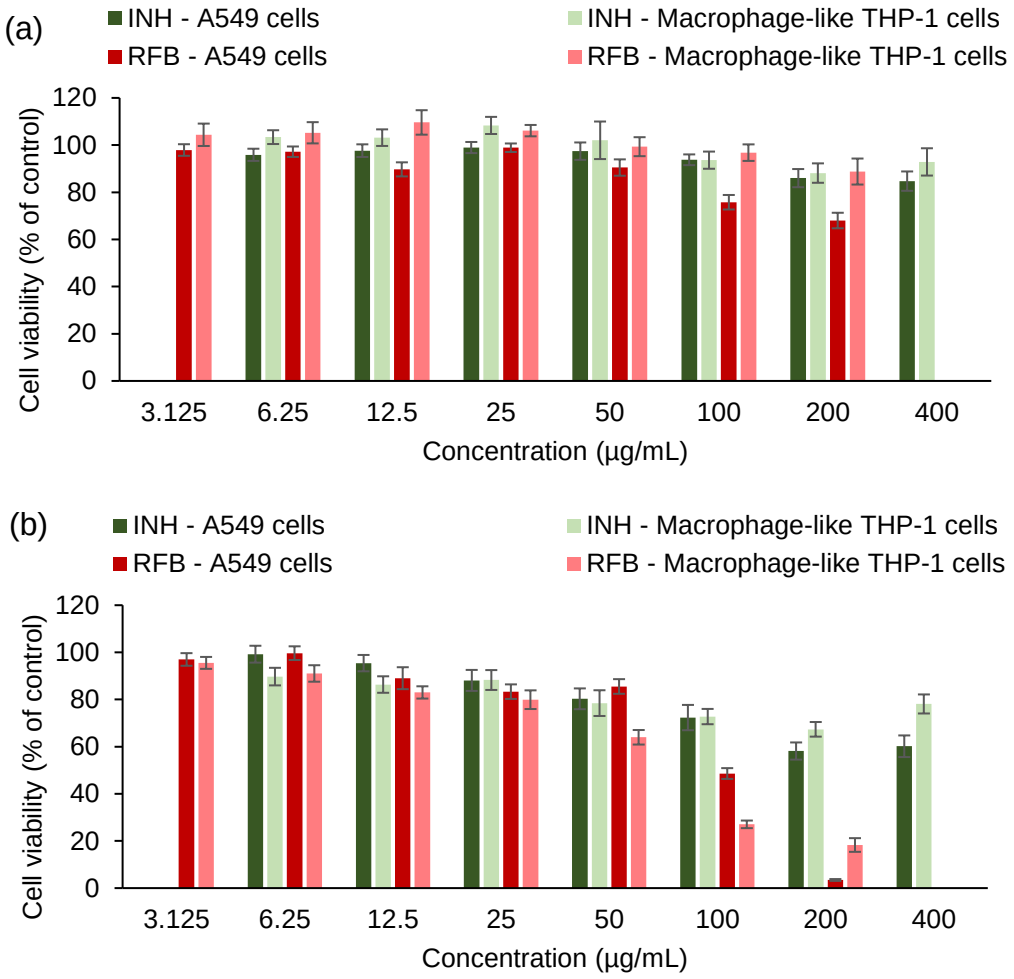

Figure 6.2. Viability of A549 and macrophage-like THP-1 cells as determined by the MTT assay upon exposure of (a) 3 h and (b) 24 h to isoniazid (INH) and rifabutin (RFB) as free drugs. Data represent mean ± SEM (n = 3).

In summary, the analysis of data pertaining to the free drugs indicated time- and concentration-dependent effect, along with stronger toxic effect of RFB comparing with INH. These results were expected, being aligned with those of previous works testing the same drugs in A549 and macrophage-like THP-1 cells.[87,176]

Similar conditions (cells lines and exposure times) were applied to analyse the effect of hydrolysed KGM and KGM microparticles, both unloaded and drug-loaded. Data obtained upon 3 h of exposure are depicted in Figure 6.3. A549 cells had a concentration-dependent decrease in viability upon contact with KGM or unloaded KGM microparticles (Figure 6.3a), reaching around 40% at the highest concentration tested (2 000 µg/mL). Curiously, at concentrations above 500 µg/mL, drug-loaded KGM microparticles always registered superior levels of cell viability comparing with KGM or unloaded KGM microparticles. Macrophage-like cells, in turn, did not evidence any relevant impact of sample exposure upon 3 h (Figure 6.3b).

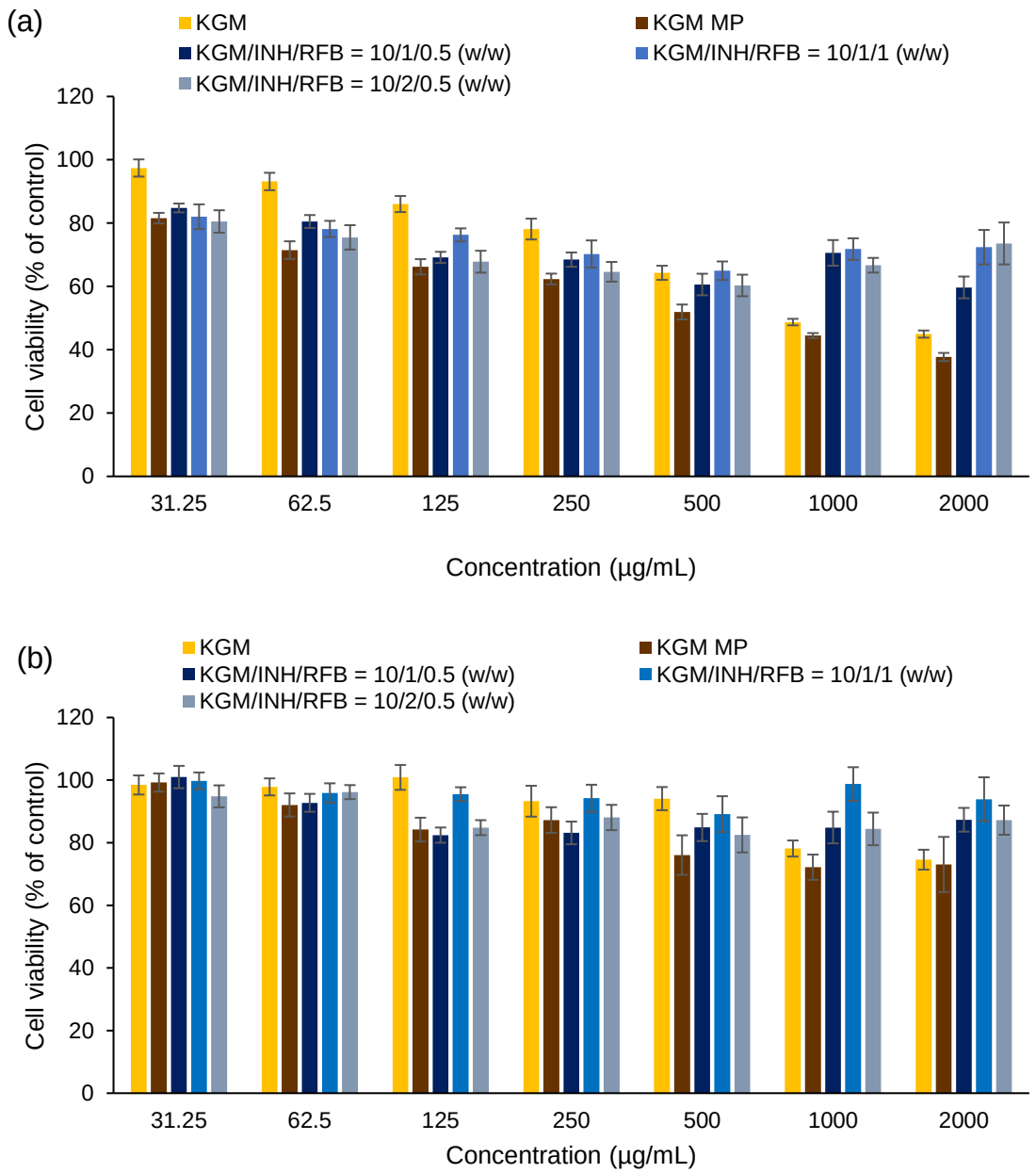

Figure 6.3. Cell viability of (a) A549 and (b) macrophage-like THP-1 cells as determined by MTT assay upon 3 h exposure to konjac glucomannan (KGM) and the corresponding microparticles (MP). Data are presented as mean ± SEM (n = 3).

Similarly to the observations occurred with the free drugs, the prolongation of the exposure to 24 h produced a time- and concentration-dependent effect in both cell lines, the cell viability decreasing significantly with the increase of these parameters ($p < 0.05$). In both cell lines, a significant decrease of cell viability to levels below 70% was generally observed at concentrations of 250 µg/mL or

higher ($p < 0.05$; Figure 6.4). The strongest effects were naturally seen for the highest concentrations tested. In A549 cells, the stronger cytotoxic effect was observed for the microparticles KGM/INH/RFB = 10/1/1 (w/w), with only 6.5% of viability when tested at the concentration of 2 000 µg/mL. As it was mentioned above, RFB itself proved to be very toxic when tested at concentrations between 100 and 200 µg/mL for 24 h. The high amount of RFB in KGM/INH/RFB = 10/1/1 (w/w) microparticles could potentiate the toxic effect of this formulation in A549 cells comparing with the other two formulations, where the RFB concentration is halved (Figure 6.4a). Nevertheless, this distinctive effect was not visible in differentiated THP-1 cells (Figure 6.4b). Furthermore, in general there were no significant differences between the three KGM formulations, regardless the amounts of drugs associated to the microparticles. The presence of KGM endowed upon drug microencapsulation seems to have slightly improved the toxic effect that drugs would induce in the cells after 24 h exposure, especially RFB, if these data were compared with the results pertaining to the free drugs (Figure 6.2b). The ameliorating effect of microencapsulation towards the cytotoxic profile of antitubercular drugs, RFB in particular, was already proposed in previous works of the team.[87,88]

Taking into consideration that KGM is proposed as the matrix of inhaled microparticles, the KGM (hydrolysed polymer) and unloaded microparticles were also evaluated to disclose any effect of the carrier itself. The analysis of the results indicates that, on several occasions, KGM microparticles induce cell viability lower than that induced by the unprocessed polymer, particularly at the lower concentrations tested. The justification for this observation is possibly related with the dissolution profile of each sample on CCM. In fact, while KGM forms a dispersion in CCM, not reaching complete dissolution, KGM microparticles seem to be completely dissolved in the medium when cell exposure takes place, certainly providing a more intimate contact with the cells which induced higher toxicity.

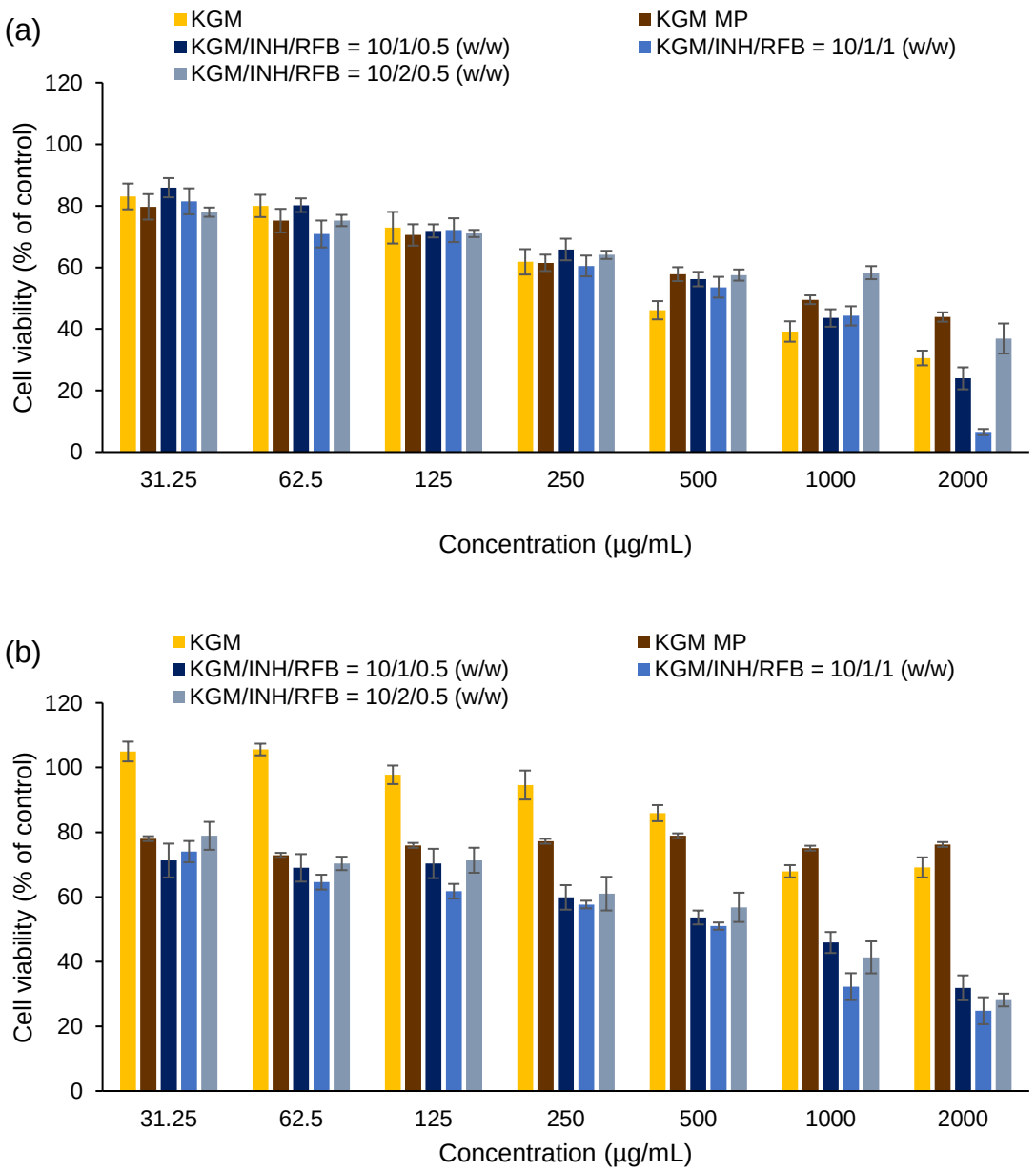

Figure 6.4. Cell viability of (a) A549 and (b) macrophage-like THP-1 cells as determined by MTT assay upon 24 h exposure to konjac glucomannan (KGM) and corresponding microparticles (MP). Data are presented as mean ± SEM (n = 3).

The generality of results seems to point to an absence of toxicity when carrier concentrations up to 125 µg/mL are used. This is in fact supportive of lung delivery applications, as currently marketed formulations do not go beyond that and are inclusive quite far from generating such concentrations, because of the large surface area of the lung (up to 80 m^2).[177] In addition, the highest

concentrations tested in this work were a means to extreme assessment conditions and evaluate the behaviour of the developed drug delivery systems, towards understanding general performances. This is of relevance particularly because the used excipient is not approved for lung delivery applications and related information is scarce in the literature.

In order to complement the information provided by the cell viability data, the half-maximal inhibitory concentration (IC_{50}) at 24 h was determined for all the samples reaching cell viability levels lower than 50% in the MTT assay (Table 6.1). The lowest IC_{50} was determined for RFB (61-92 µg/mL) but, contrasting these results with those of KGM/INH/RFB microparticles, makes visible the protecting effect of microencapsulation already mentioned in section 6.2.1.1. In fact, IC_{50} values increase between 3.5 and 17 times upon microencapsulation. It was also possible to verify that the presence of a higher amount of RFB in microparticles KGM/INH/RFB = 10/1/1 (w/w) decrease the IC_{50} in comparison with the other KGM microparticle formulations, a tendency verified for both cell lines. This reinforces the fact that RFB plays an important role in the toxicity elicited by the developed carriers.

Table 6.1. IC_{50} values (µg/mL) determined on A549 and macrophage-like THP-1 cells after 24 h exposure to isoniazid (INH) and rifabutin (RFB) as free drugs, konjac glucomannan (KGM) and various KGM microparticles (MP).

Samples	A549 cells	Macrophage-like THP-1 cells
INH	N/A	N/A
RFB	91.55	61.4
KGM	492.8	N/A
KGM MP	1011.0	N/A
KGM/INH/RFB = 10/1/0.5 (w/w)	572.4	564.7
KGM/INH/RFB = 10/1/1 (w/w)	401.4	315.6
KGM/INH/RFB = 10/2/0.5 (w/w)	1058.0	529.6

N/A: not applicable

6.2.1.2. Cell membrane integrity

As a complement to the results obtained from the MTT assay, the integrity of the cell membrane was evaluated by the quantification of LDH released from A549 and macrophage-like THP-1 cells upon 24 h exposure to microparticles and KGM (500 and 1 000 µg/mL), as well as INH (100 and 200 µg/mL) and RFB (50 and 100 µg/mL) as free drugs. LDH is a cytoplasmatic enzyme, which is released from the cells when their membrane is damaged, thus its quantification permitting the assessment of the damage. The quantification is performed using a colorimetric assay that involves the reduction of NAD+ to NADH by the cytoplasmatic enzyme, converting lactate into pyruvate. The resultant NADH is used in the conversion of the tetrazolium salt into red formazan crystals, which might be quantified by spectrophotometry.

The amount of LDH released upon exposure to each sample was compared with that released in the sequence of incubation with CCM (negative control). As depicted in Figure 6.5a, no statistically significant differences were observed in the LDH released by A549 cells. Despite the indications of some toxic effect of the higher concentrations of the samples on these cells in the MTT assay (Figures 6.2b and 6.4a), these results seem to indicate that the toxicological effect does not involve cell membrane disruption. As expected though, the LDH release induced by the positive control was significantly higher than that obtained for the tested samples ($p < 0.05$). Contrary to the observations in A549 cells, both free drugs induced significantly higher release of LDH from macrophage-like THP-1 cells when incubated at the highest concentrations, comparing with CCM, an effect also observed in KGM/INH/RFB microparticles and, as expected, in the positive control ($p < 0.05$; Figure 6.5b). In this case, the obtained data were generally in line with results of the evaluation of cell metabolic activity (Figure 6.4b).

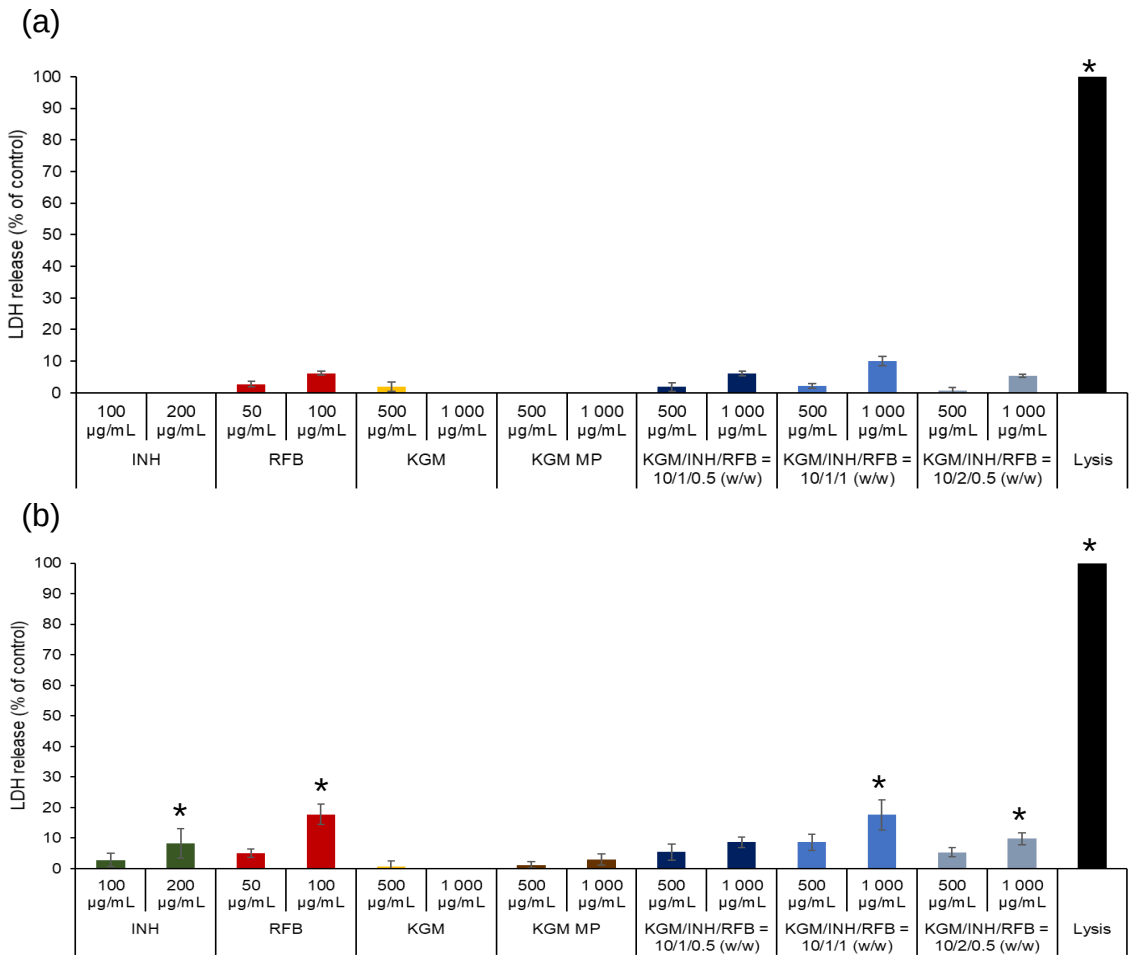

Figure 6.5. LDH released from (a) A549 cells and (b) macrophage-like THP-1 cells after 24 h exposure to isoniazid (INH), rifabutin (RFB), konjac glucomannan (KGM) and microparticles (MP). Data represent mean ± SEM (n = 3). Statistically significant differences are indicated as *$p < 0.05$ compared with respective cell culture medium (negative control).

As previously commented, the assessment of cell metabolic activity and cell membrane integrity are typically performed in the context of evaluating toxicological effects associated to the exposure to potentially toxicant substances. Nevertheless, the interpretation of the obtained data must be careful and integrated. When cells are exposed to potential harmful stimulus, the loss of cell membrane integrity occurs late in the process of cell death, while the metabolic activity of the cells is expectedly affected at earlier stages. The evaluation of the cell membrane integrity should thus be done after the cells initiate apoptosis[178] and 24 h is considered an adequate time period for that.

However, it is clear that both assays focus on different aspects of cellular metabolism and activity, thus not being surprising that the results of the assays are not exactly coincident, but instead complementary. Additionally, the difference observed in the results reinforces the need to perform assays that focus distinct aspects of cellular activity to conclude on the toxicological profile of materials undergoing evaluation. Overall, the obtained results indicate the absence of overt toxic effects of the produced microparticles, considering that at concentrations up to 125 µg/mL no relevant toxicological effects are expected to be observed, thus supporting an application in inhalable tuberculosis therapy.

6.2.2. Macrophage activation

During tuberculosis infection, the PAMPs of mycobacteria are identified by the macrophage surface receptors, leading to macrophage activation and polarisation towards the M1 phenotype. This initiates the production of pro-inflammatory mediators that will foster bacterial elimination and triggers an adaptive immune response.[24] The KGM composition, rich in glucose and mannose units, theoretically enables a similar effect, mediating the recognition of microparticles by the surface receptors. The interaction between KGM microparticles and the macrophage receptors, with consequent internalisation of the particles, could activate these cells, leading to the production and release of pro-inflammatory mediators. Therefore, the ability of KGM to activate the macrophages could play an important role in the course of the tuberculosis infection, due to improved bactericidal activity of activated macrophages,[179] and worth investigation. In order to evaluate this potential role of KGM in the activation of the macrophages, macrophage-like THP-1 cells were exposed (24 h) to KGM in the form of polymer and drug-loaded microparticles (KGM/INH/RFB = 10/1/0.5, w/w), and the production of TNF-α and IL-8 quantified. TNF-α is a well-known pro-inflammatory mediator secreted by activated M1 macrophages.[180,181] In tuberculosis, this molecule initiates the T-cell and macrophage migration, as well as the granuloma formation during the infection.[182] IL-8 is another pro-inflammatory chemokine produced during tuberculosis infection,[183], known to induce the recruitment of immune cells to the lungs and also participating in the

granuloma formation. Moreover, Krupa *et al*.[184] have shown enhanced antimicrobial ability of macrophages and neutrophils upon interaction with *M. tuberculosis*.

Data regarding the release of the cytokines are displayed in Figure 6.6, which also provides data obtained upon stimulation of macrophage-like THP-1 cells with LPS, used as positive control because of its demonstrated ability to induce macrophage activation resulting in the over-secretion of cytokines. Untreated cells were used as negative control. Figure 6.6a evidences that macrophage-like THP-1 cells exposed to KGM for 24 h, either in the form of polymer or microparticles, did not reveal altered production of TNF-α. Similarly, the production of IL-8 by the cells upon exposure to a solution of the polymer was minimal, but the exposure to microparticles induced statistically significant production of IL-8 as compared with cells exposed only to the CCM ($p < 0.05$). Previous works with polysaccharides have shown the ability of these materials to induce the release of pro-inflammatory mediators, suggesting the activation of the macrophages. Indeed, fucoidan and chondroitin sulfate were reported to stimulate cytokine production.[86,88] However, this increase could also be a consequence of endotoxin contamination in the samples, which was demonstrated to occur with chondroitin sulfate.[88] Despite no endotoxin test was performed in KGM samples and considering that KGM is a polysaccharide with anti-inflammatory properties, the moderate production of IL-8 by macrophage-like THP-1 cells could be due to KGM microparticle contamination during manufacture, since the unprocessed polymer did not cause this effect in cells.

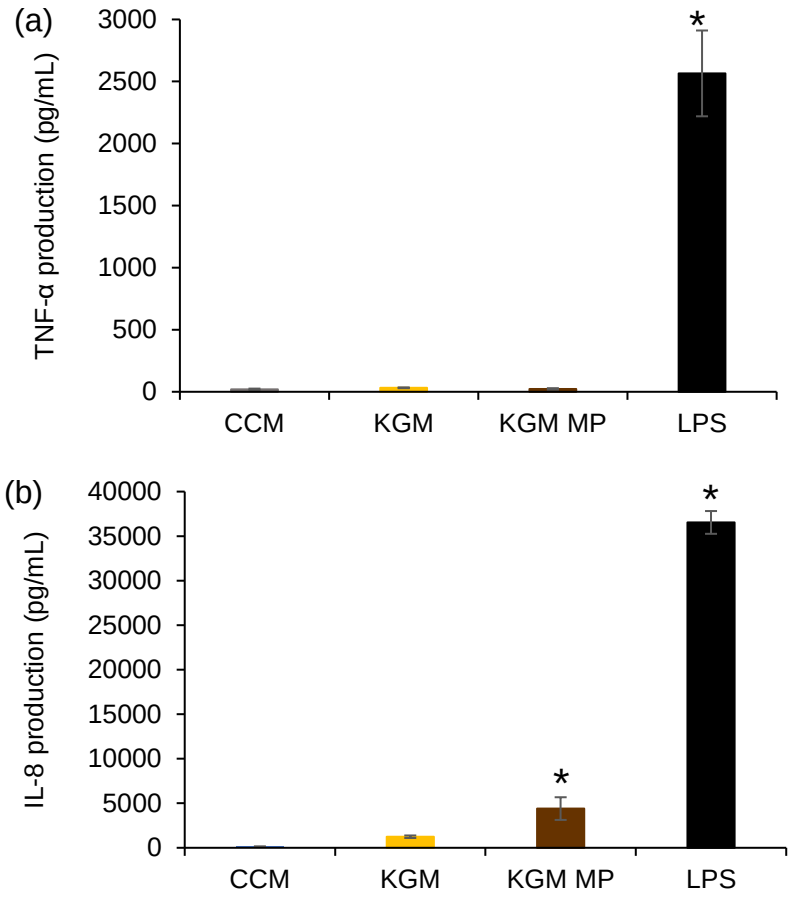

Figure 6.6. Amount of (a) tumour necrosis factor α (TNF-α) and (b) interleukin-8 (IL-8) released from macrophage-like THP-1 cells after 24 h exposure to konjac glucomannan (KGM) and KGM/INH/RFB = 10/1/0.5 (w/w) microparticles (KGM MP), as determined using ELISA kits. Data represent mean ± SEM (n = 2). Statistically significant levels are indicated as *p < 0.05 compared with CCM (negative control).

The macrophage activation and the expression of pro-inflammatory cytokines are critical in the control of tuberculosis infection through bacteria degradation and induction of an adaptive response by the immune system.[25,29] Therefore, the strategy of developing an inhalable treatment for pulmonary tuberculosis that, apart from co-localising the drugs and the pathogenic agents, could further contribute for macrophage stimulation, could be appealing. However, recent findings related with tuberculosis pathogenesis indicate that the expression of some inflammatory biomarkers during an inflammatory response, such as nitric oxide, could benefit mycobacteria growth rather than potentiate the elimination of the pathogen.[185] Following this perspective, the apparent limited capacity of KGM

to activate the macrophages, observed upon an exposure of 24 h, can be considered favourable rather than limiting, and supports the evidence of KGM anti-inflammatory properties.[7]

6.2.3. Uptake of konjac glucomannan microparticles by macrophages

For the successful treatment of pulmonary tuberculosis, the antitubercular drugs must penetrate cell membrane of macrophages and inhibit/kill the intracellular *M. tuberculosis.*[186] Hence, using the phagocytic role of macrophages, inhaled particles targeted to these cells could be used to deliver and load the infected macrophages with antibiotics in order to treat the disease.[187] To assess the ability of the developed KGM microparticles for the first step of macrophage internalisation, the polymer was labelled with fluorescein, fluorescent microparticles produced and the ability of macrophage-like THP-1 cells to uptake these particles evaluated. The cells were exposed to the microparticles for 2 h, after which the percentage of cells phagocytosing KGM microparticles was determined. The results are shown in Figure 6.7, which shows that the event of KGM microparticle phagocytosis is concentration-dependent. In fact, while the dose of 100 μg/cm^2 yielded 89% phagocytosis, when the dose increased to 300 μg/cm^2 the percentage of cells with signs of phagocytosis was close to 100%. As it is well-known, alveolar macrophages will engulf substances/materials tagged for elimination regardless of their composition, a function that is part of their natural role in maintaining the lung homeostasis.[188] It is also known that macrophages preferentially uptake particulate matter[189] and may exhibit preferential affinity for specific molecules/groups/residues in comparison with others. This was demonstrated in this work using PVA microparticles produced in similar conditions and exhibiting characteristics similar to those of KGM microparticles (geometric diameter around 2 μm), which were used as control. PVA is also a polysaccharide, having a structure similar to that of KGM, but contrary to that polymer, PVA is devoid of sugar residues described as potentiating macrophage recognition through receptor interaction. The percentage of macrophage-like THP-1 cells determined to phagocytose PVA microparticles was significantly lower compared with those phagocytosing KGM

microparticles ($p < 0.05$), reaching a maximum of 62% when the higher dose was tested (Figure 6.7).

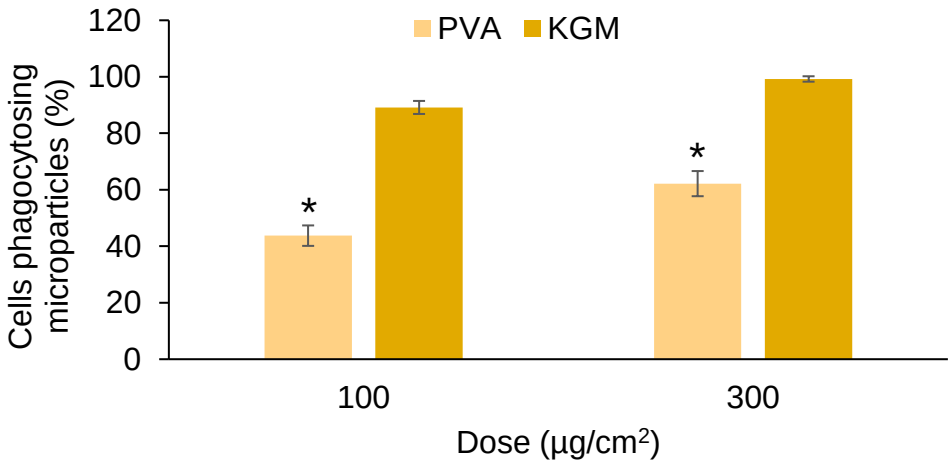

Figure 6.7. Percentage of macrophage-like THP-1 cells phagocytosing fluorescently-labelled poly(vinyl alcohol) (PVA) and konjac glucomannan (KGM) microparticles upon 2 h of exposure. Results are expressed as mean ± SEM (n = 3). Statistically significant levels are indicated as *$p < 0.05$, comparing results of PVA with those of KGM for the same dose.

The ability of macrophages to phagocytose specific molecules, often due to the recognition of patterns/residues by the interaction with surface receptors, allows and potentiates the development of therapeutic approaches through the use of suitable particulate carriers to treat diseases where these cells play a central role.[190] The mannose/glucose composition of KGM may have potentiated macrophage recognition and consequent enhancement of phagocytosis of KGM microparticles. Similar results were reported for other natural polymers regarding to the capacity of macrophages for particle internalisation. Locust bean gum, a galactomannan, reached a phagocytic level around 100% when testing the same cells.[85] Overall, the obtained data suggests that KGM microparticles are promising carriers to deliver drugs to macrophages, a strategy that may find applications in the treatment of intracellular diseases like tuberculosis. However, these data should be complemented with confocal microscopy images in the future, since flow cytometry does not give information regarding to the localisation of the microparticles in the cell.

6.2.4. In vivo assay

The inhalation of particles may pose risks related with the generation of inflammatory or immune responses, characterised by changes in lung cell populations and inflammatory biomarkers that may be identified and quantified.[191] Evaluating the safety of KGM microparticles *in vivo* is, thus, a relevant issue as this material is being proposed as a potential excipient for the formulation of lung drug carriers. In fact, *in vivo* studies provide the possibility to evaluate possible effects and responses that are out of reach *in vitro*.

A preliminary assessment of *in vivo* safety of KGM microparticles after inhalation was performed, addressing a limited set of parameters. Mice received by inhalation either 1 or 10 doses of dry powder comprising unloaded KGM microparticles, thus addressing possible acute and subacute toxicity issues as indicated in regulatory guidelines.[192,193] The inflammatory response was determined by analysing the differentiated blood leucocytes, while a potential allergic response was evaluated by quantifying IgE levels in plasma and BALF samples. BALF was further analysed for toxicity biomarkers, such as LDH and total protein. Body weight was monitored over the experimental procedure and tissue index values for selected organs, namely lung, liver, spleen and kidneys were determined at the end of the *in vivo* assay, as another indicator of toxicology. Moreover, the lung has undergone histological analysis. Importantly, nose-only inhalation and histopathology are the standards for preclinical regulatory inhalation toxicology.[192] The results obtained in all these analyses are described in the following sections.

6.2.4.1. Monitorisation of body weight

The body weight of mice undergoing the subacute toxicity study (prolonged exposure, KGM 10x) was registered and results are depicted in Figure 6.8. Over the two weeks of the *in vivo* study, no significant variations were observed in terms of body weight either for mice receiving microparticles or naïve animals (control group). The same pattern was observed for mice exposed to a single dose of KGM microparticles (data not shown).

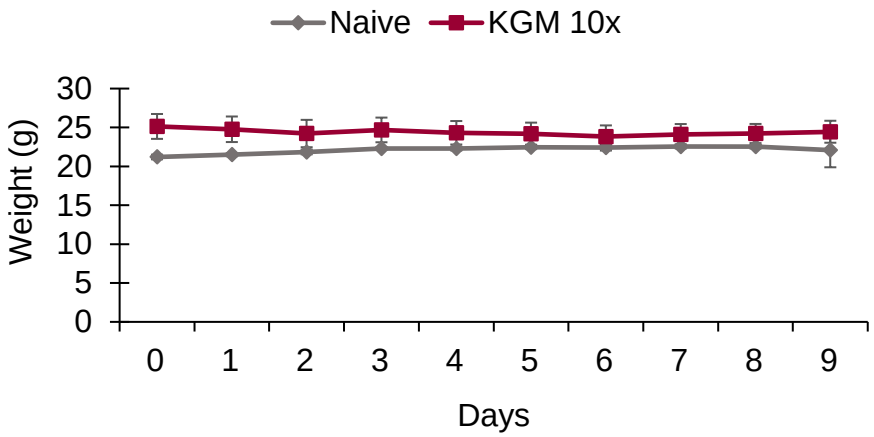

Figure 6.8. Evolution of body weight of naïve mice (Naïve) or animals submitted to daily pulmonary administration of dry powder comprising unloaded konjac glucomannan (KGM) microparticles in a total number of 10 administrations (mean ± SD, n = 6).

6.2.4.2. Counting of diferentiated leucocytes in blood

Leucocytes are a group of cells of utmost relevance having a central role in the elimination of foreign substances, infections and/or injuries.[194] Moreover, they constitute important inflammatory biomarkers when immune responses are evaluated, analysed or studied.[194] Hence, the analysis of leucocytes present in the blood of mice receiving unloaded KGM microparticles by inhalation may provide relevant data regarding the induction of a potential inflammatory response as a consequence of the exposure to the excipient. Leucocyte analysis was performed by counting the different classes of these cells in blood after acute and subacute exposure (Figure 6.9).

Except for monocytes, naïve mice were determined to have leucocyte counts within the expected interval of reference (as referred in Charles River Laboratories International),[195] indicating normal and expected conditions. Moreover, the values determined for neutrophils, basophils and lymphocytes also remained within the interval of reference upon both the treatment protocols of KGM microparticle inhalation. During an inflammatory response, neutrophils influx is typically evident and thus a very good marker.[196,197] The obtained data revealed no significant differences of neutrophils counts in comparison with naïve

mice, regardless of the frequency of administration of KGM microparticles (Figure 6.9a). These results suggest the absence of inflammatory response upon inhalation of KGM, or at least that this was not expressed by neutrophils increase. Similarly, the percentage of lymphocytes and basophils also remained approximate to that determined for naïve mice, without statistically significant differences (Figure 6.9b, c).

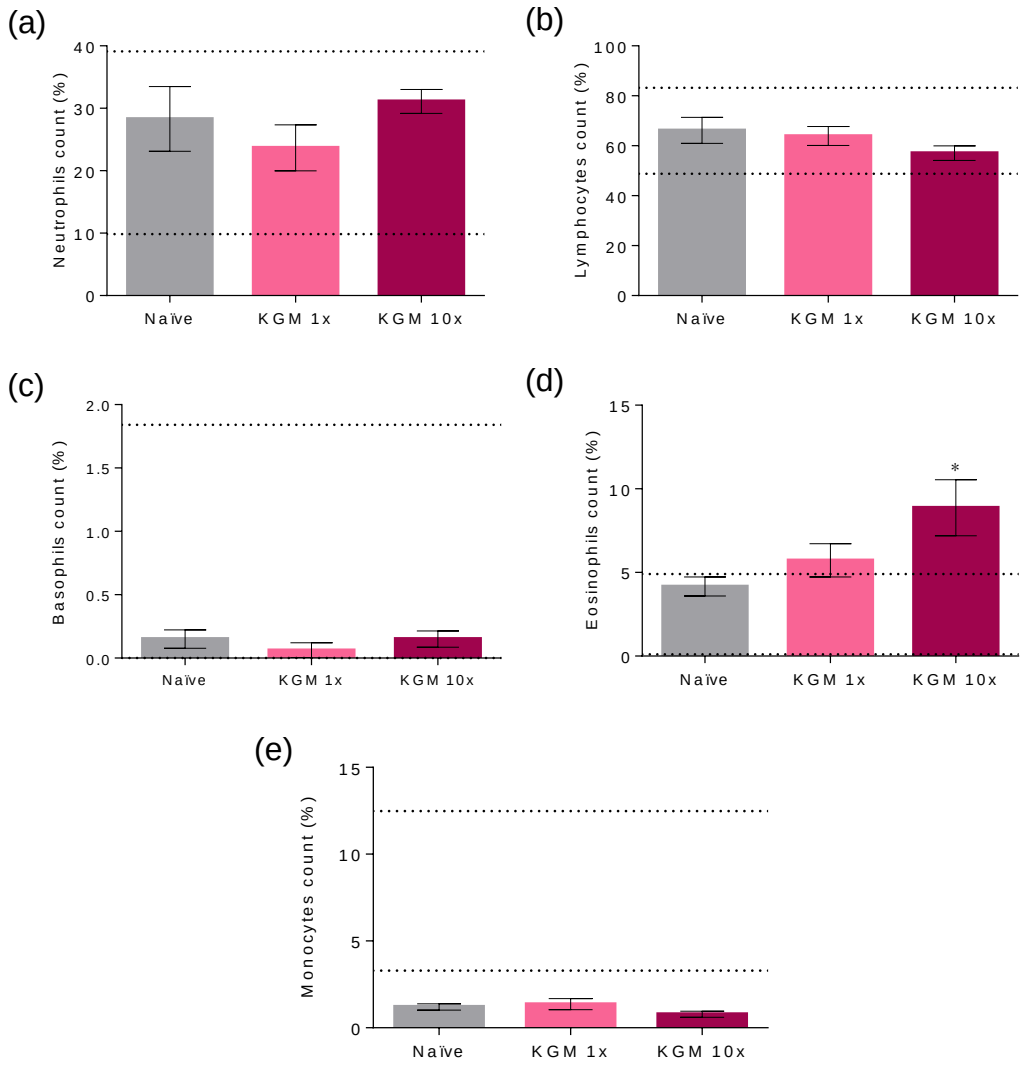

Figure 6.9. Leucocyte count in mice blood. (a) Neutrophils; (b) lymphocytes; (c) basophils; (d) eosinophils; (e) monocytes. Dashed lines represent the reference intervals for each type of white blood cell (mean ± SEM, n = 6). Statistically significant levels are indicated as *p < 0.05.

In turn, the number of eosinophils registered a visible impact upon the inhalation of unloaded KGM microparticles (Figure 6.9d). Indeed, a tendency to increase

was observed even when a single dose was administered. However, statistically significant differences, in comparison to naïve group, were only attained for mice receiving 10 doses of KGM microparticles ($p < 0.05$). These cells have an important role on the regulation of local immune and inflammatory responses, and a condition of eosinophilia in blood or tissues may be associated to several disorders, including allergic reactions.[198] The observed increase in eosinophils potentially indicates the induction of a local immune response. Surprisingly, data obtained in the present work are discordant with literature that reports the ability of KGM to supress an eosinophilia condition after its intake through a mixture with food (5%, w/w) by NC/Nga mice.[199]

Finally, as commented above, a condition of monocytopenia was found in all tested conditions, including in naïve mice (Figure 6.9e). Monocytes are part of the mononuclear phagocytic system and represent approximately 4% of peripheral leucocytes in mice (around 10% in humans).[200] Nevertheless, as shown in the figure, mice from all groups exhibited monocyte counts around 1%. Among the major causes of monocytopenia are the intake of myelotoxic drugs, acute infectious stress, aplastic anaemia, hairy cell leukaemia and myeloid leukaemia.[201] No justification was found so far for the registered values, which require further studies for clarification, but they cannot be attributed to causes related with KGM inhalation.

6.2.4.3. Determination of IgE

IgE is an immunoglobulin that plays an important role in acute and chronic inflammatory allergic conditions. When individuals are exposed to specific antigens, this typically generates the production of high levels of IgE. These molecules have the ability to bind the receptor FcεRI expressed in some effector cells, such as mast cells and basophils, thus triggering allergic reactions.[202,203] Therefore, the quantification of expressed IgE levels is often used as a biomarker to evaluate the occurrence of allergic responses.[204] In this perspective, the levels of IgE expressed in the sequence of the inhalation of unloaded KGM microparticles were analysed in plasma and BALF samples extracted from mice, and the obtained data are depicted in Figure 6.10. In plasma samples (Figure

6.10a), the inhalation of KGM microparticles did not induce significant production of IgE in comparison with naïve mice. Despite the increase of the number of doses of KGM microparticles that were inhaled, the production of IgE remained around 1 300 ng/mL in both groups corresponding to KGM inhalation.

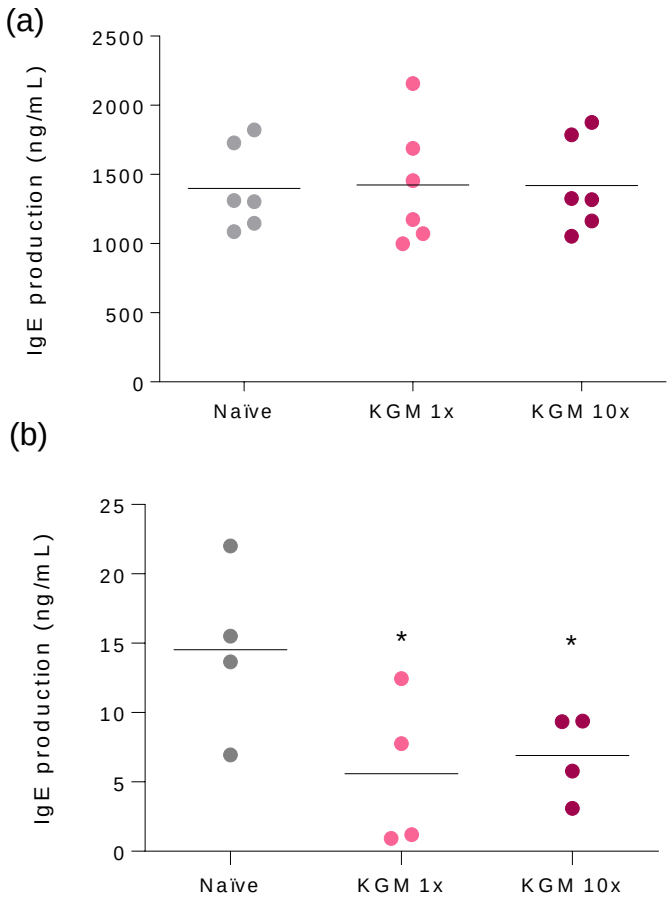

Figure 6.10. IgE levels determined in (a) plasma and (b) bronchoalveolar lavage fluid (BALF) of mice from naïve and konjac glucomannan (KGM) groups exposed to a single dose (1x) and ten doses (10x) of unloaded KGM microparticles. Lines represent the mean of IgE secretion expressed in ng/mL (plasma: n = 6; BALF: n = 4). Statistical significance levels comparing with control (naïve mice) are indicated as *p < 0.05.

Regarding to BALF samples and as it was expected, the IgE levels were significantly lower than the levels expressed in plasma ($p < 0.05$).[205] Moreover, the production of IgE induced by the inhalation of KGM microparticles was significantly lower compared with that of the naïve group ($p < 0.05$). In fact, while the latter registered approximately 15 ng/mL, the inhalation of unloaded KGM

microparticles induced mean IgE levels of 6 and 7 ng/mL for a single dose (1x) and ten doses (10x) of microparticles, respectively (Figure 6.10b).

KGM is reported as a natural polymer with anti-inflammatory properties.[7] This capacity is apparently supported by the obtained IgE data, not only because no allergic reaction was induced, but also because it is apparently counteracted. Indeed, the production of IgE was similar (in plasma) or lower (in BALF) compared with the IgE values observed in mice from the naïve group. Previous works developed by Onishi *et al*.[199] and Suzuki *et al*.[206] have already demonstrated the anti-inflammatory activity of KGM, where the exposure to this polymer supressed the IgE production, improving cases of allergic rhinitis and atopic diseases in mice.

6.2.4.4. LDH and total protein in BALF

The release of LDH and the total protein present in BALF samples are considered indicators of toxicity and predictors of inflammatory response.[191,196,207] Therefore, BALF samples of mice from naïve and KGM (1x and 10x) groups were analysed regarding these two parameters (Figure 6.11 and Figure 6.12).

In cases of injury, the levels of LDH can be increased as a result of an inflammatory response upon exposure to specific antigens.[196] Data in Figure 6.11 indicate that, regardless of the frequency of inhalation of KGM microparticles, no significant changes on LDH values comparing with the control naïve group were observed.

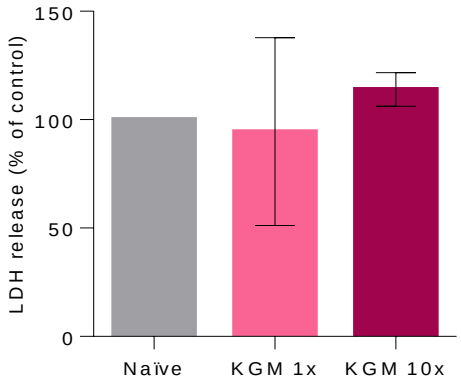

Figure 6.11. Content of lactate dehydrogenase (LDH) in bronchoalveolar lavage fluid (BALF) samples obtained from naïve mice and animals receiving 1 (KGM 1x) or 10 (KGM 10x) inhalations of dry powder comprised of unloaded KGM microparticles (mean ± SEM, n = 4).

In parallel, levels of total protein were also determined, and results are depicted in Figure 6.12. Similarly to the observations regarding to LDH quantification, the levels of total protein in the BALF samples did not vary significantly between the groups receiving 1 or 10 doses of KGM and were also similar to those of naïve mice. For all the three groups under study, the protein concentration was approximately 100 µg/mL (Figure 6.12).

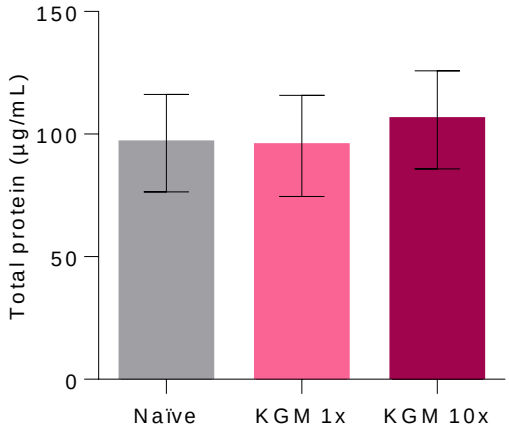

Figure 6.12. Content of total protein in bronchoalveolar lavage fluid (BALF) samples obtained from naïve mice and animals receiving 1 (KGM 1x) or 10 (KGM 10x) inhalations of dry powder comprised of unloaded KGM microparticles (mean ± SEM, n = 4).

6.2.4.5. Tissue index

The determination of tissue index after inhalation of dry powder corresponding to unloaded KGM microparticles was another step towards the evaluation of KGM safety as an excipient for pulmonary delivery applications.[208] One day after the last administration, the animals were sacrificed and organs of interest collected, including liver, spleen, lungs, and kidneys, and macroscopically analysed. The respective tissue index was also determined and compared with the naïve group. Values of tissue index are detailed in Table 6.2. No significant differences were observed between the three groups under study, indicating that the inhalation of KGM microparticles, even in the more prolonged schedule, did not affect the weight of the organs.

Table 6.2. Tissue index of liver, spleen, lung, and kidneys of mice from naïve group or upon inhalation of one (1x) or ten doses (10x) of konjac glucomannan (KGM) microparticles (mean ± SD, n = 6). Different letters represent significant differences between the groups in each analysed organ ($p < 0.05$).

	Liver (%)	**Spleen (%)**	**Lungs (%)**	**Kidneys (%)**
Naïve	22.6 ± 0.8^{a}	5.7 ± 0.2^{b}	8.6 ± 1.1^{c}	12.7 ± 0.3^{d}
KGM 1x	23.1 ± 0.7^{a}	5.7 ± 0.1^{b}	8.9 ± 1.1^{c}	13.0 ± 0.5^{d}
KGM 10x	22.6 ± 0.6^{a}	5.6 ± 0.4^{b}	8.9 ± 0.7^{c}	12.9 ± 0.4^{d}

6.2.4.6. Histology

Finally, inflammatory and morphological alterations in the lung tissue were analysed as a complementary indicator of toxicity.[209] After the inhalation of ten doses of unloaded KGM microparticles (KGM, 10x) , histological analyses of mice lungs were performed (Figure 6.13). As a whole, the histological observations indicate that the inhalation of KGM microparticles did not affect lung structures. In fact, when comparing the group that received KGM microparticles by inhalation with naïve mice, similar histological features were visualised. However, while bronchi and bronchioles display what is considered a normal structure (Figure 6.13a and 6.13b), the same was not observed in the alveoli. The observations of

this area revealed the existence of aggregates of mononuclear cells in perivascular position and some areas exhibited wider alveolar septa due to the infiltration of mononuclear cells, and consequent decrease of the alveolar lumen. Surprisingly, this effect was visible in both naïve mice and animals receiving KGM microparticles (Figures 6.13c and 6.13d). Usually, the accumulation of mononuclear cells in perivascular position and the infiltration of mononuclear cells is associated to inflammatory response,[210,211] but the fact that both naïve mice and animals receiving dry powder formulations show similar histological observations, hinders the justification of microparticle inhalation.

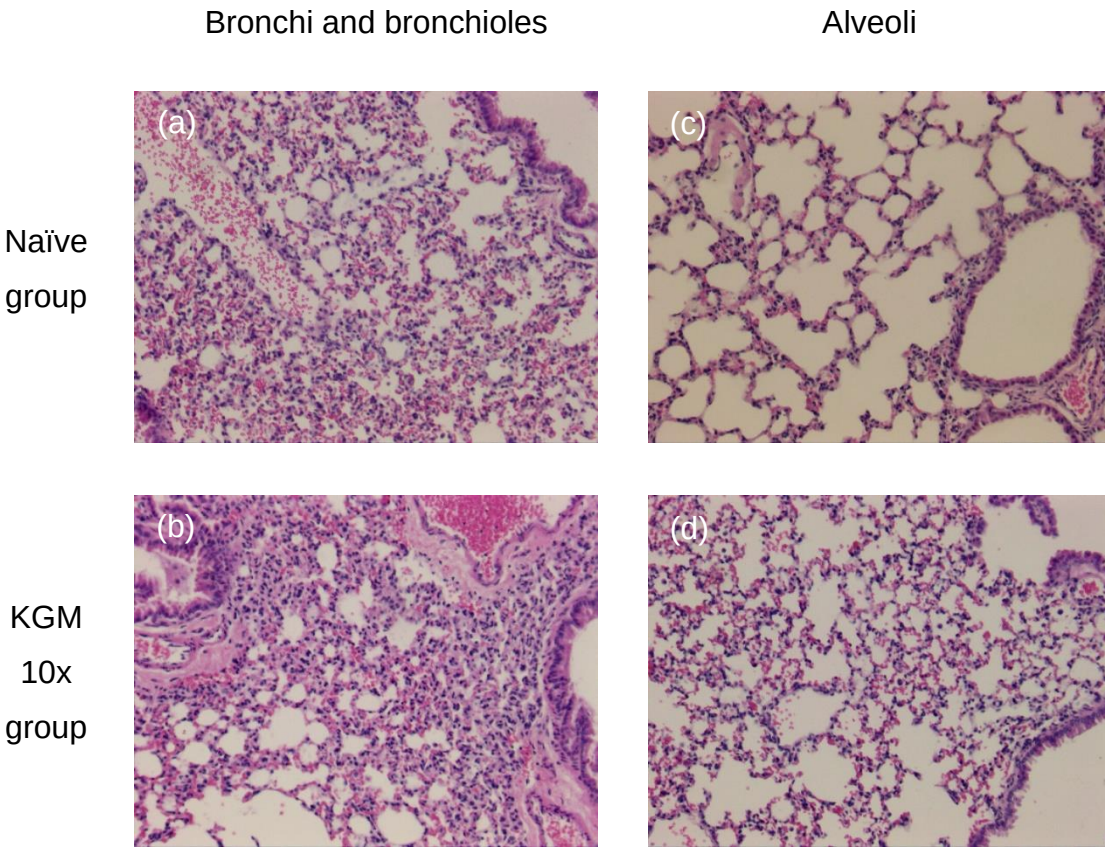

Figure 6.13. Lung histology. Representative images of haematoxylin and eosin (H&E) stained lung sections (100x) from bronchi and bronchioles (a, b) and alveoli (c, d) of naïve mice (a, c) of animals receiving 10 inhalations of dry powder comprising unloaded KGM microparticles (KGM 10x) (b, d).

As referred above, the anti-inflammatory profile of KGM is well established in the literature.[103,199,206] Therefore, the eliciting of an inflammatory reaction in the sequence of the inhalation of KGM microparticles would not be expected. Indeed,

most of the results described herein suggest a mild effect of the excipient, with absence of neutrophils influx and similar values of IgE, LDH and total protein comparing with the naïve mice (control group). However, some observations suggest the need of further studies to deeply understand KGM safety regarding the potential use in lung drug delivery applications. The observed eosinophilia (Figure 6.9d) raises concern as it is typically associated to allergic reactions[198] and may be an indicator of the ability of KGM microparticles to trigger such a reaction. Nevertheless, the absence of alteration of IgE values upon KGM inhalation (Figure 6.10) opposes to this effect, as this immunoglobulin is increased in allergic reactions. Thus, the observed eosinophilia cannot be directly assigned to allergic response subsequent to inhalation of KGM microparticles. The fact that other works report the ability of KGM to improve allergic conditions through suppression of eosinophil infiltration and IgE production, reinforce this observation.[199,206] Unexpected events in lung histology also require clarification, namely the observation of cell infiltrates in the alveolar septa, indicating a possible inflammatory response.[210] Nevertheless, as no differences were observed between mice exposed to KGM and the naïve group, the infiltration of the mononuclear cells in the alveolar space cannot to be assigned to the inhalation of unloaded KGM microparticles. The obtained results apparently indicate absence of damaging effects attributable to KGM inhalation, but the set of assays must be reinforced and expanded to further clarify the safety of KGM for lung delivery applications.

6.3. Conclusions

Nowadays, there are few excipients approved by regulatory agencies for pulmonary delivery applications, mainly due to the unknown behaviour and fate of the materials after inhalation. Therefore, characterising the *in vitro* and *in vivo* safety profile of a determined excipient and respective delivery system is an important step towards understanding reactions/behaviours potentially triggered upon inhalation. One of the advantages of the pulmonary delivery of drugs for local disease treatment is the potential to increase lung concentrations without the need to administer a large amount of drug, as the administration directly

targets the primarily affected area. Expectations in turn of the approach proposed in this project rely on the potential to decrease drug doses when these are delivered to the lung using KGM microparticles. Despite some toxicity was registered for high concentrations of KGM-based samples in A549 and macrophage-like THP-1 cells, encouraging safety indications were provided *in vitro* at the expected lung concentrations (< 125 µg/mL). Additionally, efficient uptake of KGM microparticles was demonstrated without eliciting significant response by macrophages, evaluated through the production of TNF-α and IL-8. In parallel to the *in vitro* data, data obtained *in vivo* upon inhalation of unloaded KGM microparticles have shown promising results. Most inflammatory and toxicity biomarkers analysed during the *in vivo* study suggest the absence of major deleterious effects in mice exposed to the carriers, except for the detected eosinophilia and some signs of inflammation that appeared in lung histology. Notwithstanding the relevance of the positive indications on KGM safety and on the interaction with macrophages, the major players in the development of tuberculosis, these aspects require a more profound evaluation to clarify safety issues and to better enlighten the interaction of KGM microparticles with macrophages.

This page was intentionally left in blank

CHAPTER 7 - FINAL CONSIDERATIONS

This page was intentionally left in blank

7. Final considerations

7.1. General conclusions

This PhD thesis proposed the development of an inhalable therapeutic strategy for the treatment of lung tuberculosis. In this context, KGM microparticles were thus proposed as antitubercular drug carriers, aiming at targeting the alveolar macrophages infected with *M. tuberculosis*, while further exploring the potential of KGM as a pharmaceutical excipient for lung delivery applications.

The obtained results allowed drawing the following conclusions:

1. Inhalable KGM microparticles associating different amounts of INH and RFB in combination were successfully produced by spray-drying, with drug association efficiency varying within 78-91% for INH and 66-74% for RFB. Long-term stability studies indicated, however, the inability of microparticles to remain stable beyond 3 months regarding to the drug content;
2. The associated drugs evidenced complete release from KGM microparticles upon 24 h in conditions resembling those of pulmonary environment;
3. KGM microparticles exhibited suitable aerodynamic properties to reach the alveolar region (mass median aerodynamic diameter around 3 µm) where the drug targets (alveolar macrophages hosting *M. tuberculosis*) are located;
4. The spherical shape and geometric size around 2 µm exhibited by KGM microparticles are theoretically adequate to foster particle uptake by macrophages and high rate of internalisation was demonstrated *in vitro*;
5. The size of KGM microparticles was demonstrated to decrease in presence of β-mannosidase, an enzyme present in the lung, thus providing potential indications on KGM biodegradability;
6. The process of microencapsulation did not affect the antibacterial activity of INH and RFB, as the MIC remained similar between free and

microencapsulated drugs. However, the amount of drug corresponding to MIC was found to not suffice bacterial elimination after macrophage infection or growth inhibition upon continued exposure to KGM microparticles for 7 days;

7. At concentrations considered realistic in the context of lung delivery (up to 125 µg/mL), KGM/INH/RFB microparticles did not show significant cell toxicity in A549 and macrophage-like THP-1 cells upon 24 h exposure;

8. Daily inhalation of KGM microparticles in a total of 10 doses did not induce an inflammatory response in BALB/c mice. This is coincident with reduced activation of macrophages determined *in vitro* and agrees with the literature reporting KGM as an anti-inflammatory polysaccharide. An allergic reaction expressed through IgE increase in plasma or BALF was not detected but eosinophilia was observed. This and the detection of some histological alterations in the lung require further clarification to establish the real potential of KGM as an excipient for pulmonary delivery, particularly in the context of tuberculosis treatment.

Overall, the data obtained through this PhD thesis are encouraging to persist on exploring the potential of KGM as matrix material of inhalable antitubercular drug carriers to treat pulmonary tuberculosis.

7.2. Future perspectives

KGM microparticles have shown to have potential for pulmonary drug delivery, particularly in the context of tuberculosis, justifying the continuation of studies. The need for other studies envisages complementing the generated information and reinforcing the capabilities as inhalable system to treat pulmonary tuberculosis, while considering an eventual translation to clinics. Relevant aspects that must be addressed in the future include:

1. The loss of stability of the formulation is one of the main issues arising from the work. Further studies are necessary to understand the cause of this effect. If it is due to humidity ingress during the test period inside the

climatic test cabinet, the closure system needs to be worked out. However, if the problem is the formulation itself, it will require optimisation to enhance stability over the time.

2. The bactericidal effect of drug-loaded KGM microparticles against mycobacteria must be explored to establish the required dose of KGM microparticles to eliminate the mycobacteria. Preliminary data have shown that the determined MIC values for free drugs and KGM microparticles were not enough to inhibit *M. bovis* growth, either within the macrophages or as a bacterial culture.

3. The *in vitro* interaction of KGM microparticles with the cells could be further explored to know what is the mechanism of internalisation and which receptors are used to mediate the uptake. Moreover, these uptake assays should be supplemented with confocal microscopy images to know the exact localisation of KGM microparticles in the cell.

4. Regarding to the *in vivo* safety profile of KGM microparticles, the observed eosinophilia and the alterations in the lung histology of mice that inhaled KGM microparticles need to be clarified with more analyses. Moreover, further studies are required to better characterise the safety profile, which could include determination of the levels of C reactive protein in plasma, the concentration of pro-inflammatory cytokines in plasma and BALF, the counting of differentiated leucocytes in BALF, etc.

5. An *in vivo* assay of therapeutic efficacy, involving the exposure of mice infected with *M. tuberculosis* to the drug-loaded KGM microparticles by inhalation, at the required dose to inhibit or kill the mycobacteria, would be adequate to establish the real potential of KGM microparticles as inhalable antitubercular drug carriers for tuberculosis treatment.

This page was intentionally left in blank

References

1. World Health Organization. *Global Tuberculosis Report 2020*. (2020).
2. Pham, D.-D., Fattal, E. & Tsapis, N. Pulmonary drug delivery systems for the treatment of tuberculosis. *Int. J. Pharm.* **478**, 517–529 (2015).
3. Zumla, A., Raviglione, M., Hafner, R. & Fordham von Reyn, C. Tuberculosis. *N. Engl. J. Med.* **368**, 745–755 (2013).
4. Dube, D., Agrawal, G. P. & Vyas, S. P. Tuberculosis: from molecular pathogenesis to effective drug carrier design. *Drug Discov. Today* **17**, 760–73 (2012).
5. Ahsan, F., Rivas, I. P., Khan, M. A. & Torres Suárez, A. I. Targeting to macrophages: Role of physicochemical properties of particulate carriers - Liposomes and microspheres - On the phagocytosis by macrophages. *J. Control. Release* **79**, 29–40 (2002).
6. Parumasivam, T. *et al.* Dry powder inhalable formulations for anti-tubercular therapy. *Adv. Drug Deliv. Rev.* **102**, 83–101 (2016).
7. Devaraj, R. D., Reddy, C. K. & Xu, B. Health-promoting effects of konjac glucomannan and its practical applications: A critical review. *Int. J. Biol. Macromol.* **126**, 273–281 (2019).
8. Huang, Z. *et al.* An orally administrated nucleotide-delivery vehicle targeting colonic macrophages for the treatment of inflammatory bowel disease. *Biomaterials* **48**, 26–36 (2015).
9. Auld, S. C. & Staitieh, B. S. HIV and the tuberculosis 'set point': How HIV impairs alveolar macrophage responses to tuberculosis and sets the stage for progressive disease. *Retrovirology* **17**, 1–12 (2020).
10. Direção-Geral da Saúde. *Manual de tuberculose e micobactérias não tuberculosas - Recomendações 2020*. (2020).
11. Ministério da Saúde. *Relatório Anual - Acesso a cuidados de saúde nos estabelecimentos do SNS e entidades convencionadas em 2019*. (2020).
12. Direção-Geral da Saúde. *Programa nacional de vacinação 2020*. (2020).
13. World Health Organization. *The End TB Strategy*. (2014).
14. Pezzella, A. T. History of Pulmonary Tuberculosis. *Thorac. Surg. Clin.* **29**, 1–17 (2019).
15. Chai, Q., Zhang, Y. & Liu, C. H. Mycobacterium tuberculosis: An Adaptable Pathogen Associated With Multiple Human Diseases. **8**, 158 (2018).
16. Talbot, E. A. & Raffa, B. J. Mycobacterium tuberculosis. in *Molecular Medical Microbiology: Second Edition* vol. 3 1637–1653 (Elsevier Ltd, 2015).
17. Kalscheuer, R. *et al.* The Mycobacterium tuberculosis capsule: a cell structure with key implications in pathogenesis. *Biochem. J.* **476**, 1995–

2016 (2019).

18. Maitra, A. *et al.* Cell wall peptidoglycan in Mycobacterium tuberculosis: An Achilles' heel for the TB-causing pathogen. *FEMS Microbiol. Rev.* **43**, 548–575 (2019).

19. Gygli, S. M., Borrell, S., Trauner, A. & Gagneux, S. Antimicrobial resistance in Mycobacterium tuberculosis: Mechanistic and evolutionary perspectives. *FEMS Microbiol. Rev.* **41**, 354–373 (2017).

20. Smith, T., Wolff, K. A. & Nguyen, L. Molecular Biology of Drug Resistance in Mycobacterium tuberculosis. *Curr Top Microbiol Immunol* **374**, 53–80 (2013).

21. Guirado, E., Schlesinger, L. S. & Kaplan, G. *Macrophages in tuberculosis: Friend or foe*. *Seminars in Immunopathology* vol. 35 (2013).

22. Pai, M. *et al.* Tuberculosis. *Nat. Rev. Dis. Prim.* **2**, (2016).

23. Das, S., Tucker, I. & Stewart, P. Inhaled Dry Powder Formulations for Treating Tuberculosis. *Curr. Drug Deliv.* **12**, 26–39 (2015).

24. Arora, S., Dev, K., Agarwal, B., Das, P. & Syed, M. A. Macrophages: Their role, activation and polarization in pulmonary diseases. *Immunobiology* **223**, 383–396 (2018).

25. Marino, S. *et al.* Macrophage polarization drives granuloma outcome during Mycobacterium tuberculosis infection. *Infect. Immun.* **83**, 324–338 (2015).

26. Weiss, G. & Schaible, U. E. Macrophage defense mechanisms against intracellular bacteria. *Immunol. Rev.* **264**, 182–203 (2015).

27. Wang, Y., Smith, W., Hao, D., He, B. & Kong, L. M1 and M2 macrophage polarization and potentially therapeutic naturally occurring compounds. *Int. Immunopharmacol.* **70**, 459–466 (2019).

28. Fricker, M. & Gibson, P. G. Macrophage dysfunction in the pathogenesis and treatment of asthma. *Eur. Respir. J.* **50**, (2017).

29. Rodrigues, S. & Grenha, A. Activation of macrophages: Establishing a role for polysaccharides in drug delivery strategies envisaging antibacterial therapy. *Curr. Pharm. Des.* **21**, 4869–4887 (2015).

30. He, W., Kapate, N., Shields, C. W. & Mitragotri, S. Drug delivery to macrophages: A review of targeting drugs and drug carriers to macrophages for inflammatory diseases. *Adv. Drug Deliv. Rev.* **165**–**166**, 15–40 (2020).

31. Funes, S. C., Rios, M., Escobar-Vera, J. & Kalergis, A. M. Implications of macrophage polarization in autoimmunity. *Immunology* **154**, 186–195 (2018).

32. Queval, C. J., Brosch, R. & Simeone, R. The macrophage: A disputed fortress in the battle against Mycobacterium tuberculosis. *Front. Microbiol.* **8**, 1–11 (2017).

33. Ramachandra, L. *et al.* Phagosomal processing of Mycobacterium

tuberculosis antigen 85B is modulated independently of mycobacterial viability and phagosome maturation. *Infect. Immun.* **73**, 1097–1105 (2005).

34. O'Leary, S., O'Sullivan, M. P. & Keane, J. IL-10 blocks phagosome maturation in Mycobacterium tuberculosis-infected human macrophages. *Am. J. Respir. Cell Mol. Biol.* **45**, 172–180 (2011).

35. Silva Miranda, M., Breiman, A., Allain, S., Deknuydt, F. & Altare, F. The tuberculous granuloma: An unsuccessful host defence mechanism providing a safety shelter for the bacteria? *Clin. Dev. Immunol.* **2012**, (2012).

36. Jagatia, H. & Tsolaki, A. G. The Role of Complement System and the Immune Response to Tuberculosis Infection. *Medicina (B. Aires).* **57**, 84 (2021).

37. Ndlovu, H. & Marakalala, M. J. Granulomas and inflammation: Host-directed therapies for tuberculosis. *Front. Immunol.* **7**, 434 (2016).

38. Momin, M. A. M., Tucker, I. G. & Das, S. C. High dose dry powder inhalers to overcome the challenges of tuberculosis treatment. *Int. J. Pharm.* **550**, 398–417 (2018).

39. Sica, A. & Mantovani, A. Macrophage plasticity and polarization: In vivo veritas. *J. Clin. Invest.* **122**, 787–795 (2012).

40. World Health Organization. *Global Tuberculosis Report 2019*. (2019).

41. Ufimtseva, E. *et al.* Mycobacterium tuberculosis with different virulence reside within intact phagosomes and inhibit phagolysosomal biogenesis in alveolar macrophages of patients with pulmonary tuberculosis. *Tuberculosis* **114**, 77–90 (2019).

42. Furin, J., Cox, H. & Pai, M. Tuberculosis. *Lancet* **393**, 1642–1656 (2019).

43. Vilchèze, C. & Jacobs, W. R. The mechanism of isoniazid killing: clarity through the scope of genetics. *Annu. Rev. Microbiol.* **61**, 35–50 (2007).

44. World Health Organization. *Treatment of tuberculosis: guidelines - 4th ed. World Health Organization 2010* (2010).

45. Fogel, N. Tuberculosis: A disease without boundaries. *Tuberculosis* **95**, 527–531 (2015).

46. Coelho, T. *et al.* Enhancement of antibiotic activity by efflux inhibitors against multidrug resistant Mycobacterium tuberculosis clinical isolates from Brazil. *Front. Microbiol.* **6**, (2015).

47. Rendon, A. *et al.* Classification of drugs to treat multidrug-resistant tuberculosis (MDR-TB): Evidence and perspectives. *J. Thorac. Dis.* **8**, 2666–2671 (2016).

48. Sulis, G. & Pai, M. Isoniazid-resistant tuberculosis: A problem we can no longer ignore. *PLoS Med.* **17**, e1003023 (2020).

49. Zhu, C., Liu, Y., Hu, L., Yang, M. & He, Z. G. Molecular mechanism of the synergistic activity of ethambutol and isoniazid against Mycobacterium

tuberculosis. *J. Biol. Chem.* **293**, 16741–16750 (2019).

50. Purkan, P. *et al.* Molecular Analysis of katG Encoding Catalase-Peroxidase from Clinical Isolate of Isoniazid-Resistant Mycobacterium tuberculosis. *J. Med. Life* **11**, 160–167 (2018).

51. Lange, C. *et al.* Management of drug-resistant tuberculosis. *Lancet* **394**, 953–966 (2019).

52. O'Neil, M. J. Merck Index. *The Merck index: an encyclopedia of chemicals, drugs, and biologicals* (2001).

53. Razak, S. A., Fariq, S., Syed, F., Abdullah, J. M. & Adnan, R. Characterization , phase solubility studies and molecular modeling of Isoniazid and its β -Cyclodextrin complexes. *J. Chem. Pharm. Res.* **6**, 291–299 (2014).

54. Crabol, Y., Catherinot, E., Veziris, N., Jullien, V. & Lortholary, O. Rifabutin: Where do we stand in 2016? *J. Antimicrob. Chemother.* **71**, 1759–1771 (2016).

55. Pinheiro, M., Silva, A. S. & Reis, S. Molecular interactions of rifabutin with membrane under acidic conditions. *Int. J. Pharm.* **479**, 63–69 (2015).

56. Phillips, M. C., Wald-Dickler, N., Loomis, K., Luna, B. M. & Spellberg, B. Pharmacology, Dosing, and Side Effects of Rifabutin as a Possible Therapy for Antibiotic-Resistant Acinetobacter Infections. *Open Forum Infect. Dis.* **7**, 1–9 (2020).

57. Pfizer Canada Inc. *Mycobutin*. *Pfizer Canada Inc.* (2015).

58. Muttil, P., Wang, C. & Hickey, A. J. Inhaled drug delivery for tuberculosis therapy. *Pharm. Res.* **26**, 2401–2416 (2009).

59. Kasozi, S. *et al.* Addressing the drug-resistant tuberculosis challenge through implementing a mixed model of care in Uganda. *PLoS One* **15**, e0244451 (2020).

60. Sansare, V. A., Warrier, D. U. & Shinde, U. A. Cellular trafficking of nanocarriers in alveolar macrophages for effective management of pulmonary tuberculosis. **3**, (2020).

61. Kukut Hatipoglu, M., Hickey, A. J. & Garcia-Contreras, L. Pharmacokinetics and pharmacodynamics of high doses of inhaled dry powder drugs. *Int. J. Pharm.* **549**, 306–316 (2018).

62. Borghardt, J. M., Kloft, C. & Sharma, A. Inhaled Therapy in Respiratory Disease: The Complex Interplay of Pulmonary Kinetic Processes. *Can. Respir. J.* **2018**, 1–11 (2018).

63. Floroiu, A., Klein, M. & Lehr, C. Towards Standardized Dissolution Techniques for In Vitro Performance Testing of Dry Powder Inhalers. *Dissolution Technol.* **23**, 6–19 (2018).

64. Hadiwinoto, G. D., Kwok, P. C. L. & Lakerveld, R. A review on recent technologies for the manufacture of pulmonary drugs. *Ther. Deliv.* **9**, 47–

70 (2018).

65. Scherließ, R. & Etschmann, C. DPI formulations for high dose applications – Challenges and opportunities. *Int. J. Pharm.* **548**, 49–53 (2018).

66. Sibum, I., Hagedoorn, P., de Boer, A. H., Frijlink, H. W. & Grasmeijer, F. Challenges for pulmonary delivery of high powder doses. *Int. J. Pharm.* **548**, 325–336 (2018).

67. Zhong, H., Chan, G., Hu, Y., Hu, H. & Ouyang, D. A comprehensive map of FDA-approved pharmaceutical products. *Pharmaceutics* **10**, 1–19 (2018).

68. Moreno-Sastre, M., Pastor, M., Salomon, C. J., Esquisabel, A. & Pedraz, J. L. Pulmonary drug delivery: A review on nanocarriers for antibacterial chemotherapy. *J. Antimicrob. Chemother.* **70**, 2945–2955 (2015).

69. Usmani, O. S. Choosing the right inhaler for your asthma or COPD patient. *Ther. Clin. Risk Manag.* **15**, 461 (2019).

70. Javadzadeh, Y. & Yaqoubi, S. Therapeutic nanostructures for pulmonary drug delivery. in *Nanostructures for Drug Delivery* 619–638 (Elsevier Inc., 2017). doi:10.1016/b978-0-323-46143-6.00020-8.

71. McShane, D. *et al.* Normal nasal mucociliary clearance in CF children: Evidence against a CFTR-related defect. *Eur. Respir. J.* **24**, 95–100 (2004).

72. El-sherbiny, I. M., El-baz, N. M. & Yacoub, M. H. Inhaled nano- and microparticles for drug delivery. *Global Cardiology Science and Practice* 1–14 (2015).

73. Osman, N., Kaneko, K., Carini, V. & Saleem, I. Carriers for the targeted delivery of aerosolized macromolecules for pulmonary pathologies. *Expert Opin. Drug Deliv.* **15**, 821–834 (2018).

74. Cun, D., Zhang, C., Bera, H. & Yang, M. Particle engineering principles and technologies for pharmaceutical biologics. *Adv. Drug Deliv. Rev.* **174**, 140–167 (2021).

75. Lengyel, M., Kállai-Szabó, N., Antal, V., Laki, A. J. & Antal, I. Microparticles, microspheres, and microcapsules for advanced drug delivery. *Sci. Pharm.* **87**, (2019).

76. Pontes, J. F. & Grenha, A. Multifunctional nanocarriers for lung drug delivery. *Nanomaterials* **10**, 183 (2020).

77. Grenha, A., Seijo, B. & Remuñán-López, C. Microencapsulated chitosan nanoparticles for lung protein delivery. *Eur. J. Pharm. Sci.* **25**, 427–437 (2005).

78. Tomoda, K. *et al.* Preparation and properties of inhalable nanocomposite particles: Effects of the temperature at a spray-dryer inlet upon the properties of particles. *Colloids Surfaces B Biointerfaces* **61**, 138–144 (2008).

79. Liang, Z., Ni, R., Zhou, J. & Mao, S. Recent advances in controlled

pulmonary drug delivery. *Drug Discov. Today* **20**, 380–389 (2015).

80. Prasher, P. *et al.* Current-status and applications of polysaccharides in drug delivery systems. *Colloids Interface Sci. Commun.* **42**, 100418 (2021).

81. Rehman, A. *et al.* Drug nanodelivery systems based on natural polysaccharides against different diseases. *Adv. Colloid Interface Sci.* **284**, 102251 (2020).

82. Cunha, L. *et al.* Inhalable chitosan microparticles for simultaneous delivery of isoniazid and rifabutin in lung tuberculosis treatment. *Drug Dev. Ind. Pharm.* **45**, 1313–1320 (2019).

83. Kundawala, A. J., Patel, V. a, Patel, H. V & Choudhary, D. Isoniazid loaded chitosan microspheres for pulmonary delivery : Preparation and characterization. *Pelagia Res. Libr. Der Pharm. Sin.* **2**, 88–97 (2011).

84. Rodrigues, S. *et al.* Dual antibiotherapy of tuberculosis mediated by inhalable locust bean gum microparticles. *Int. J. Pharm.* **529**, (2017).

85. Alves, A. D. *et al.* Inhalable antitubercular therapy mediated by locust bean gum microparticles. *Molecules* **21**, (2016).

86. Cunha, L., Rodrigues, S., Buttini, F. & Grenha, A. Inhalable Fucoidan Microparticles Combining Two Antitubercular Drugs with Potential Application in Pulmonary Tuberculosis Therapy. *Polymers (Basel).* **10**, 636 (2018).

87. Cunha, L. *et al.* Spray-dried fucoidan microparticles for pulmonary delivery of antitubercular drugs. *J. Microencapsul.* **35**, 392–405 (2018).

88. Rodrigues, S. *et al.* Cytocompatibility and cellular interactions of chondroitin sulfate microparticles designed for inhaled tuberculosis treatment. *Eur. J. Pharm. Biopharm.* **163**, 171–178 (2021).

89. Rodrigues, S. *et al.* Inhalable spray-dried chondroitin sulphate microparticles: Effect of different solvents on particle properties and drug activity. *Polymers (Basel).* **12**, 1–13 (2020).

90. Acharya, D., Li, X. R., Heineman, R. E. S. & Harrison, R. E. Complement Receptor-Mediated Phagocytosis Induces Proinflammatory Cytokine Production in Murine Macrophages. *Front. Immunol.* **10**, 3049 (2020).

91. Speert, D. P. Macrophages in bacterial infection. in *The Macrophage* 217–263 (1992).

92. Joffe, A. M., Bakalar, M. H. & Fletcher, D. A. Macrophage phagocytosis assay with reconstituted target particles. *Nat. Protoc.* **15**, 2230–2246 (2020).

93. Hirayama, D., Iida, T. & Nakase, H. The phagocytic function of macrophage-enforcing innate immunity and tissue homeostasis. *Int. J. Mol. Sci.* **19**, 92 (2018).

94. Rosales, C. & Uribe-Querol, E. Phagocytosis: A Fundamental Process in Immunity. *Biomed Res. Int.* **2017**, (2017).

95. Gordon, S. & Plüddemann, A. Role of Macrophages in Autoimmunity. in *The Autoimmune Diseases* 161–174 (2013). doi:10.1016/B978-0-12-384929-8.00011-3.

96. Wang, T. *et al.* Targeted polymer-based antibiotic delivery system: A promising option for treating bacterial infections via macromolecular approaches. *Prog. Polym. Sci.* **116**, 101389 (2021).

97. Vieira, A. C. C. *et al.* Mannosylated solid lipid nanoparticles for the selective delivery of rifampicin to macrophages. *Artif. Cells, Nanomedicine Biotechnol.* **46**, 653–663 (2018).

98. Maretti, E. *et al.* Newly synthesized surfactants for surface mannosylation of respirable SLN assemblies to target macrophages in tuberculosis therapy. *Drug Deliv. Transl. Res.* **9**, 298–310 (2019).

99. Su, F. Y. *et al.* Polymer-augmented liposomes enhancing antibiotic delivery against intracellular infections. *Biomater. Sci.* **6**, 1976–1985 (2018).

100. Baranov, M. V., Kumar, M., Sacanna, S., Thutupalli, S. & van den Bogaart, G. Modulation of Immune Responses by Particle Size and Shape. *Front. Immunol.* **11**, 3854 (2021).

101. Tabata, Y. & Ikada, Y. Effect of the size and surface charge of polymer microspheres on their phagocytosis by macrophage. *Biomaterials* **9**, 356–362 (1988).

102. Pacheco, P., White, D. & Sulchek, T. Effects of Microparticle Size and Fc Density on Macrophage Phagocytosis. *PLoS One* **8**, e60989 (2013).

103. Tang, J., Chen, J., Guo, J., Wei, Q. & Fan, H. Construction and evaluation of fibrillar composite hydrogel of collagen/konjac glucomannan for potential biomedical applications. *Regen. Biomater.* **5**, 239–250 (2018).

104. Behera, S. S. & Ray, R. C. Konjac glucomannan, a promising polysaccharide of Amorphophallus konjac K. Koch in health care. *Int. J. Biol. Macromol.* **92**, 942–956 (2016).

105. Luan, J. *et al.* pH-Sensitive drug delivery system based on hydrophobic modified konjac glucomannan. *Carbohydr. Polym.* **171**, 9–17 (2017).

106. Zhu, F. Modifications of konjac glucomannan for diverse applications. *Food Chem.* **256**, 419–426 (2018).

107. Abbasi, Y. F. & Bera, H. Konjac glucomannan-based nanomaterials in drug delivery and biomedical applications. in *Biopolymer-Based Nanomaterials in Drug Delivery and Biomedical Applications* 119–141 (2021).

108. Alvarez-Manceñido, F., Landin, M., Lacik, I. & Martínez-Pacheco, R. Konjac glucomannan and konjac glucomannan/xanthan gum mixtures as excipients for controlled drug delivery systems. Diffusion of small drugs. *Int. J. Pharm.* **349**, 11–18 (2008).

109. Bhardwaj, T. R., Kanwar, M. & Lal, R. Natural Gums and Modified Natural Gums as Sustained-Release Carriers. *Drug Dev. Ind. Pharm.* **26**, 1025–1038 (2000).

110. Chen, L. G., Liu, Z. L. & Zhuo, R. X. Synthesis and properties of degradable hydrogels of konjac glucomannan grafted acrylic acid for colon-specific drug delivery. *Polymer (Guildf).* **46**, 6274–6281 (2005).

111. Liu, J. *et al.* Preparation of konjac glucomannan-based pulsatile capsule for colonic drug delivery system and its evaluation in vitro and in vivo. *Carbohydr. Polym.* **87**, 377–382 (2012).

112. Ding, Y. F. *et al.* Oral Colon-Targeted Konjac Glucomannan Hydrogel Constructed through Noncovalent Cross-Linking by Cucurbit[8]uril for Ulcerative Colitis Therapy. *ACS Appl. Bio Mater.* **3**, 10–19 (2020).

113. Kök, M. S., Abdelhameed, A. S., Ang, S., Morris, G. a. & Harding, S. E. A novel global hydrodynamic analysis of the molecular flexibility of the dietary fibre polysaccharide konjac glucomannan. *Food Hydrocoll.* **23**, 1910–1917 (2009).

114. Alonso-Sande, M., Teijeiro-Osorio, D., Remuñán-López, C. & Alonso, M. J. Glucomannan, a promising polysaccharide for biopharmaceutical purposes. *European Journal of Pharmaceutics and Biopharmaceutics* vol. 72 453–462 (2009).

115. Guerreiro, F., Pontes, J. F., Rosa da Costa, A. M. & Grenha, A. Spray-drying of konjac glucomannan to produce microparticles for an application as antitubercular drug carriers. *Powder Technol.* **342**, (2019).

116. Beccari, T., Bibi, L., Stinchi, S. & Stirling, J. L. Mouse Beta-Mannosidase : cDNA Cloning , Expression , and Chromosomal Localization. *Biosci. Rep.* **21**, 315–323 (2001).

117. Chaurasiya, B. & Zhao, Y.-Y. Dry Powder for Pulmonary Delivery: A Comprehensive Review. *Pharmaceutics* **13**, 31 (2020).

118. Poozesh, S. & Bilgili, E. Scale-up of pharmaceutical spray drying using scale-up rules: A review. *Int. J. Pharm.* **562**, 271–292 (2019).

119. Salama, A. H. Spray drying as an advantageous strategy for enhancing pharmaceuticals bioavailability. *Drug Deliv. Transl. Res.* **10**, 1–12 (2020).

120. Ziaee, A. *et al.* Spray drying of pharmaceuticals and biopharmaceuticals: Critical parameters and experimental process optimization approaches. *Eur. J. Pharm. Sci.* **127**, 300–318 (2019).

121. Haggag, Y. A. & Faheem, A. M. Evaluation of nano spray drying as a method for drying and formulation of therapeutic peptides and proteins. *Front. Pharmacol.* **6**, (2015).

122. Verma, M. *et al.* A gastric resident drug delivery system for prolonged gram-level dosing of tuberculosis treatment. *Sci. Transl. Med.* **11**, eaau6267 (2019).

123. Maretti, E. *et al.* Inhaled Solid Lipid Microparticles to target alveolar macrophages for tuberculosis. *Int. J. Pharm.* **462**, 74–82 (2014).

124. Almeida, A. J. & Grenha, A. Technosphere®: an inhalation system for pulmonary delivery of biopharmaceuticals. in *Mucosal delivery of*

biopharmaceuticals 483–498 (2014).

125. Newman, S. P. Drug delivery to the lungs: Challenges and opportunities. *Ther. Deliv.* **8**, 647–661 (2017).

126. Peng, T. *et al.* Influence of physical properties of carrier on the performance of dry powder inhalers. *Acta Pharm. Sin. B* **6**, 308–318 (2016).

127. Hamishehkar, H., Rahimpour, Y. & Javadzadeh, Y. The role of carrier in dry powder inhaler. in *Recent Advances in Novel Drug Carrier System* (eds. Hamishehkar, H., Rahimpour, Y. & Javadzadeh, Y.) 39–66 (INTECH Open Access Publisher, 2012).

128. Liu, Q., Guan, J., Qin, L., Zhang, X. & Mao, S. Physicochemical properties affecting the fate of nanoparticles in pulmonary drug delivery. *Drug Discov. Today* **25**, 150–159 (2020).

129. Filatova, L. Y., Klyachko, N. L. & Kudryashova, E. V. Targeted delivery of anti-tuberculosis drugs to macrophages: targeting mannose receptors Targeted delivery of anti-tuberculosis drugs to macrophages : targeting mannose receptors. *Russ. Chem. Rev.* **87**, 374–391 (2018).

130. Guerreiro, F. Spray-dried polysaccharide microparticles aimed at pulmonary delivery of antitubercular drugs. (Universidade do Algarve, 2015).

131. Cheng, L. H., Nur Halawiah, H., Lai, B. N., Yong, H. M. & Ang, S. L. Ultrasound mediated acid hydrolysis of konjac glucomannan. *Int. Food Res. J.* **17**, 1043–1050 (2010).

132. Barth, H. G. Accuracy validation of size-exclusion chromatography. *LCGC North Am.* **36**, 142–145 (2018).

133. Flórez-Fernández, N., Domínguez, H. & Torres, M. D. Advances in the biorefinery of Sargassum muticum: Valorisation of the alginate fractions. *Ind. Crops Prod.* **138**, 111483 (2019).

134. Chua, M., Baldwin, T. C., Hocking, T. J. & Chan, K. Traditional uses and potential health benefits of Amorphophallus konjac K. Koch ex N.E.Br. *J. Ethnopharmacol.* **128**, 268–278 (2010).

135. Wang, Y., Liu, J., Li, Q., Wang, Y. & Wang, C. Two natural glucomannan polymers, from Konjac and Bletilla, as bioactive materials for pharmaceutical applications. *Biotechnol. Lett.* **37**, 1–8 (2015).

136. Crescenzi, V. *et al.* A high field NMR study of the products ensuing from Konjak glucomannan C(6)-oxidation followed by enzymatic c(5)-epiderization. *Biomacromolecules* **3**, 1343–1352 (2002).

137. Torres, M. D., Hallmark, B., Wilson, D. I. & Hilliou, L. Natural Giesekus: Shear and Externsional Behavior of Food Gum Solutions in the Semidilute Regime. *AIChE J.* **60**, 3902–3915 (2014).

138. Hassoun, M., Royall, P. G., Parry, M., Harvey, R. D. & Forbes, B. Design and development of a biorelevant simulated human lung fluid. *J. Drug Deliv. Sci. Technol.* **47**, 485–491 (2018).

139. ICH Expert Working Group. *Stability testing of new drug substances and products Q1A(R2)*. *International Conference on Harmonization of Technical Requirements for registration of pharmaceuticals for human use* (2003) doi:10.1136/bmj.333.7574.873-a.

140. European Medicines Agency. *ICH Topic Q 1 E Evaluation of Stability Data Step*. *European Medicines Agency* http://www.ema.europa.eu/ema/ (2003).

141. European Directorate for the Quality of Medicines & HealthCare (EDQM). Section 2.9.18. Preparations for inhalations: Aerodynamic assessment of fine particles. in *EUROPEAN PHARMACOPOEIA 8.0* 309–320 (2013).

142. Gaspar, D. P. *et al.* Rifabutin-loaded solid lipid nanoparticles for inhaled antitubercular therapy: Physicochemical and in vitro studies. *Int. J. Pharm.* **497**, 199–209 (2016).

143. Rojanarat, W. *et al.* Isoniazid proliposome powders for inhalation-preparation, characterization and cell culture studies. *Int. J. Mol. Sci.* **12**, 4414–4434 (2011).

144. Abdallah, A. M. *et al.* Genomic expression catalogue of a global collection of BCG vaccine strains show evidence for highly diverged metabolic and cell-wall adaptations. *Sci. Rep.* **5**, 1–15 (2015).

145. Ritz, N. *et al.* Susceptibility of Mycobacterium bovis BCG vaccine strains to antituberculous antibiotics. *Antimicrob. Agents Chemother.* **53**, 316–318 (2009).

146. Alves, A. *et al.* Inhalable Antitubercular Therapy Mediated by Locust Bean Gum Microparticles. *Molecules* **21**, 702 (2016).

147. Seville, P. C., Learoyd, T. P., Li, H. Y., Williamson, I. J. & Birchall, J. C. Amino acid-modified spray-dried powders with enhanced aerosolisation properties for pulmonary drug delivery. *Powder Technol.* **178**, 40–50 (2007).

148. Hirota, K. *et al.* Optimum conditions for efficient phagocytosis of rifampicin-loaded PLGA microspheres by alveolar macrophages. *J. Control. Release* **119**, 69–76 (2007).

149. Miranda, M. S. *et al.* Exploring inhalable polymeric dry powders for anti-tuberculosis drug delivery. *Mater. Sci. Eng. C* **93**, 1090–1103 (2018).

150. Yoo, J.-W. & Mitragotri, S. Polymer particles that switch shape in response to a stimulus. *Proc. Natl. Acad. Sci.* **107**, 11205–11210 (2010).

151. Du, P., Du, J. & Smyth, H. D. C. Evaluation of Granulated Lactose as a Carrier for Dry Powder Inhaler Formulations 2: Effect of Drugs and Drug Loading. *J. Pharm. Sci.* **106**, 366–376 (2017).

152. Kyle, H., Ward, J. P. T. & Widdicombe, J. G. Control of pH of airway surface liquid of the ferret trachea in vitro. *J. Appl. Physiol.* **68**, 135–140 (1990).

153. Kumar, A. *et al.* A Biocompatible Synthetic Lung Fluid Based on Human Respiratory Tract Lining Fluid Composition. *Pharm. Res.* **34**, 2454–2465

(2017).

154. Li, L. *et al.* Study on swelling model and thermodynamic structure of native konjac glucomannan. *J. Zhejiang Univ. Sci. B* **10**, 273–279 (2009).

155. Alpert, A. J. Effect of salts on retention in hydrophilic interaction chromatography. *J. Chromatogr. A* **1538**, 45–53 (2018).

156. Alkhayat, A. H. *et al.* Human beta-mannosidase cDNA characterization and first identification of a mutation associated with human beta-mannosidosis. *Hum. Mol. Genet.* **7**, 75–83 (1998).

157. The Human Protein Atlas. *MANBA* https://www.proteinatlas.org/ENSG00000109323-MANBA/blood (2019).

158. Koshikawa, N. *et al.* Expression of trypsin by epithelial cells of various tissues, leukocytes, and neurons in human and mouse. *Am. J. Pathol.* **153**, 937–944 (1998).

159. Enlo-Scott, Z., Bäckström, E., Mudway, I. & Forbes, B. Drug metabolism in the lungs: opportunities for optimising inhaled medicines. *Expert Opin. Drug Metab. Toxicol.* (2021).

160. Grimm, W. Storage conditions for stability testing (Part 2). *Drugs Made Ger.* **29**, 39–47 (1986).

161. Grimm, W. Extension of the international conference on harmonization tripartite guideline for stability testing of new drug substances and products to countries of climatic zones III and IV. *Drug Dev. Ind. Pharm.* **24**, 313–325 (1998).

162. Patton, J. S. & Byron, P. R. Inhaling medicines: Delivering drugs to the body through the lungs. *Nat. Rev. Drug Discov.* **6**, 67–74 (2007).

163. Magee, K. P., Wimberley, D., Crane, G., Sobhi, S. & Bawdon, R. E. Ex Vivo Human Placental Transfer of Rifampin and Rifabutin. *Infect. Dis. Obstet. Gynecol.* **4**, 319–322 (1996).

164. Nazarova, E. V. & Russell, D. G. Growing and handling of Mycobacterium tuberculosis for macrophage infection assays. in *Phagocytosis and Phagosomes* vol. 1519 325–331 (2017).

165. Clinical and Laboratory Standards Institute. Susceptibility Testing of Mycobacteria, Nocardiae, and Other Aerobic Actinomycetes. in *Clinical and Laboratory Standards Institute* M24–A2 (2003).

166. Kolibab, K., Derrick, S. C. & Morris, S. L. Sensitivity to isoniazid of Mycobacterium bovis BCG strains and BCG disseminated disease isolates. *J. Clin. Microbiol.* **49**, 2380–2381 (2011).

167. Pinheiro, M. *et al.* The influence of Rifabutin on human and bacterial membrane models: Implications for its mechanism of action. *J. Phys. Chem. B* **117**, 6187–6193 (2013).

168. Pinheiro, M., Silva, A. S. & Reis, S. Molecular interactions of rifabutin with membrane under acidic conditions. *Int. J. Pharm.* **479**, 63–69 (2015).

169. Perdigão, J. *et al.* Unraveling Mycobacterium tuberculosis genomic diversity and evolution in Lisbon, Portugal, a highly drug resistant setting. *BMC Genomics* **15**, 991 (2014).

170. Becker, C. *et al.* Biowaiver monographs for immediate release solid oral dosage forms: isoniazid. *J. Pharm. Sci.* **96**, 522–31 (2007).

171. Grenha, A. *et al.* Inhalable locust bean gum microparticles co-associating isoniazid and rifabutin: Therapeutic assessment in a murine model of tuberculosis infection. *Eur. J. Pharm. Biopharm.* **147**, 38–44 (2020).

172. Van Hoecke, L., Job, E. R., Saelens, X. & Roose, K. Bronchoalveolar lavage of murine lungs to analyze inflammatory cell infiltration. *J. Vis. Exp.* **2017**, 1–8 (2017).

173. Riss, T. L. *et al.* Cell Viability Assays. in *Assay Guidance Manual* (2016).

174. Geiser, M. Update on Macrophage Clearance of Inhaled. *J. Aerosol Med. Pulm. Drug Deliv.* **23**, 207–217 (2010).

175. International Organization for Standardization. *ISO 10993-1 Biological Evaluation of Medical Devices—Part 5: Tests for in Vitro Cytotoxicity*. (2009).

176. Rodrigues, S. *et al.* Dual antibiotherapy of tuberculosis mediated by inhalable locust bean gum microparticles. *Int. J. Pharm.* **529**, 433–441 (2017).

177. Cookson, W. O. C. M., Cox, M. J. & Moffatt, M. F. New opportunities for managing acute and chronic lung infections. *Nat. Rev. Microbiol.* **16**, 111–120 (2018).

178. Colton, C. K. *et al.* Characterization of Islet Preparations. in *Cellular Transplantation* 85–133 (Elsevier Inc., 2007). doi:10.1016/B978-012369415-7/50007-7.

179. Mosser, D. M. & Edwards, J. P. Exploring the full spectrum of macrophage activation. *Nat Rev Immunol.* **8**, 958–969 (2008).

180. Wu, X. *et al.* TNF-a mediated inflammatory macrophage polarization contributes to the pathogenesis of steroid-induced osteonecrosis in mice. *Int. J. Immunopathol. Pharmacol.* **28**, 351–361 (2015).

181. Page, M. J., Bester, J. & Pretorius, E. The inflammatory effects of TNF-α and complement component 3 on coagulation. *Sci. Rep.* **8**, 1–9 (2018).

182. Horiuchi, T., Mitoma, H., Harashima, S. I., Tsukamoto, H. & Shimoda, T. Transmembrane TNF-α: Structure, function and interaction with anti-TNF agents. *Rheumatology* **49**, 1215–1228 (2010).

183. Meniailo, M. E. *et al.* Interleukin-8 favors pro-inflammatory activity of human monocytes/macrophages. *Int. Immunopharmacol.* **56**, 217–221 (2018).

184. Krupa, A. *et al.* Binding of CXCL8/IL-8 to Mycobacterium tuberculosis Modulates the Innate Immune Response. *Mediators Inflamm.* **2015**, (2015).

185. Dallenga, T. *et al.* M. tuberculosis-Induced Necrosis of Infected Neutrophils

Promotes Bacterial Growth Following Phagocytosis by Macrophages. *Cell Host Microbe* **22**, 519-530.e3 (2017).

186. Maphasa, R. E., Meyer, M. & Dube, A. The Macrophage Response to Mycobacterium tuberculosis and Opportunities for Autophagy Inducing Nanomedicines for Tuberculosis Therapy. *Front. Cell. Infect. Microbiol.* **10**, (2021).

187. Visser, J. G., Van Staden, A. D. P. & Smith, C. Harnessing macrophages for controlled-release drug delivery: Lessons from microbes. *Front. Pharmacol.* **10**, 22 (2019).

188. Mosser, D. M., Hamidzadeh, K. & Goncalves, R. Macrophages and the maintenance of homeostasis. *Cell. Mol. Immunol.* **18**, 579–587 (2021).

189. Patel, B., Gupta, N. & Ahsan, F. Particle engineering to enhance or lessen particle uptake by alveolar macrophages and to influence the therapeutic outcome. *Eur. J. Pharm. Biopharm.* **89**, 163–174 (2015).

190. Moghimi, S. M. *et al.* Particulate systems for targeting of macrophages: Basic and therapeutic concepts. *J. Innate Immun.* **4**, 509–528 (2012).

191. Bermudez, E. *et al.* Pulmonary responses of mice, rats, and hamsters to subchronic inhalation of ultrafine titanium dioxide particles. *Toxicol. Sci.* **77**, 347–357 (2004).

192. ICH. *ICH guideline M3(R2) on non-clinical safety studies for the conduct of human clinical trials and marketing authorisation for pharmaceuticals*. (2009).

193. De Jong, W., Carraway, J. & Geertsma, R. In vivo and in vitro testing for the biological safety evaluation of biomaterials and medical devices. in *Biocompatibility and Performance of Medical Devices* (ed. Boutrand, J.) 123–166 (2020).

194. Wirth, M. D. *et al.* The Dietary Inflammatory Index is Associated with Elevated White Blood Cell Counts in the National Health and Nutrition Examination Survey. *Brain Behav Immun* **69**, 296–303 (2018).

195. Charles River Laboratories International. *BALB/C Mouse Hematology North American Colonies January 2008 - December 2012*. (2012).

196. Henderson, R. F. *et al.* New approaches for the evaluation of pulmonary toxicity: Bronchoalveolar lavage fluid analysis. *Toxicol. Sci.* **5**, 451–458 (1985).

197. Rosales, C. Neutrophil: A cell with many roles in inflammation or several cell types? *Front. Physiol.* **9**, 113 (2018).

198. Fulkerson, P. C. & Rothenberg, M. E. Targeting Eosinophils in Allergy, Inflammation and Beyond. *Nat. Rev. Drug Discov.* **12**, 1–23 (2013).

199. Onishi, N. *et al.* Dietary pulverized konjac glucomannan suppresses scratching behavior and skin inflammatory immune responses in NC/Nga mice. *Int. Arch. Allergy Immunol.* **144**, 95–104 (2007).

200. Guilliams, M., Mildner, A. & Yona, S. Developmental and Functional Heterogeneity of Monocytes. *Immunity* **49**, 595–613 (2018).

201. Nazir, T. *et al.* Monocytopenia; Induction by Vinorelbine, Cisplatin and Doxorubicin in Breast, Non-Small Cell Lung and Cervix Cancer Patients. *Int. J. Health Sci. (Qassim).* **10**, 542 (2016).

202. Rosenwasser, L. J. Mechanisms of IgE inflammation. *Curr. Allergy Asthma Rep.* **11**, 178–183 (2011).

203. Navinés-ferrer, A., Serrano-candelas, E. & Martín, M. IgE-Related Chronic Diseases and Anti-IgE-Based Treatments. **2016**, (2016).

204. Ferastraoaru, D. *et al.* AllergoOncology: Ultra-low IgE, a potential novel biomarker in cancer - A Position Paper of the European Academy of Allergy and Clinical Immunology (EAACI). *Clin. Transl. Allergy* **10**, 1–16 (2020).

205. Patel, K. K., Anderson, E., Salva, P. S. & Webley, W. C. The prevalence and identity of Chlamydia-specific IgE in children with asthma and other chronic respiratory symptoms. *Respir. Res.* **13**, 1–11 (2012).

206. Suzuki, H. *et al.* Hydrolyzed Konjac glucomannan suppresses IgE production in mice B cells. *Int. Arch. Allergy Immunol.* **152**, 122–130 (2010).

207. Aragao-Santiago, L. *et al.* Compared in vivo toxicity in mice of lung delivered biodegradable and non-biodegradable nanoparticles. *Nanotoxicology* **10**, 292–302 (2016).

208. Michael, B. *et al.* Evaluation of organ weights for rodent and non-rodent toxicity studies: a review of regulatory guidelines and a survey of current practices. *Toxicol. Pathol.* **35**, 742–750 (2007).

209. Larsen, S. T. *et al.* Airway irritation, inflammation, and toxicity in mice following inhalation of metal oxide nanoparticles. *Nanotoxicology* **10**, 1254–1262 (2016).

210. Jiao, Z., Wen, Z., Yang, W., Hu, L. & Li, J. Influence of fine particulate matter and its pure particulate fractions on pulmonary immune cells and cytokines in mice. *Exp. Ther. Med.* **21**, 1–9 (2021).

211. Poole, J. A. *et al.* Intranasal organic dust exposure-induced airway adaptation response marked by persistent lung inflammation and pathology in mice. *Am. J. Physiol. - Lung Cell. Mol. Physiol.* **296**, 1085–1095 (2009).